BUSINESS

Ideal chip of future may hide in true grit

☐ An Oregon professor hopes he can develop a better semiconductor material from the stuff that covers sandpaper

By RICHARD COLBY
of The Oregonian staff

In the quest for new semiconductors that will compute and do countless other electronic tasks faster than semiconductors can do them already, a substance called beta silicon carbide has been called the semiconducting material of the future.

The only problem, says Jim Parsons, is that in the case of beta silicon carbide, the "future" started 40 years ago and has yet to arrive.

That situation will change if Parsons has anything to do with it.

Since the 1950s, beta silicon carbide has been recognized as a theoretically better conductor of heat and electricity and thus a more heat-tolerant alternative to pure silicon, the basis for most semiconductors now.

Beta silicon carbide, Parsons explains, is among more than 170 different structures of silicon carbide, commonly used as the grit on sandpaper.

"The beta structure's properties make it ideal for electronic applications," he explains.

Parsons says the beta silicon carbon compound also shows certain technical advantages over another substitute for silicon called gallium arsenide, which has been slowly growing in use as a semiconductor material because it conducts electricity faster.

However, according to Parsons, the extreme difficulty of making usable quantities of beta silicon carbide has kept it out of semiconductor makers' reach.

Parsons, an Oregon Graduate Institute associate professor and researcher who joined the institute's faculty last year, says the compound's production problems have been overcome, at least in his laboratory.

Using what he calls a chemical vapor deposition system, the scientist has been able to grow beta silicon carbide crystals into usable quantities with the necessary purity for minute electronics to be put into them.

Along with allowing higher density for the electronics, a major advantage is that beta silicon carbide semiconductors can operate in temperatures as high as 1,800 degrees Fahrenheit, compared with silicon's maximum temperature of about 575 degrees.

Thus, the carbide compound should prove especially valuable for uses such as sophisticated aircraft electronics, including weaponry, that now require either weighty cooling attachments or huge vacuum tubes instead of silicon-chip controllers.

"Beta silicon carbide would eliminate cooling requirements in aircraft wings, where fuel lines now cool the equipment," says Parsons, who spent nine years with Hughes Aircraft Co.'s research subsidiary near Los Angeles before coming to Oregon.

It all won't happen overnight.

"From the economic aspect, we're not going to be supplanting silicon anytime soon. We're not going to be making a 486," Parsons says of Intel Corp.'s latest and fastest computing chip.

"That would be 10 years off, I think."

What should be possible, perhaps within another year or two, will be making simpler electronic components out of beta silicon carbide. Promising candidates are diodes that control the electrical energy flow to other equipment or thermistors that measure heat being generated, Parsons says.

And as scientists' and engineers' knowledge about how to deal with the substance grows, more sophisticated electronics will follow, he predicts, including computer chips.

And new semiconductor uses should also come about, he says, such as electronic substitutes for aircraft hydraulics or new automotive-engine controls — perhaps embedded in the engine block.

"We're with beta silicon carbide now where we were with silicon in 1955," Parsons says.

Hundreds of thousands of silicon products have been developed in the past 35 years; Parsons thinks it would take only 10 to 15 years to get as far with the carbide compound.

He also talks of consumer products, such as replacing the main microwave oven component called a magnetron. A magnetron converts normal house current to much higher electrical frequencies that bombard food and thus heat it. A small beta silicon carbide chip doing the same thing would require far less electricity and less space, he says.

"One of the reasons we think this is important is that we might be able to create an industry here," Parsons says of the compound and its prospective applications.

Others are more cautious about beta silicon carbide.

"I wouldn't expect to see products based on silicon carbide anytime soon, if at all," said William O'Mara, an electronics consultant with Rose Associates in Los Altos, Calif.

"I'm a little bit skeptical, although the theoretical possibilities are there. More than five years is what I would say before we see any commercial products made of silicon carbide," said O'Mara, who said he was not familiar with Parsons' laboratory processes.

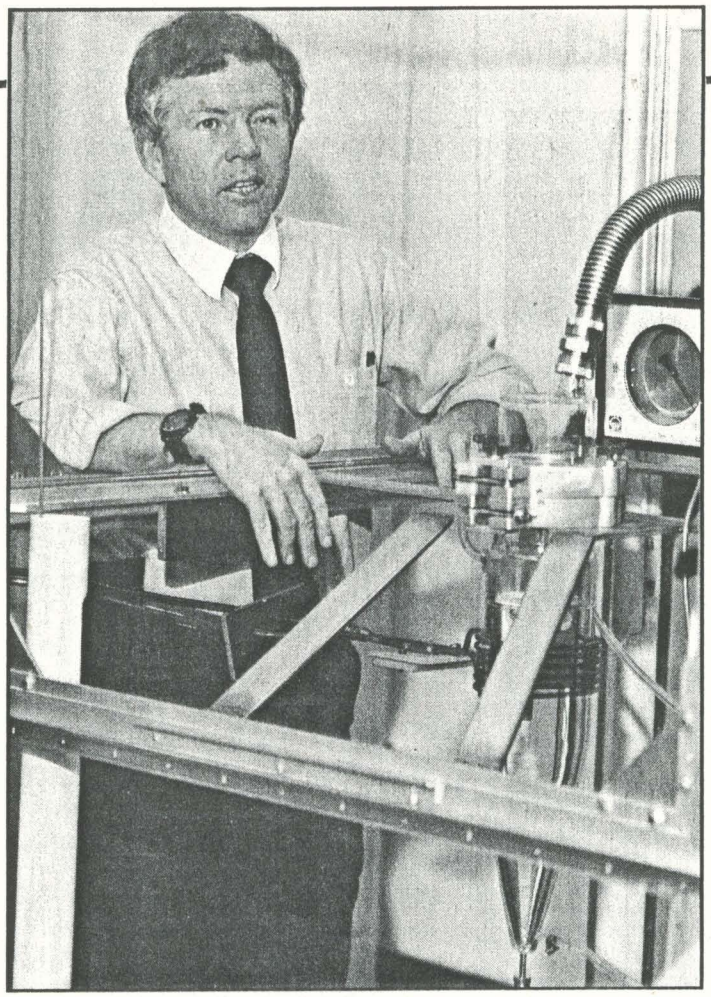

The Oregonian/BRENT WOJAHN

Jim Parsons, of the Oregon Graduate Institute, displays the system that forms beta silicon carbide, which he touts as a promising material for semiconductors.

"From the economic aspect, we're not going to be supplanting silicon anytime soon."

— Jim Parsons, Oregon Graduate Institute

Companies recruiting with an eye on the future

☐ Diversification is taking place not just to meet affirmative action goals, but because it's good business

By JIM NESBITT
Newhouse News Service

ST. LOUIS — At a reception his company held last year in Boston for the top business students of Harvard and MIT, Monsanto chairman Richard Mahoney watched corporate America's future leaders sweep up a broad marble staircase to meet his senior executives.

Half of the students were white males — a youthful reflection of the demographic group that dominates the white-collar hierarchy. But half were women, blacks, Hispanics and Asians — a preview of the fastest-growing talent pool for the 21st century.

As the students approached, Mahoney turned to some of his senior executives and asked: "How would you like that group to plunge into a sea of white male faces? How effective would our recruiting effort be? Thank God, we have some — not as many as we should, not as many as we will — but some women and minorities to meet them."

For Mahoney, this encounter was a clear sign that U.S. corporations need to change their old-boy ways and make themselves more attractive to women and minorities — not to right ancient wrongs, not to make affirmative action goals, but to meet the challenge of corporate competitiveness and maintain the bottom line.

Under the banner of the buzzword "diversity," corporate giants like Monsanto, American Telephone and Telegraph Co., Procter and Gamble, Corning, Digital Equipment and IBM are launching a variety of programs aimed at preparing for a workplace that will be a crossroad of racial, ethnic and gender differences.

Overt racism isn't the prime target here; it is rarely the root cause of the "glass ceiling" that keeps women and minorities from advancing to the top tier. Subtler biases, cultural differences and social disadvantages — underscored by the "old-boy network" of white males — are the main reasons women and minorities have been bypassed.

"The most frustrating thing is knowing you can do the job and not being given the opportunity to do so," said Jim Trice, 51, a black personnel manager with Monsanto.

Some corporations have put real teeth behind this push. Corning and US West tie executives' bonuses and promotions to their success in recruiting and promoting blacks and women.

Others, like Monsanto, emphasize programs that increase the sensitivity of employees to racial and cultural bias. The focus goes beyond a single group or gender; the idea is to cut through cultural differences and make people more comfortable about working together.

"The issue isn't about blacks, it isn't about women," said Ed Jones, president of Corporate Organizational Dynamics, a South Orange, N.J., consulting firm that advises companies how to manage a diverse workplace. "It's about how you bring diverse people together. It's about how we move the best people ahead."

Jones advises companies that they have

Please turn to MINORITIES, Page C12

Gritty problem faces Vancouver

By LEONARD BACON
of The Oregonian staff

VANCOUVER, Wash. — Some Vancouver residents faced a gritty problem Tuesday, an abrasive fine grit covering automobiles left in the downtown Vancouver area Monday night.

The particulate was identified as silicon carbide and identical to that taken from a monitoring station adjacent to The Carborundum Co. plant in Vancouver by the Southwest Washington Air Pollution Authority.

Harold O'Connor, an official of The Carborundum Co., which manufactures silicone carbide for abrasives on such items as grinding wheels and sandpaper, said the company prohibits discussing air pollution with the press. He is to meet with air pollution authorities in Vancouver Wednesday, July 30.

O'Connor did question results of the tests, claiming involved laboratory procedures are required to identify silicon carbide from several similiar substances.

Samples of the particulate tested Tuesday by the Southwest Washington Air Pollution Authority were removed from an automobile parked at Vancouver City Hall between 8 and 9:30 p.m. Monday. The second sample was taken from a monitoring station at the Port of Vancouver, about 100 yards from the Carborundum plant. The two were compared under a high-powered microscope.

Ed Taylor, director of the air pollution authority, termed the question of pollution control at The Carborundum Co. "a very long story."

In 1970, the agency went to court and received a court order that the company comply with Washington's air pollution standards.

At that time, Taylor said estimates indicated the firm was discharging about 5,000 tons of particulate matter into the atmosphere each year. About 2,000 tons of the total were being emitted from furnaces at the plant, Taylor said.

The firm was partially successful in appealing the order to comply with air pollution standards, said Taylor.

During a hearing before the Washington State Pollution Control Board, the firm claimed technological know-how to control emissions from the furnaces did not exist. The firm did agree to implement control procedures on the remainder of the process, which involved handling materials outside the furnaces.

The board agreed to wait until these controls were in operation before taking up the question of the furnaces.

Taylor said a meeting of air pollution authorities in Vancouver Wednesday will review the process. He said all plans, procedures and equipment used by The Carborundum Co. to control particulate discharge during the handling phases of the operation have been approved by the air pollution agency.

Asked about furnace emissions, O'Connor said the firm has a "variance" from the state.

The estimated 2,000 tons of particulate matter being discharged annually bt The Carborundum Co. furnaces compares to about 40 tons annually from the larger, nearby Aluminum Company of America (Alcoa) smelter, Taylor said.

Agency records show Alcoa was discharging about 2,000 tons of particulates into the atmosphere in 1970. Taylor said controls installed by Alcoa since then have reduced emissions by 98 per cent.

Agency installs toll-free line

SALEM (AP) — Oregon residents with questions or complaints about insurance have a toll-free number to call in the office of the state insurance commissioner.

Commissioner Lester Rawls said the toll-free line will be open from 8 a.m. to noon and 1 p.m. to 5 p.m. every weekday.

The toll-free number is 1-800-452-9110.

Rawls urged Portland and Salem residents to continue using the local phones, 229-5722 in Portland and 378-4271 in Salem.

THE CARBORUNDUM COMPANY
VANCOUVER WASHINGTON

GENERAL FLOW DIAGRAM

SILICON CARBIDE FURNACE PLANT

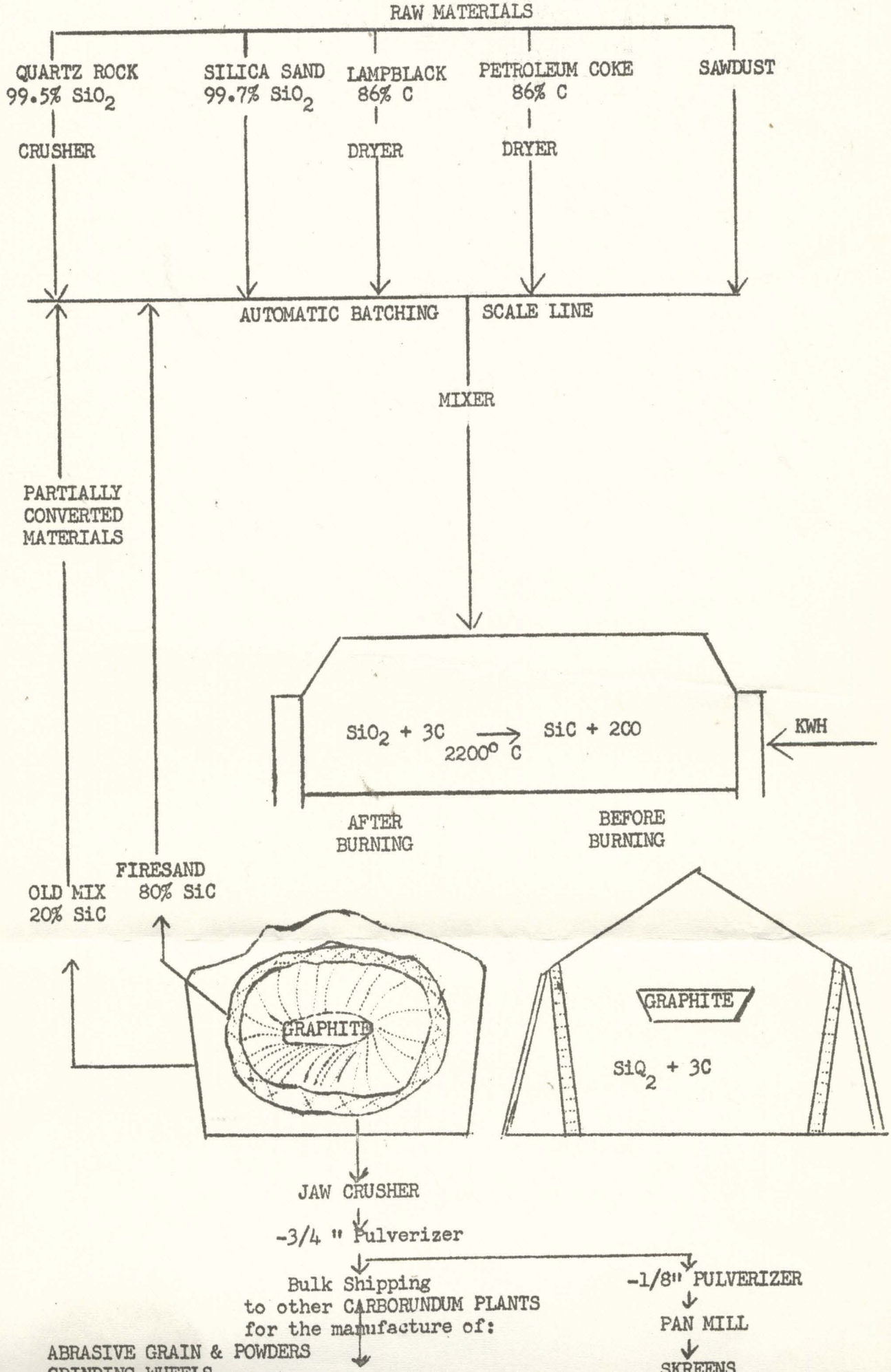

Silicon carbide

grades, prices and uses

Silicon carbide (SiC) is a substance not found in nature. It was first produced in 1891 by the American, Acheson, who produced crystals of silicon carbide by heating carbon and clay in an electric furnace. Commercial production today is achieved by heating a mixture of petroleum coke and silica sand in an electrical resistance furnace. A voltage is applied to a graphite core running through the centre of a trough-shaped furnace, and the heat generated causes the formation of silicon carbide crystals at about 2400°C. It was first produced for its abrasive properties and, along with another electric furnace product — fused aluminium oxide (synthetic corundum) — is the principal abrasive material in use today. The abrasive uses of silicon carbide were discussed in some detail in the IM Abrasives articles of June and July 1971, but the distinctive properties of the material have led to new applications in a number of other industries — particularly refractories and the ferrous metals industry. Some aspects of its refractory applications have been discussed in our current series of articles on the refractories industry. We shall attempt now to look at all the main fields of consumption and, within the European context, to give a guide to the various grades and prices of silicon carbide for each application.

In abrasives

Silicon carbide for abrasives is subject to very stringent specifications, particularly concerning size. For any fine-polishing or grinding operation, uniformity of the grain-size is of the utmost importance, since even one oversize particle may ruin the surface of a workpiece. It is therefore essential that a manufacturer of abrasive products — such as bonded abrasives (grinding wheels, etc.), coated abrasives (coated on to paper, cloth, or fibre), and fine-polishing and lapping compounds—shall know exactly what he is buying. To this end the producers of abrasive grains have grouped together to set up international standards and testing procedures. In Europe this comes under the auspices of the Abrasive Grains Committee of the Federation of European Producers of Abrasive Products (FEPA), whose standards are based so far as possible on the long-standing ASTM (American Society for the Testing of Materials) sieve sizes. FEPA works in collaboration with the abrasives associations of the member countries, namely Austria, Belgium, Denmark, France, West Germany, Italy, the Netherlands, Norway, Portugal, Spain, Sweden, Switzerland and the UK.

Macro-grits

The bulk of abrasive-grade production covers material ranging from 8-mesh to 220-mesh in size — the so-called macro-grits. Our quoted price for this material is now **£180-£210** per ton c.i.f. North European ports (see Prices Section), a substantially higher price than that quoted at the same time last year. There are a number of reasons for this. The UK has no production of its own, of course, since it lacks the principal ingredient of silicon carbide manufacture — cheap hydro-electric power. Hence all the country's requirements are imported, principally from Norway, Italy, West Germany, and Switzerland. At the beginning of 1972 a price range, expressed in sterling, of **£145-£173** per ton was fairly representative, but by the end of the year new contracts were being signed in the **£170-£200** per ton range. The principal cause for this increase was the floating of sterling, which by the year-end was about 12% below the old parity. In addition, silicon carbide producers' costs had risen during this period, owing to inflation throughout Europe, and increases by price leaders in Norway accounted for about a further 6%. Other European producers generally followed suit. The situation in the UK has been complicated even more, however, since the devaluation of the US dollar on February 12, which led to a further downward float of sterling against most European currencies. During February the pound fell by about 6% against the Norwegian krone and the Deutschmark. Since the new currency exchange rates are not necessarily stable ones, it is perhaps more useful to express the price in Norwegian kroner. The current price for macro-grits is **NKr. 2,700-3,150** per metric ton, c.i.f. North European port (for bulk shipments to the large manufacturers of bonded and coated abrasives).

Micro more expensive

Although macro-grits form the major part of abrasive silicon carbide production, the manufacturers also produce a range of micro-grits ranging from 230-mesh down to 1200-mesh. The micro are prepared in a somewhat different way from the macro. In both cases the raw silicon carbide must first be crushed, but whereas the macro-grits are classified by being passed through a series of vibrating screens (dry process), the micro-grits are generally sized by a wet-grading or sedimentation process based on the rate of settling of the particles in water. Since this second process is more costly, and since quantities are generally smaller, the micro-grits are more expensive than macro-grits; their price moreover increases with fineness. The macro-grits, on the other hand, are generally sold at one price regardless of size—the price differential we quote reflects the division of silicon carbide into the two main varieties, namely black and green (discussed below).

This prompts the question: if one price can be applied to macro-grits, why not to micro-grits also? In both cases one particular grade is produced along with various other sizes in a classification process. The answer is partly historical and partly one of scale. The macro-grits were for a long time the only type produced, and the single-price structure was accepted as the fairest and most convenient method of sale. As a relatively new class of abrasive, the micro-grits are

subjected to different patterns of demand, so that a multi-price structure has evolved. The question of scale is reflected in the case where a sudden surge in demand for one particular grade causes a temporary imbalance in the complementary production of other grades. The scale of macro-grit output is large enough to absorb such fluctuations in demand, whereas the scale of micro-grit output is not.

Black and green

The colour of silicon carbide depends on its purity. Very pure material (over 99.5% SiC) is light green in colour, but as the impurity content increases it becomes darker green. By the time the impurity content has reached about 1.0% (i.e. 99.0% SiC), the product is black, and with a still higher impurity content it takes on a greyish shade. The pure, green variety is the prime abrasive material and is employed where a sharper, more brittle abrasive is required—for instance, in grinding alloy steels and metal carbides. It is usually prepared entirely from virgin raw materials, whereas the black variety can economically re-use the unreacted charge from green SiC furnaces—or, of course, other black SiC furnaces. Green carbide therefore sells at £20-£30 p.t. above the abrasive-quality black material.

Silicon carbide refractories

Although silicon carbide was first produced for its abrasive properties, its refractory properties could not go unrecognised for long, and the refractory uses now rival the abrasive in importance. Among its most outstanding refractory characteristics are strength over a wide range, resistance to thermal shock and chemical attack, high thermal conductivity, and—being an abrasive material—high resistance to abrasion. These properties are employed in a wide range of refractories but particularly in kiln furniture and other special shapes. These are made by mixing granular silicon carbide with some form of bonding medium, which must hold the silicon carbide together during moulding at low temperatures and then form a hard, ceramic bond when the shape is fired (at 1,450-1,550° C). Still the most common bonding material is clay, but other forms of bond have been developed for products designed to operate under more severe conditions. These include silicon nitride, silicon oxynitride, and direct-bonded silicon carbide (essentially a pure SiC product).

Silicon carbide for use in refractories is not subject to quite the same degree of size and impurity tolerances as abrasive materials. It is difficult to give an exact specification for refractory grade carbide, since requirements vary according to the size and type of refractory product. In general, however, a much wider grain-size range is allowed—or, in some cases, is preferred because a range of particle sizes can give closer packing. In purity terms there are two main types, one in the 97-98% SiC range (black), and the other of 95-97% SiC (greyish). It is understood that recent sales of the higher quality type have been made at prices of **£120-£140** per ton c.i.f., and the greyish variety at a bit less. For some less demanding applications, lower purity material is sometimes adequate, and naturally the cost of such material is somewhat lower still.

Metallurgical uses

Silicon carbide is used in certain iron and steel processes as a deoxidant. Its most established use is in the cast-iron foundry, where it is added to the cupola charge in the form of briquettes. Once the metal has melted, the silicon carbide dissociates into silicon and

carbon—both powerful reducing agents whose effect is to prevent oxidation of the metal. Furthermore, as the oxidation of both silicon and carbon are strongly exothermic reactions, they serve to superheat the molten metal at the time of casting. This effect is especially important in casting thin sections, as it prevents premature solidification. Silicon carbide's main rival in this field is ferrosilicon—also a deoxidant, and a slightly cheaper material. The advantage of using silicon carbide is that, because of its superheating property, lower quality scrap can be used for thin-section castings. Normally very pure scrap must be used to ensure that premature solidification does not occur. Silicon carbide briquettes are widely used in Continental Europe and in the USA, but so far their use has been insignificant in the UK. This situation may soon change, however, and it is understood that one of the UK's major motor manufacturers is carrying out tests with French silicon carbide briquettes for use in casting thin-section cylinder heads. It should also be noted that silicon carbide has a third beneficial effect in cast irons—it assists in the crystallising of graphite in the iron. The small particles of atomic silicon and carbon act as 'seeds' for the nucleation of graphite and thereby give a fine and even distribution of graphite in the solidified metal.

Great interest has been shown in recent years in the use of silicon carbide in another area of the ferrous metals industry—namely, the adding of granular silicon carbide in LD steelmaking. Use is again made of the exothermic reaction when silicon and carbon oxidise in the melt (naturally its deoxidising effect is also useful but is of secondary importance to the heat-releasing effect in this case). Adding silicon carbide allows a much higher proportion of cold scrap to be used in the LD converter (claimed to be 45% instead of 30%). This is understood to be common practice in some steelworks, but often the quantities used vary with the amount of scrap available at any given time. SiC has certainly been used in this way in West Germany, the USA, and the UK.

Quality

As one would expect, the quality of silicon carbide for metallurgical consumption is subject to far less stringent demands than for either abrasives or refractories. The principal conditions are that the SiC shall not add undesirable impurities, such as alumina or sulphur, to the melt, and that it shall be uniform, so that the iron-founder or steel-maker may know the effective contribution of the addition he makes. Prices vary widely according to source, size of shipment, and purity, but **£70** per ton c.i.f. is probably a reasonable average.

UK imports of silicon carbide—Year 1972

Country	*Tonnage (metric)*	*Value (£)*	*Average cost per ton*
Norway	11,526	1,539,858	£134
Luxembourg	1,180	55,939	£47
Italy	960	143,657	£150
West Germany	801	135,830	£170
Switzerland	390	85,871	£220
Poland	232	28,485	£122
United States	207	41,837	£200
Belgium	140	16,337	£115
Netherlands	105	5,081	£48
France	89	12,802	£145
USSR	20	2,532	£126
Total	15,650	2,068,229	£132

Metallurgical-grade silicon carbide from Eastern Europe enters Western markets from time to time, including the UK via Luxembourg or the Netherlands. During 1972 some of this material has been priced at as little as **£40-£45** per ton (see table of UK silicon carbide imports). In another instance, this time in West Germany, used silicon carbide refractories have been crushed and remade into briquettes for metallurgical consumption. Naturally such products are of lower quality than briquettes prepared from virgin material, but they are cheaper and quite adequate for certain casting operations.

Miscellaneous uses

Other areas of consumption for silicon carbide include grain for wire-sawing stone, dust-extraction linings, non-slip surface in concrete, and filler pigments in paint. Although grain used in wire-sawing may be thought of as an abrasive, fairly coarse splits of material are used as opposed to individual FEPA grains. (The coarse grit is added to the cutting crack during the wire-sawing operation.) The other three fields mentioned above are quite interesting in that the abrasion-resistant properties of silicon carbide are employed. Grit added to the surface of concrete gives a hard, durable, non-slip surface. In this respect it competes with flint, emery, calcined bauxite, caustic-calcined magnesia, and a number of synthetic products. In dust extraction equipment, silicon carbide is used to give an abrasion-resistant lining. In paints it is a useful ingredient for surfaces subjected to severe abrasive and corrosive conditions. In France, paint containing silicon carbide has been used on the exterior of ships. In general, material for these miscellaneous uses is of fairly low grade and therefore of low price. So far as the SiC producers are concerned, it is an interesting sideline to the main production. Hence there are rarely any set prices, and any contract is entirely a matter of negotiation

EUROPEAN PRODUCERS OF SILICON CARBIDE

Company	*Plant location*	*Approximate capacity*	*Remarks*
France			
Péchiney-Ugine-Kuhlmann	Aiguebelle	18,000 tpa	Formerly operated by Sté. Ugine-Kuhlmann
Germany [West]			
Elektroschmelzwerk Kempten GmbH	Gretrath	28,000 tpa	Owned by Wacker-Chemie GmbH
Lonza-Werke GmbH	Waldshut	18,000 tpa	Owned by Lonza SA of Basle
Italy			
AMMI SpA	Scurelle	8,000 tpa	These operations were formerly operated by SET (Elettro Termochimica) and Montedison but were taken over by the state-owned AMMI during 1972
	S. Michelle	18,000 tpa	
Norway			
Arendal Smelteverk A/S	Arendal	35,000 tpa	Subsid. of Carborundum Co. of the USA
Norton A/S	Lillesand	12,000 tpa	Subsid. of Norton Co. of the USA
Orkla Exolon A/S & Co.	Orkanger	12,000 tpa	Owned by Orkla-Grube AB, Elkem-Spigerverk, and The Exolon Co. of the USA
Spain			
Navarro SA	Vadiflos	5,000 tpa	Technical licence from Carborundum Co.
Switzerland			
Lonza SA	Bodio	10,000 tpa	Headquarters at Basle

Principal East European producing countries are the USSR, Poland, and Czechoslovakia

Democrat-Herald/Stanford Smith

John Kelly flexes rubber-and-emery surface material.

Old tires could make floors in zoos, stables

By CARTER WOOD
Democrat-Herald Writer

JEFFERSON — John Kelly has been on the lookout for ground-up tires, hoping to use the old rubber in products he calls only "the elephant floor" and the "horse floor."

As president of Wear Technology Inc. in Jefferson, Kelly has been combining the old rubber, emery and epoxy to develop new surfaces fit for animals in zoos, stables and other buildings.

Such surfaces could eventually provide another way to use tires that might otherwise end up in landfills or be dumped off the side of some road, he says.

Tests of the new flooring are going on at Oregon State University's veterinary hospital and zoos in Portland and Seattle.

"We have developed an elastomeric-type floor material that answers OSU's needs," Kelly said, a materials science

Ground-up old tires are already used to manufacture such things as railroad crossings and matting, and Kelly says that his rubberized floors could consume even more recycled rubber.

Each square foot of the material contains about one pound of old tires.

"So on a floor of 30,000 square feet, that's 15 tons of rubber," he said.

Old tires are a headache for dealers to dispose of; they generally must pay someone to haul them away.

"There's a cost factor there," Kelly said. "But there's also aesthetically a value in using something that's a waste product."

With continued research, more possible applications present themselves. Boeing Industries in Seattle is interested in a non-skid floor that would stand up to acids, for example.

At an estimated $10 per square feet, the flooring would start to be profitable only on such big projects, Kelly said.

Kelly will soon be moving to Beaver-

type floor material that answers OSU's needs," Kelly said, a materials science expert who retired after 24 years with the Bureau of Mines.

"It had to be washable, cushioned, non-skid and have good bonding to concrete." He and his partners, Epoxy Resin Technology (ERT) of Beaverton, have been custom designing the surfaces depending on what kind of animals tread on them.

"It's been very interesting looking at the special problems of the animals," said Kelly. Rubber provides the insulation needed by animals from Africa's warm savannahs, and the emery — mined in the Cascades — offers abrasive qualities that can help trim the hooves of cows.

The surfaces must also stand up to the corrosive affects of animal urine.

only on such big projects, Kelly said.

Kelly will soon be moving to Beaverton to set up shop with ERT. The two have also been working on a variety of non-skid coatings for bridge and boat decks.

Entrepreneur rolls out jewel of an idea

By PAUL DUNWIDDIE
For The Associated Press

EUGENE — At first blush, the venture sounds like an elaborate smuggling operation. Bags of semiprecious stones are mixed into the treads of truck tires.

But this is no get-rich-quick scheme. The semiprecious stones are industrial-grade garnet sand. The garnet gives truck tires a sandpaper grip on wet, icy or snowy roads.

Jim Scheller has spent $50,000 and the last 12 years of his life trying to make Garnetread tires a reality. And now that the bugs have been worked out of the production process, the Portland man has teamed with Oregon Rubber Co. of Eugene in an effort to crack the retread truck tire business.

Nationwide, retreaded tires for big, 18-wheel highway rigs are a $15 million-a-year business, according to John Wagner, managing director of the American Retreaders Association.

G. David Lowe Sr., owner of Oregon Rubber Co. and Wyatt's Tire Co. of Eugene, hopes Garnetread can capture as much as $700,000 of the market.

Garnetreads add about $7 to the cost of a $70 truck tire retread, but they have a big advantage in traction.

Lt. LaVere Klewin, commander of the equipment and standards review section of the Washington State Patrol, says Garnetreads are considered approved traction devices by themselves in Washington. The distinction could help truckers avoid chaining up in slippery conditions.

Scheller is not the first to add material to tire rubber in the quest for better traction. Wagner says inventors in the past have tried walnut shells, wood chips, rocks and old rubber.

Frank Timmons, spokesman for the Rubber Manufactureers Association, adds cork and wire springs to the list. If Garnetreads work, Timmons says, they will certainly find a place in the market.

One believer is John Cook, professor emeritus and former reserach engineer at Washington State University.

About 10 years ago, Cook was working on a pavement that would stand up to studded tires. Scheller, who graduated from Washington State with an engineering degree, was driving a truck for his family business in Idaho and was looking for a way to improve traction in icy conditions.

The two men got together during the testing process for Cook's pavement idea: to add garnet to the asphalt.

Garnet is an extremely hard mineral usually used as an abrasive, especially for sandpaper. High-quality red garnets often are used as gems, and are the birthstone for the month of January.

Scheller figured that industrial-grade garnet could be added to tire rubber, eliminating the need for studs and thereby saving wear and tear on highways. He had a local tire company make some garnet tires, and Cook says they worked fine, improving traction and reducing wear on the road.

One important feature of the tire is its relatively constant traction, he says. As the tires wear down, new bits of garnet are exposed, maintaining traction.

Scheller bought a special piece of machinery for Oregon Rubber Co. to entice Lowe into making the Garnetreads. Lowe liked the idea, and the Garnetread tire is now on the market.

Evaluation of commercial US grinding balls by laboratory impact and abrasion tests

R. Blickensderfer and J. H. Tylczak

Abstract — *Impact and abrasion properties of various commercial US grinding balls were evaluated and compared by the Bureau of Mines, US Department of the Interior. Laboratory tests were conducted on balls obtained from eight major US manufacturers. The balls included forged steel, cast steel, and alloyed white cast iron and were subjected to repeated impacts until they broke or until 300,000 impacts were exceeded. Pin abrasion tests also were conducted. The results showed wide differences in impact lives, ranging from a few thousand to over 500,000 impacts. The life of inferior commercial balls was increased five to six times by a laboratory tempering heat treatment. For balls that did not break, the major impact wear mode was spalling and ranged from an average rate of 0.28 to 4.46 mg per impact. The softest balls (steel) had excellent impact resistance but low abrasion resistance. The abrasion resistance of the steel balls generally increased with hardness. The alloyed white cast irons had about twice the abrasion resistance of the steel balls. Users should become aware of the wide variations among commercial balls, and ball manufacturers should be aware that their product can be improved.*

Introduction

Wear and breakage of grinding media result in a major expense to the US minerals industry, therefore improving the cost-to-wear ratio associated with these materials is crucial. In 1973 alone, an industry survey documented consumption of over 214,000 tons of grinding media. (Nass, 1974). In an effort to assist the minerals industry in reducing the cost of grinding, the Bureau of Mines, US Department of the Interior, is conducting research directed at reducing the breakage and abrasion of commercial grinding balls.

Most commercial balls are made of steel with a carbon content of about 0.5 to 1.0 wt % and heat treated to maximize resistance to abrasion, fracture, and spalling. Fully hardened balls have a tendency to fracture and spall. The odd shaped "balls" found inside ball mills are a result of fracture and spalling which result in higher ball consumption.

An even more abrasion-resistant material is high-chromium white cast iron; however, it has major problems with breaking and spalling. Under milling conditions of low impact and high abrasion, the more expensive high-Cr white cast irons can be cost effective (Farge and Barclay, 1975). Our previous research (Blickensderfer, et al., 1983) showed that the impact resistance of high-chromium white cast iron is greatly affected by heat treatment.

Improvement of grinding media has been a slow process. Grinding balls can be evaluated by the user by keeping records of ball consumption and ore tonnage. But this procedure requires long testing times of months or years (Norman, 1948; El-Koussy, et al., 1981; Moroz and Lorenzetti, 1981; Howat, 1983; Malghan, 1982). In addition, if the operating parameters such as ore size, type, charge, etc., change, the evaluation may lead to the wrong conclusion as to which type of balls are best (Avery, 1961). Small-scale ball mill tests are convenient but could give misleading results because they do not produce the severe ball impacts of full-sized mills.

During ball milling, balls are subjected to three conditions: impact, abrasion, and corrosion. Much effort has been made to simulate these conditions in the laboratory. The impact of balls in mills is known to result in fracture and spalling, but spalling has been especially difficult to duplicate in the laboratory. Fracture of balls that occur in real ball mills does not correlate well with fracture toughness measurements. Dixon (1961) and Durman (1973) conducted ball-on-block drop tests that produced fracture of alloyed white cast iron balls. But it wasn't until the development of the ball-on-ball impact-spalling test by the Bureau of Mines (Blickensderfer and Tylczak, 1983) that spalling was produced by repeated impact under laboratory conditions. Furthermore, by producing impacts at a much faster rate than previously possible in laboratory tests, the impact evaluation of balls became feasible.

Abrasion accounts for the primary wear mode when balls do not fracture or spall. The pin abrasion test used in the present work is similar to those of Muscara and Sinnot (1972) and Mutton (1978). The pin abrasion test produces sufficiently high loading to crush the abrasive particles, thus simulating the grinding of ore between balls in a ball mill (Diesburg and Borik, 1975; Gundlach and Parks, 1978).

Corrosion can account for a third cause of ball degradation when grinding ore wet. In laboratory tests under very acidic conditions of pH 2, we found that corrosion and abrasion combined to aggravate wear (Tylczak, et al., 1986). Moore et al., (1984) found corrosion effects during wet milling of Cu-Ni gabbro sulfide ore and magnetic taconite ore in a very small laboratory mill. It is known that as mill diam is increased, the impact and abrasion conditions increase and consequently abrasion becomes much more significant than corrosion. Under the neutral or basic conditions existing during the bulk of milling, corrosion effects are negligible relative to abrasion. Therefore, laboratory corrosion tests were not conducted as part of the evaluation of commercial grinding balls.

An evaluation of commercial grinding balls was undertaken as part of the wear research program of the Bureau of Mines. The findings may be helpful to operators of grinding mills and to ball manufacturers.

Description of the balls

General

Numerous grinding balls were obtained from eight major

R. Blickensderfer and **J. H. Tylczak** are with Albany Research Center, US Bureau of Mines, Albany, OR. M&MP paper 88-653. Manuscript June 16, 1988. Discussionof this paper must be submitted, in duplicate, prior to Jul. 31, 1989.

effectively seal the pad off from solution flow. Continued spraying increases the area of sealed pad, leading to ponding problems. Recovery is lost due to poor percolation and the ponds themselves represent hazards to watering wildlife. Solution application rates in excess of 0.41 L/min/m2 (0.010 gpm per sq ft) have been possible with the emitters with little or no ponding. Lower flow rates are also possible with the emitter system. Flow rates as low as 0.02 L/min/m^2 (0.0005 gpm per sq ft) have been used on old pads to minimize dilution. The wide range of flow rates available with the drip emitters permits easy flow management when dealing with fresh pads and older pads.

One of the most significant benefits of the emitter system has been the virtual elimination of the labor-intensive chore of sprinkler maintenance. The leach area at Rochester required the use of over 1900 sprinklers. One employee was dedicated to sprinkler maintenance on the day shift while additional hours were spent by other operations personnel in repairing malfunctioning sprinklers. Daily observations of surface emitter lines has shown that carefully monitored scale control and clean operating solutions result in a well operating drip system. Evaporative scaling on sprinklers utilizing the same leach solution caused sprinkler impairment requiring constant attention. As mentioned earlier, evaporative scaling has not affected emitter operation.

The evaporation of leach solutions can be a major problem to operators in hot, arid climates. Many of these operations work under strict water consumption guidelines. The use of drip emitters rather than sprays cuts the evaporative loss of process solutions dramatically. The environmental problems associated with windblown spray are also overcome with the use of a drip emitter system.

Cyanide losses due to volatilization and ultraviolet light degradation inherent in a spray system should also be reduced with the use of emitters due to the fact that exposure of solution to the sun is minimal. The effect of drip irrigation on cyanide consumption is more inferred than measured because less than one year of operational data is available.

Disadvantages

The most significant drawback to the emitter system has been the inability to reuse the drip line after burial. While it is possible to eventually retrieve ice-covered sprinkler systems for reuse, it is not economically feasible to dig up the buried drip line. The operational benefits derived from using the buried emitter system such as reduced maintenance and the elimination of the ice field in the winter offset the tubing costs. The current plan at Rochester calls for using new tubing on the surface during the summer months and burying old tubing in the winter.

Two other concerns with the operation of the emitter system are scale buildup and blockage of the emitters with particles. It was mentioned earlier that scale formation with the emitters at Rochester occurred on the outside of the emitters and did not affect their operation. However, severe scale buildup could effectively seal the emitters, rendering them inoperable. Maintenance at this point would be impractical due to the large number of individual emitters involved, while sprinklers could be cleaned relatively easily in acid and restored to the pad. For this reason, scale treatment is of paramount concern at Rochester. Scale inhibitor is applied to the system in an amount approximately 25% greater than theoretically needed. The added cost is minimal and is thought of as insurance which benefits all aspects of the plant. Successive filtration associated with the Merrill-Crowe process and the use of floating suction pumps yields a relatively particle-free solution for irrigation. Operations utilizing bottom suction pumps or carbon absorption have experienced clogging problems in emitters. This problem has been corrected at several operations with the use of in-line screens.

The loss of solution contact with the ore immediately on the surface would be of concern to an operator not building successive heaps on top of old heaps. Observations at Rochester indicate that less than 3% of the total volume of ore is not leached with the emitters laid on the surface. The emitters can be moved on the heap to get full coverage with little effort. The amount of ore not leached by buried drip lines is greater than with surface lines and the operational benefits seen in the winter would have to outweigh the loss of leached ore. Solutions to this problem include stripping the cover layer of ore for use in building new pads or using waste or low grade ore for the cover layer.

Conclusions

The use of drip irrigation at the Rochester mine has been a significant improvement over conventional spray techniques. Profitability has been enhanced since silver and gold production have remained constant while operating costs have been lessened. Some of the operational benefits include: (1) reduction in maintenance of the irrigation system, (2) improved environmental controls, (3) reduction in solution evaporation and heat loss, (4) reduction in cyanide consumption, and (5) optimization of solution control on the heap.

Disadvantages include: (1) loss of buried drip tubing, (2) severe scale formation in the lines would be almost impossible to remedy where-as sprinklers can be cleaned, (3) clogging due to particles in solution can be expected if bottom suction pumps or carbon absorption are used, and (4) less than 100% solution contact is inherent with the emitter system.

Acknowledgments

The authors sincerely acknowledge the support and guidance of the staff and management of Coeur-Rochester, Inc. and Coeur d'Alene Mines Corp. in the preparation of this paper.

US manufacturers. All balls were nominally 75-mm diam. Steel grinding balls came from 6 manufacturers in 13 different lots, and alloyed white cast iron balls came from 3 manufacturers in 1 lot each. At least three balls selected at random from each lot were evaluated. The balls are described in Table 1 and the chemical composition is given in the appendix. The original hardness of the steel balls ranged from HB 234 to 822, with 77 % of them being harder than HB 650.

The shape and the surface condition of the balls differed considerably. Although some of the forged balls were nearly spherical, most had two opposing flat spots as a result of using a cylindrical forge blank that did not quite fill the dies. Many of the groups of balls were out of round, that is, the two halves were offset because of misalignment of the forging dies. Type

Table 1 — Hardness and Description of the Commercial 75-mm Balls

Ball Type	Prod.	Lot No.	Hardness HB*	Hardness HRC†	Type	
A_1	A	1	795	58.7	HiC–Cr steel	Minor forge scars
A_2	A	2	775	60.0	HiC–Cr steel	Forge scars
B_1	B	1	803	63.0	HiC–Cr steel	Flat ends, offset halves, minor forge scars
C_1	C	1	822	59.6	HiC–Cr steel	Cast cold flow, parting line
D_1	D	1	744	58.5	HiC–Cr steel	Forge scars
D_2	D	2	234	15.1	HiC–Cr steel	Forge scars
D_3	D	3	659	58.1	HiC–Cr steel	Forge roughness
E_1	E	1	354	37.3	HiC steel	Excessive scale
E_2	E	2	498	47.6	HiC steel	Excessive scale
F_1	F	1	789	57.9	HiC–Cr steel	Forge scars, flat ends
F_2	F	2	789	59.7	HiC–Cr–Mo steel	Forge scars, flat ends
G_1	G	1	804	58.2	HiC–Cr steel	Excessive scale
G_2	G	2	813	60.7	HiC–Cr steel	Excessive scale
H	H	1	529	-	White cast iron	Roughness, gates, parting line
J	J	9	655	-	White cast iron	Minor roughness
K	K	8	659	-	White cast iron	Minor roughness

* Brinell hardness, 3000 kg load on 3.2-mm tungsten carbide indentor on a flat spot ground on ball. Average of four readings on two balls.

† Rockwell C hardness on the abrasion test pin at a depth of 6 mm beneath surface of ball.

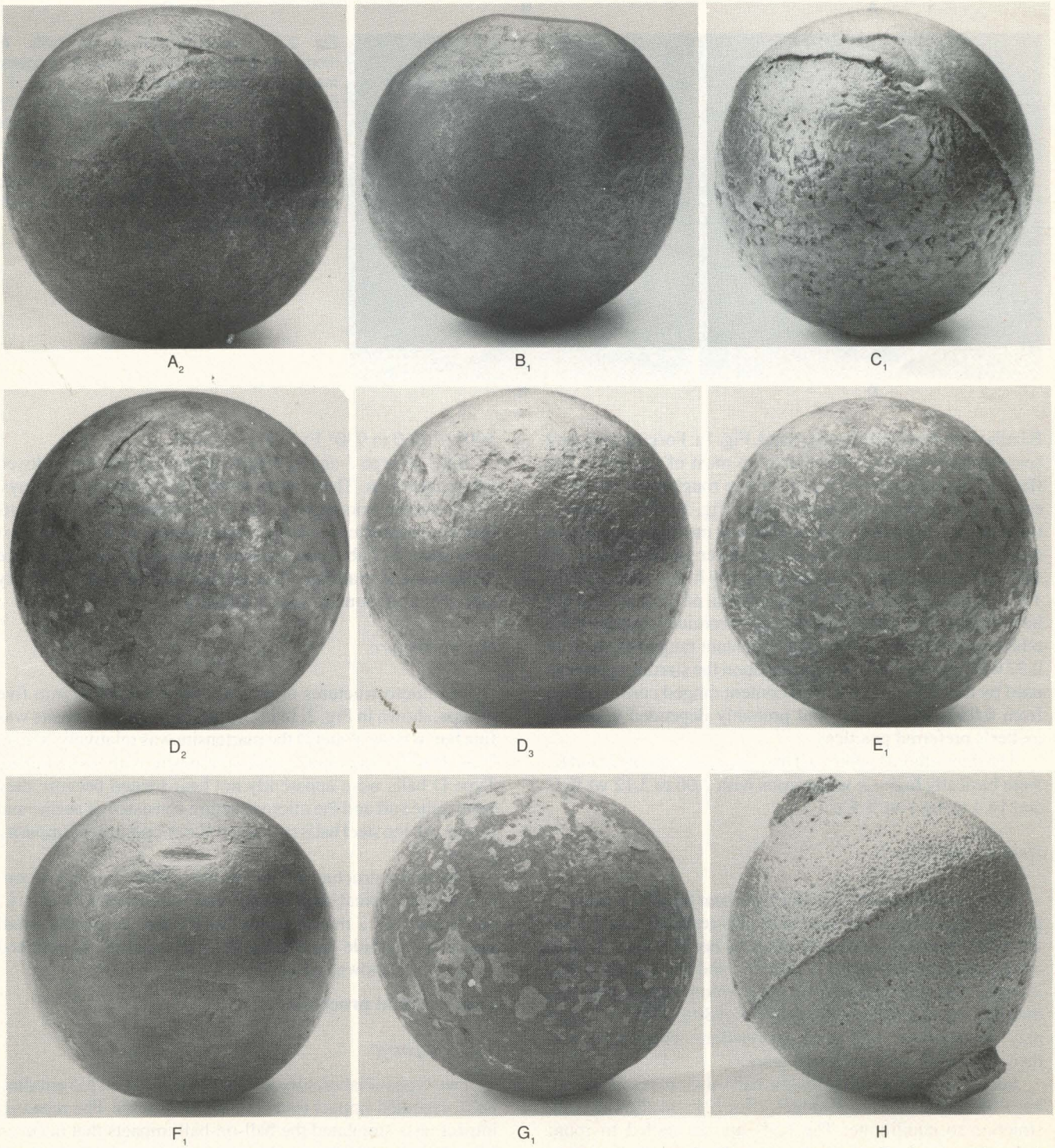

Fig. 1 — Typical commercial grinding balls, 75-mm diam. A_2. D_2, D_3, F_1, forge marks. B_1 flats. C_1, H, casting roughness, E_1, G_1, excessive scale.

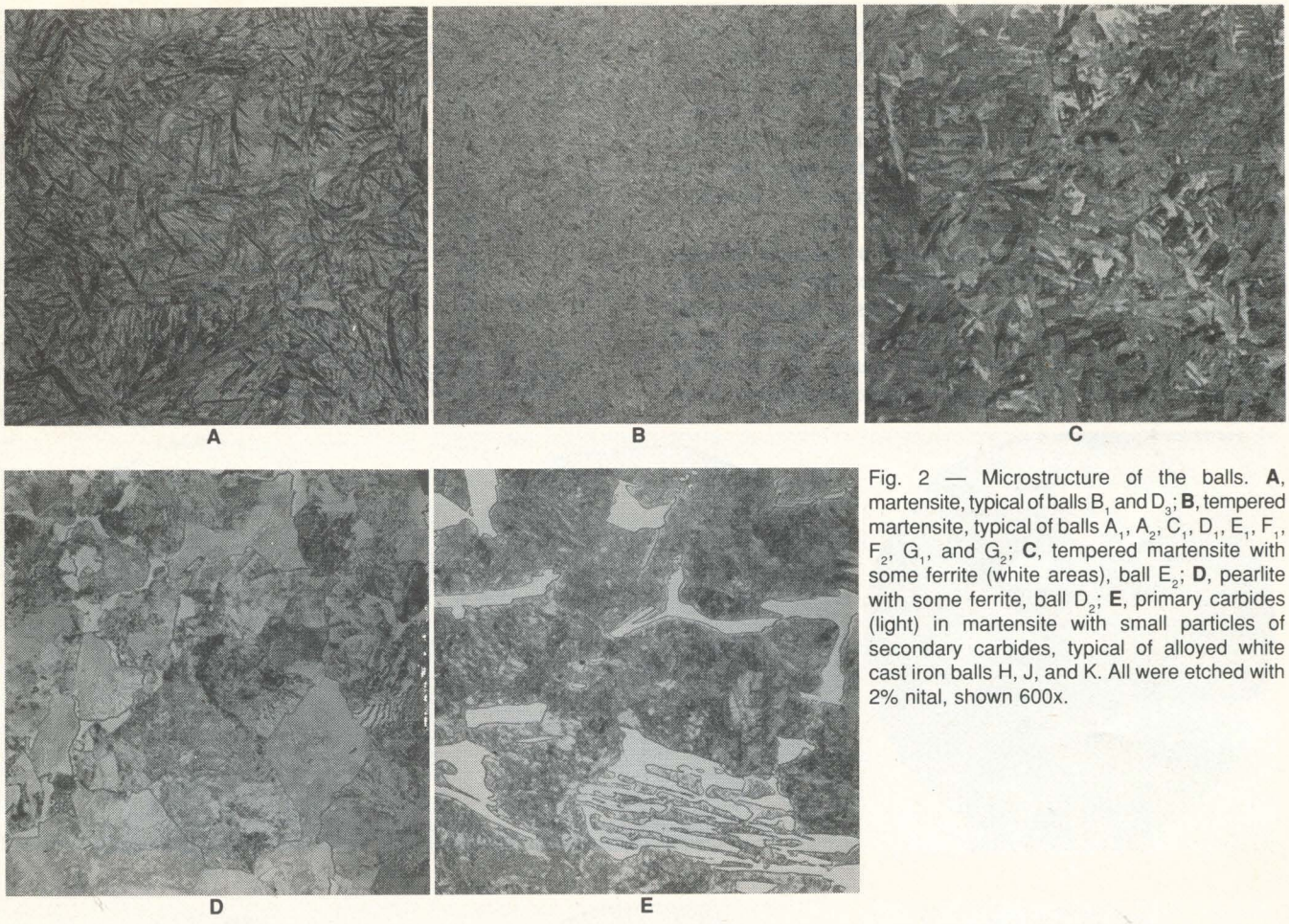

Fig. 2 — Microstructure of the balls. **A**, martensite, typical of balls B_1 and D_3; **B**, tempered martensite, typical of balls A_1, A_2, C_1, D_1, E_1, F_1, F_2, G_1, and G_2; **C**, tempered martensite with some ferrite (white areas), ball E_2; **D**, pearlite with some ferrite, ball D_2; **E**, primary carbides (light) in martensite with small particles of secondary carbides, typical of alloyed white cast iron balls H, J, and K. All were etched with 2% nital, shown 600x.

B balls were especially out of round, Fig. 1a. Forging tears and scars to some extent were visible on most of the balls. The flaws in the cast balls included surface roughness from sand casting and presence of a parting line, Fig. 1b. The compositions of the steel balls, which constitute the greatest tonnage of grinding media in the US, did not differ greatly among the different manufacturers and are basically high-carbon (0.5 to 1.0 wt %), low-alloy steels. It appears that only E balls did not have a chromium addition; the mean chromium content of the others was 0.54 wt %. The copper content ranged from nil to 0.37 wt %, presumably depending upon the starting materials used by the melter. The silicon content ranged considerably, from 0.08 to 0.76 wt %, and probably depended upon the melter's preferred practice.

The three alloyed white cast iron types of balls, H, J, and K, were basically high-Cr white irons with 2.06 to 3.12 wt % C and 14.4 to 18.4 wt % Cr.

Heat treatments

Most manufacturers consider their heat treatments as proprietary information. For steel balls, it is generally known that the balls normally are reaustenitized by heating them in air at temperatures around 800° C (1470° F), and are then quenched in water. The balls may be quenched to room temperature and then tempered, usually at 250 to 400° C (480 to 750° F), or they may be quenched only to an intermediate temperature and then air-cooled to room temperature.

For alloyed white cast irons, the balls also are reaustenized, but Table 1 times are much longer, 10 or 12 hr, to allow the cast structure to equilibrate. The balls are air-cooled to room temperature. Subsequently, they are reheated to about 350 to 500° C (660 to 930° F) and air-cooled.

Balls of type J and K represent special cases of alloyed white cast irons. These balls, made from commercial alloys, were selected from among 10 lots of different heat treatments that were evaluated by the Bureau of Mines to provide the best combination of abrasion resistance and toughness (resistance to fracture and spalling). Type H balls were made by a foundry whose heat treatment was proprietary.

Microstructure

The microstructures of the balls were classified into five groups, shown in Fig. 2. In most steel balls the martensite was fine but in types B and D the martensite was relatively coarse. Type E balls contained coarse martensite with some ferrite. Type D balls were apparently not heat-treated because they were quite soft and the microstructure consisted of perlite and ferrite. All the steel balls contained about 1 percent of impurity phases.

The microstructure of the alloyed white cast irons consisted of the typical blade shaped eutectic carbides, (Fe,Cr) C, surrounded by a matrix of martensite that contained small secondary carbide particles and small amounts of retained austenite, as shown in Fig. 2E.

Experimental procedure

Test equipment

Two types of laboratory wear tests were run on the grinding balls, repeated impact tests and abrasion tests. The repeated impact tests simulated the ball-on-ball impacts that occur in rotating ball mills that are known to cause balls to spall and

break. The abrasion test was chosen to simulate the abrasive wear that results from contact between ore and balls in ball mills. No corrosion tests were run because corrosion effects in large ball mills are normally small relative to abrasion.

Ball-on-ball repeated impact test

The ball-on-ball impact-spalling apparatus, Fig. 3, provided large numbers of impacts in a relatively short time. During operation, balls were dropped 3.5 m on to a line of 21 balls selected at random from the various lots and contained in a curved tube. The impact shockwave was propagated, with continuously decreasing energy, through the balls, with each successive ball receiving an impact on each side. The kinetic energy of the impacts ranged from 54 J for the first impact to about 5 J for the last impact, just sufficient to cause it to leave the end of the tube and enter a ramp leading to a conveyor. The conveyor carried the ball to the top of the machine, where it was dropped. This process continued until a ball broke, or spalled to the extent of about 100 to 150 g and therefore did not roll. The balls were removed and weighed after approximately 10,000 impacts per ball. Failed balls were replaced by new ones selected at random. Balls also were replaced after they had received more than 300,000 to 500,000 impacts.

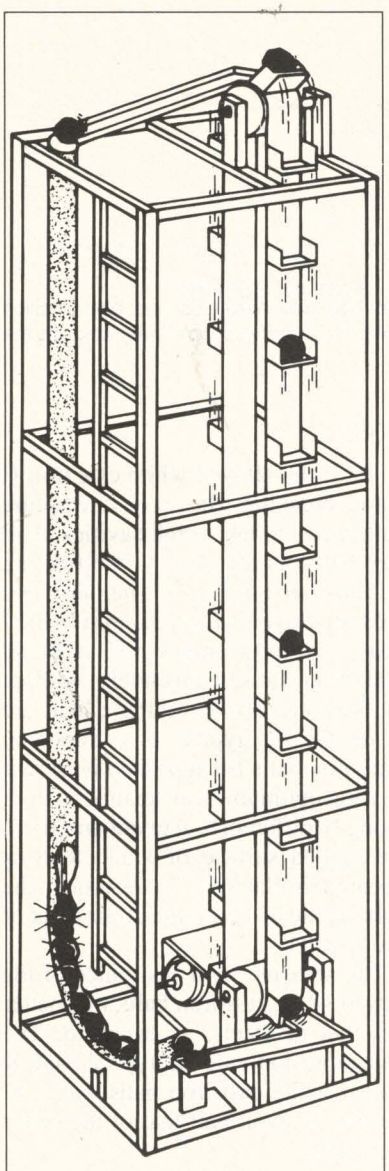

Fig. 3 — Ball-on-ball impact-spalling testing machine.

Pin-on-drum abrasive wear test

The pin-on-drum abrasive wear test machine is illustrated in Fig. 4, and is described more fully by Blickensderfer and Laird (1987). In this test, one end of a test pin moves over an abrasive cloth. The pin was loaded sufficiently to crush the abrasive particles in order to simulate the wear that takes place during the grinding of ore. Specimens were prepared by electrodischarge machining pins from unused balls and then finish grinding them in a lathe in order to minimize any surface damage or alteration of the material. The pins were 6.35 mm in diam by 2 to 3 cm in length. The end of the pin, 6 mm beneath the surface of the ball, was wear tested. Only fresh

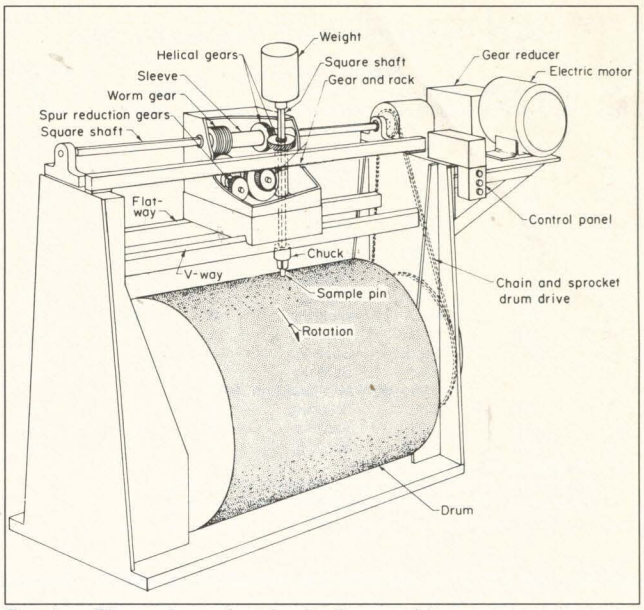

Fig. 4 — Pin-on-drum abrasion testing machine.

abrasive was encountered by the pin. The test parameters were: applied load of 66.7 N, drum surface speed of 2.7 m/min, pin rotation of 1.7 rpm, and abrasive cloth of 105 μm garnet. The wear value was corrected for variations in the abrasivity of the garnet cloth by testing a standard pin in a parallel wear track. After measuring the density of the test pin, wear values were reported in units of cubic millimeters per meter of path length.

Results

Steel balls - repeated impact tests

The steel balls subjected to repeated impacts, failed by four different modes, namely, breaking, spalling, flaking, and pitting. The results are summarized in Table 2. The breaking failures of types B_1, F_1, F_2, and G_2 are the most serious because most of the individual balls in Table 2 survived fewer than 30,000 impacts, and some fewer than 5,000 impacts. A typical fractured surface is shown in Fig. 5. One each of the D_1, D_3, and G_1 balls also broke. The impact life of the types of balls that failed prematurely by breaking was improved by giving them an additional tempering heat treatment at 200° C (400° F) in our laboratory. Type B_1 balls that originally averaged only 21,000 impacts before breaking were improved to 127,000 impacts; type G_2 balls improved from 42,000 impacts to failure originally to over 270,000 impacts without breaking.

Spalling is the second most serious mode of impact failure and resulted in average wear rates of 0.28 to 4.46 mg loss per impact. An example of severe spalling is shown in Fig. 5 for a ball of type C_1.

The other two types of wear, flaking and pitting, were quite low—less than 0.05 mg loss per impact. Flaking occurred only on the more ductile types of balls, D, E, and E, as a result of extreme cold work of the surface after more than 100,000 impacts, and is illustrated in Fig. 5. Flaking and pitting modes do not develop normally during grinding of ore in a ball mill because abrasive wear proceeds at a faster rate.

Steel balls -abrasion

The abrasive wear of the steel balls determined from the pin-on drum wear test ranged from 0.577 to 1.094 mm^3/m. However, the most abrasion resistant type of balls, B_1, had too short an impact life to be useful; and the least abrasion-resistant type of balls, D_2, with an atypical microstructure of

Table 2 — Impact and Abrasion Test Results of Balls

Ball type	Avg. No. of impacts, 1000s	Wear rate, mg/impact	Repeated impact test: Primary failure mode	Number: Tested	Number: Broken	Abrasion rate mm^3/m
			Steel Balls			
A_1	300	0.015	Pitting	6	0	0.761
A_2	300	0.278	Spalling	5	0	0.677
B_1	21[1]	N	Breaking	15	15	0.577
C_1	60	4.46	Spalling	3	0	0.687
D_1	300	0.031	Pitting	3	1	0.747
D_2	300	0.041	Flaking	3	0	1.094
D_3	300	0.470	Spalling	3	1	0.716
E_1	300	0.007	Flaking	3	0	0.897
E_2	300	0.025	Flaking	3	0	0.856
F_1	50	N	Breaking	8	8	0.735
F_2	26	N	Breaking	3	3	0.679
G_1	300	0.316	Spalling	3	1	0.742
G_2	42[2]	1.63	Spalling	3	3	0.646
			Alloyed White Cast Iron Balls			
H	18	N	Breaking	3	3	0.755
J	120	1.03	Spalling	3	0	0.399
K	300	0.292	Spalling	3	0	0.460

N — Negligable wear before breaking.
[1] Increased to 127,000 after tempering treatment in laboratory.
[2] Increased to 270,000 after tempering treatment in laboratory.

perlite, had too little abrasion resistance to be useful. Among the other steel balls with impact lives over 100,000, the abrasion rate ranged from only 0.677 to 0.897 mm^3/m.

The abrasive wear resistance (reciprocal of abrasion rate) generally increased with increasing Rockwell hardness of the pin, as seen in Fig. 6. The observed relationship between wear resistance and hardness was not linear as it is for most alloys (Krushchov and Babichev, 1956) but increased sharply above a hardness of HRC 60. The Brinell hardness taken just below the original surface of the balls did not correlate nearly as well with pin wear.

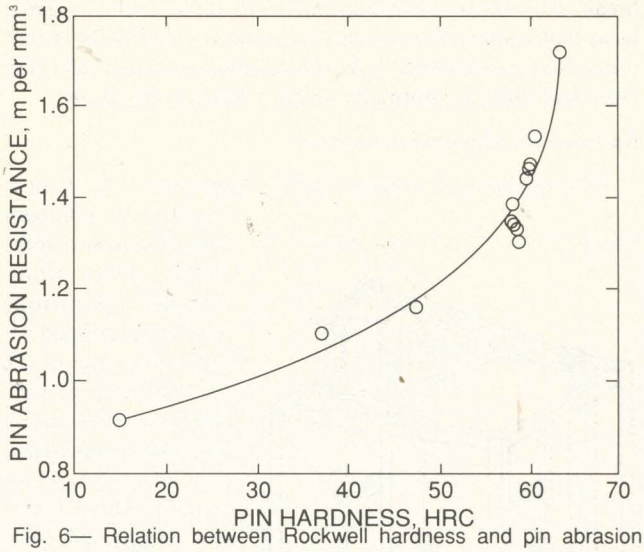

Fig. 6— Relation between Rockwell hardness and pin abrasion resistance. Pins from steel balls; hardness was measured on the pins.

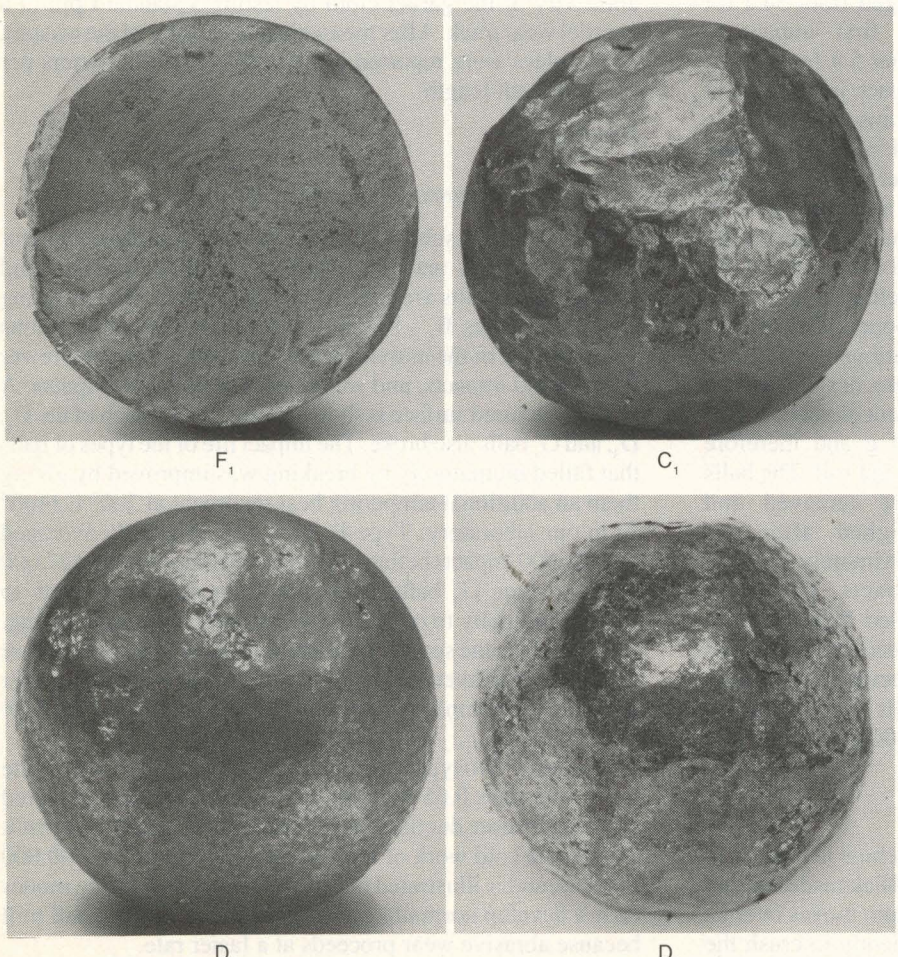

Fig. 5 — Steel balls after repeated impact testing. The F_1 ball broke after 10,800 impacts. The C_1 ball spalled excessively and D_3 slightly, shown after 60,000 and 270,000 impacts. The D_2 ball flaked and deformed, shown after 221,000 impacts, but survived over 500,000 impacts.

Alloyed white cast iron balls

The average impact life of the alloyed white cast iron H balls was only 18,000 before breaking. The premature failure is attributed to the shrink cavities in all three balls, as revealed by the fracture and illustrated in Fig. 7. The other two types of alloyed white cast iron balls, J and K, survived averages of 120,000 and 300,000 impacts, respectively, without any breaking. However, these balls are not necessarily typical of commercial white iron balls because they represent the near optimum heat treatment from among 10 different heat treatments tried. The spalled surface of J and K balls appeared similar, Fig. 7, even though the spalling rate of J was three times that of type K balls.

The abrasive wear resistance of the alloyed white cast iron balls was better than that of steels, as expected. The mean abrasion rate of type J and K alloyed white cast iron balls was 0.43 mm^3/m, or about half that of the better steel balls.

Discussion

Although the true wear test of a grinding ball is its life in a real ball mill, the laboratory tests of impact and abrasion may serve as a guide to expected ball life. The two most significant differences found among the commercial balls were the number of impacts to breakage and the impact-spalling rate. Differences in abrasive wear were less but could dictate the choice of ball when the impact properties are sufficient to not limit its life. The ball types that were prone to breaking in the laboratory test are probably suitable only for small diam mills in which impacts are relatively small. The bar graph of Fig. 8 clearly reveals differences among the types of steel balls. All of the A_2 type balls

Fig. 7 — Alloyed white cast iron balls after repeated impact testing. This H ball failed prematurely at 8,100 because of the large shrink cavity. J and K represent typical spalling of alloyed white cast irons; J, 125,000 impacts; K, 420,000 impacts.

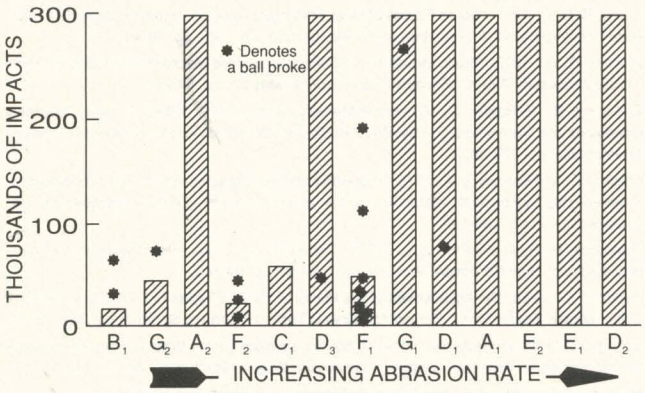

Fig. 8 — Mean impact lives of the steel balls. Type C_1 failed by spalling.

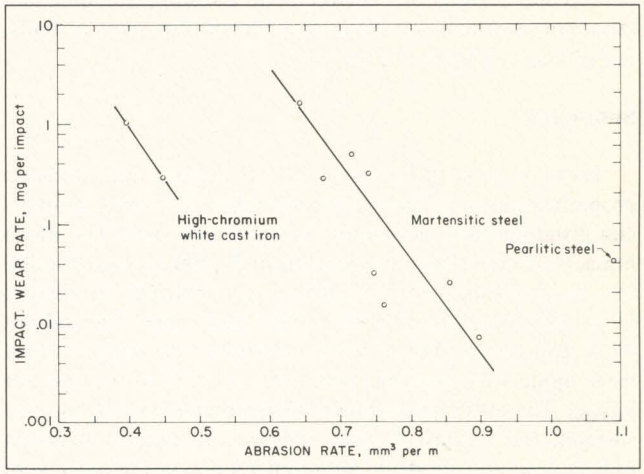

Fig. 9 — Relationship between impact wear rate and abrasion rate.

withstood 300,000 impacts and were among the lowest in wear; therefore, they would be a good choice. The F_1 type balls probably should be the last choice because many of them broke prematurely, and their abrasion resistance was only about average. However, the choice is confused by the fact that different lots from the same manufacturer, such as A_1 and A_2, also gave different results.

Among the balls that did not break prematurely, there was a relationship between impact wear rate (spalling, flaking, pitting) and abrasive wear rate. As seen in Fig. 9, a decrease in impact wear tended to result in an increase in abrasive wear and vice versa. Thus, the choice must be a compromise: balls should be selected with impact and abrasion properties that best match the conditions determined by the mill diam and type of ore.

A correlation was attempted between composition and impact properties as well as abrasive wear, but none was found. The carbon equivalent gave about the same general relationship with abrasive wear as did hardness, but neither of these is considered useful for users' specifications. Neither did the microstructure, as revealed at X600, determine the impact and abrasion properties, although it is clear that a martensitic structure is desired for abrasion resistance.

The overriding factor that determined impact properties is believed to be the heat treatment. The laboratory tempering treatment of type B_1 balls resulted in a sixfold improvement in their impact life. The manufacturer should have tempered the balls before selling them. It is doubtful that one specific heat treatment could be adequate for all of the different commercial balls, but rather, the heat treatment for each composition should be selected to provide the desired combination of impact and abrasion resistance.

The user must become aware that great differences exist among the balls supplied by various manufacturers. Furthermore, the user cannot rely on hardness, composition, or microstructure for specifying balls. It may be necessary for the user to specify a minimum impact life and spalling rate in a test such as the Bureau's ball-on-ball impact-spalling test and to specify abrasive wear standards based on a test known to simulate the given wear situation.

Manufacturers of grinding balls should improve their quality control in order to make balls having better and more consistent impact and abrasive wear properties. After ball properties are improved and made more consistent, it should be possible to classify ball types for the type of application, such as for the diam of the mill and the abrasiveness of the ore.

After the manufacturers make consistent ball products, ball consumption records kept by the user will become much more meaningful. Interaction between the manufacturer and user will help reduce ball consumption. Eventually, the best type of ball can be selected for a given mill, ore, and operating condition.

Recommendations

To reduce the consumption of grinding media, the following are recommended.

- Ball manufacturers should strive for greater consistency in their product. Adoption of standards would drive manufacturers in this direction.
- Preliminary standards should be developed for the impact, spalling, and abrasion resistance of grinding balls. The Bureau's ball-on-ball impact test and a pin abrasion test

Appendix A — Analyzed composition of the commercial 75-mm (2.95-in) balls

Ball	C	Mn	Cr	Si	Ni	Cu	Mo	P	S
					Steel Balls				
A1	0.95	0.82	0.46	0.30	0.13	0.24	-	0.011	-
A2	0.82	0.85	0.43	0.30	0.10	0.22	-	0.007	-
B1	1.00	0.82	0.62	0.20	0.27	0.37	-	0.021	-
C1	0.81	0.55	0.37	0.40	0.30	-	0.05	-	0.073
D1	0.63	0.90	0.66	0.76	<0.1	<0.1	-	0.018	-
D2	0.51	1.11	0.95	0.25	<0.08	0.17	-	0.029	0.028
D3	0.57	0.65	0.66	0.08	0.14	-	<0.01	-	-
E1	0.73	0.73	0.17	0.15	0.13	0.25	-	0.022	-
E2	0.67	0.82	<0.1	0.20	-	0.12	-	0.017	0.016
F1	0.80	0.86	0.59	0.19	0.11	0.24	-	0.33	-
F2	0.77	0.85	0.39	0.15	0.15	-	0.10	-	-
G1	0.77	0.87	0.42	0.23	0.15	0.33	-	0.018	-
G2	0.75	0.66	0.43	0.21	0.15	0.36	-	0.034	-
					Alloyed white cast iron balls				
H	2.59	0.46	14.4	0.57	0.28	-	0.12	-	-
J	3.12	0.65	17.1	0.32	0.41	-	1.10	0.04	0.10
K	2.06	0.54	18.4	0.29	0.38	0.08	0.00	-	0.49

can be used for specification of tests.

- Standards should be refined as grinding balls are improved and correlations between ball consumption data and laboratory test data are developed for various sizes of balls, mill diam, and types of ore.

Summary

There is a wide variation in the impact and abrasion properties among different lots and makes of 75-mm commercial grinding balls, according to laboratory tests. The mean impact lives to breakage ranged from 21,000 to over 300,000 for steel balls and from 18,000 to over 300,000 for alloyed white cast iron balls. For the harder steel types that did not break and for all alloyed white cast irons, the major impact wear mode was spalling, with rates of 0.28 to 4.5 mg per impact. The softer types of balls did not break or spall, but they suffered from abrasive wear. There is a tradeoff between impact wear and abrasion, although a few types of balls were relatively good in both regards.

Heat treatment has a dominant and critical effect on the impact life of grinding balls, whether they be steel or alloyed white cast iron balls.

The user needs new standards for specifying balls because hardness, composition, and microstructure are inadequate. Standards for resistance to repeated impacts and resistance to abrasion should be developed.

If ball quality were improved and if ball properties were adjusted to match the given application, grinding media consumption could undoubtedly be reduced.

References

Avery, H. S., 1961, "The Measurement of Wear Resistance," Wear, Vol. 4 , pp. 427-449.

Blickensderfer, R. and Laird, G., 1987, "A Pin-on-Drum Abrasive Wear Test and Comparison With Other Pin Wear Tests, Tribological Mechanisms and Wear Problems in Materials," ASM International, October, pp. 71-83.

Blickensderfer, R. and Tylczak, J. H., 1983, "A Large Scale Impact Spalling Test," Wear, Vol. 84, pp. 363-373.

Blickensderfer, R., Tylczak, J. H., and Dodd, J., 1983, "The Effect of Heat Treatment on Spalling of a Cr-Mo White Cast Iron," *Wear of Materials 1983*, ASME, pp. 471-47 6.

Diesburg D. F. and Borik, F., 1975, "Optimizing Abrasion Resistance," *Proceedings*, Symposium, Materials for the Mining Industry, Climax Molybdenum Co., Greenwich, CT, pp. 15-41.

Dixon, R. H. T., 1961, "Some Effects of Heat Treatment Upon the Impact Fatigue Life of Ni-Hard Grinding Balls," *Journal*, Iron and Steel Institute, Vol. 197, pp. 40-48.

Durman R. W., 1973, "Basic Metallurgical Concepts and the Mechanical Testing of Some Abrasion-resistant Alloys," *Foundry Trade Journal*, May 24, pp. 645-651.

El-Koussy R., El-Raghy, S. M., and El-Mehairy, A. E., 1981, "Effect of Heat Treatment Conditions and Composition on the Wear Resistance of Some Chromium Steels," *Tribology International*, pp. 323-28.

Farge, J. C. and Barclay, E. A., 1975, "Properties and Performance of Cast-Iron Grinding Ball," *Proceedings*, Symposium, Materials for the Mining Industry, Climax Molybdenum Co., Greenwich, CT, pp. 189-199.

Gundlach, R. B. and Parks, J. L., 1978, "Influence of Abrasive Hardness on the Wear Resistance of High Chromium Irons," *Wear*, Vol. 46, pp. 97-108.

Howat D. D., 1983, "An Assessment of the Merits of Various Types of Balls in the Milling of Ores," Mintek Report M117, Council for Mineral Tech., Randburg, South Africa, Nov., p. 20.

Krushchov, M. M. and Babichev, M. A., 1956, "Investigation of the Wear of Metals and Alloys by Rubbing on an Abrasive Surface," *Friction and Wear in Machinery*, Vol. 11, 12 pp.

Malghan, S. G., 1982, "Methods to Reduce Steel Wear in Grinding Mills," *Mining Engineering*, June pp. 684-90.

Moore, J. J., et al., 1984, "The Effect of Grinding Ball Composition and Mineral Slurry Environment on Grinding Media Wear," paper C352/84, *Tribology in Mineral Extraction War on Wear*, Institution of Mechanical Engineers Conference Publications, London, pp. 215-226.

Moroz, P. J. and Lorenzetti, J. J., 1981, "The Effects of Matrix Hardness and Microstructure on the Wear of Steel Grinding Ball During Wet Copper Ore Grinding," *Wear of Materials 1981*, ASME, pp. 280-289.

Muscara, J. and Sinnott, M. J., 1972, "Construction and Evaluation of a Versatile Abrasive Wear Testing Apparatus," *Met. Eng. Q.*, Vol. 12, No. 2, pp. 21-32.

Mutton, P. J., 1978, "High Stress Abrasion Testing of Wear Resistant Materials," Lab. Rep. MRL/PM3/78/001. Broken Hill Proprietary Co., Melbourne Res. Lab. (Australia), Aug., 49 pp.

Nass, D. E., 1974, "Steel Grinding Media Used in the United States and Canada," *Proceedings*, Symposium, Materials for the Mining Industry, Climax Molybdenum Co., Greenwich, CT, 1975, pp. 173-188.

Norman, T. E., 1948, "Wear Test of Grinding Balls," *Trans. AIME*, Vol. 176, pp. 490-526.

Tylczak, J. H., Singleton, D. J., and Blickensderfer, R., 1986, "Wear of 12 Alloys During Milling of Phosphate Rock in Phosphoric Acid Waste Water," *Minerals and Metallurgical Processing*, Aug, pp. 187-190.

Oregon lures another silicon industry player

☐ Fujimi Abrasives plans to make polishing compounds at a plant in Wilsonville

By JUDY ROOKS
of The Oregonian staff

Another supplier to the silicon wafer industry has been drawn to the Portland area, which boasts about half a dozen companies in that industry.

Fujimi Abrasives Co., Ltd. of Nagoya, Japan, a maker of polishing compounds, is converting a 18,000 square foot building in Wilsonville into a manufacturing plant.

Scheduled to open early next year, the plant will produce compounds for the semiconductor and computer industries.

Fujimi products are used by Siltec Corp. of Salem and SEH America of Vancouver, Wash., both Japanese-owned silicon wafer makers. SEH, with worldwide operations, is one of Fujimi's largest customers, said Shoji Azuma, president of the Oregon operation, Fujimi America Inc.

Employment at the Oregon plant is expected to begin with about 10 employees making one product, as a "trial" operation, Azuma said.

If it is successful, the company will move in a few years to a "large-scale" operation, making several products. An expanded operation likely would be located "in the vicinity," he added.

Company officials hope U.S. manufacturing someday might equal Japanese production, he said, but that depends on many market factors.

Fujima employs about 300 workers in Japan at three plants. Sales last year totaled nearly $80 million, Azuma said.

Fujimi is the world's largest manufacturer of fine precision abrasives, used for optical, semiconductor, computer and fine metal polishing.

The move to U.S. manufacturing was made because of increased U.S. sales volume and to ensure U.S. customers of a secure supply free from foreign exchange rate fluctuations.

Fujimi's move to Oregon is important not only for the jobs it provides, but also as another element in "an ever-increasing infrastructure of supply companies" for high-technology manufacturers, said Jim Thayer, assistant director for international trade for the Oregon Economic Development Department.

Company may use Linn emery deposits

By GUS AUGUST
Democrat-Herald Writer

A firm relocating in Oregon from California may one day be using emery mined in the mid-valley.

Emery is a natural rock produced by volcanic action when conditions are exactly right.

Its best uses are for making non-skid surfaces, such as on stairways aboard ship or on aircraft carrier decks. In addition to being non-skid, emery is long-wearing.

An Albany firm, the Oregon Emery Company, has a claim on a large deposit of "world class emery," according to one of its officials who does not want to be named at this time.

He said that the emery is of as good or better quality than that mined in Greece or Turkey, countries from which most emery is imported.

He added that it is found in four locations on four different mountains in the Cascade range from east of Sweet Home south to near Crater Lake.

Recently, a Huntington Beach, Calif. firm put down earnest money to buy four acres of land from the city of Toledo near the Oregon coast to build an emery board factory. Part of the land was donated to the city by Georgia-Pacific Corp. earlier this fall.

Sale price is $40,000 but a number of constraints must be met before the sale is final, according to Toledo officials.

The Realys Inc. plant is expected to gross up to $4 million a year and eventually will employ 50 people, according to Julian Raintree, president. He said the goal is to have the plant operating by spring, possibly by May.

Raintree said it will be a new, modern plant containing about 12,000 square feet. Machinery will be brought from California and in two years the California plant will be closed, Raintree said.

He said the California plant is 2½ years old "and is just starting to explode."

"We are contract manufacturers and are now putting out 160 different products," Raintree said.

Another plant official, Michael Falley, on the board of directors, said the company makes advertising and promotional items, in addition to latex cosmetic applicators, foams and sandpapers.

He added that they will start in Toledo with the emery board and latex applicators.

Raintree said the Toledo site was selected because of its proximity to water and rail lines for shipping and because of Oregon's natural resources, including the emery.

"Toledo has a number of good things going for it," Raintree said. "It has a port to handle barges which come up from the ocean and the community has shown that it is behind us."

Raintree said Toledo was once a thriving community and can be again.

He said Toledo has an enterprise zone, one of 10 designated by the State of Oregon as depressed areas because of high unemployment.

"We'll be able to use some of the money from the lottery to help the area reduce unemployment," Raintree said.

He added that the Oregon Economic Development Department will help cut red tape to get the plant to Oregon.

Peter Tryon, manager of business investments for the department, said no one has yet asked for financial assistance for the firm but that the department has been working with the company for some time, supplying background information, support, and sources of raw material.

"Toledo has been the most instrumental force in getting the plant to locate there," Tryon added.

Raintree said Newport, about six miles away, is one of the nicest towns on the West Coast and he will probably live there because he is "an ocean man."

Another consideration was the proximity of Oregon State University at Corvallis, which has the best research and development department around, according to Raintree.

Raintree said that the University of Oregon in Eugene will also help with research and development.

Department of Geology Oregon State University Corvallis, Oregon 97331 (503) 754-2484

Oct. 31, 1978

Jerry J. Gray
State of Oregon
Department of Geology and Mineral Industries
Albany, Oregon

Dear Jerry:

Enclosed find the report on the 17 thin sections you gave me. It took me some three hours , hence at the rate of $15/hour I quoted you the total bill amounts to $45.

I would like to request you to pay either by a check made out to "Oregon State University Foundation" or if it suits the office better pay to the Foundation account number: 30-262-7150
OSU Foundation Research.
You can send the check to me and I'll give it to the Foundation or you can send it to them noting it is for Petrographic Consultation from Enlows.

Damn interesting rocks, got any more?

Sincerely,

Harold E. Enlows

Harold E. Enlows

Department of Geology Oregon State University Corvallis, Oregon 97331 (503) 754-2484

REPORT

To: Jerry J. Gray
State of Oregon Department of Geology and Mineral Industries

From: Harold E. Enlows

Subject: Petrographic examination of 17 thin sections labeled JG-1 through 17.

The following minerals were examined for age dating purposes. Following directions, no modal analyses were made quantities of minerals are given in qualitative terms.

Mica. Biotite and or phlogopite are excellent for age dating since they are rich in potash (7 - 10%) and retain the radiogenic argon.

Hornblende. Suitable despite its low K content (0 - 2.5%).

Pyroxene. Possible if the pyroxene contains any K since it retains the radiogenic argon very well. A chemical examination would be necessary to check their suitability. Or one can merely chance it they are found with mica or other good age dating mineral.

Feldspar. Generally unsuitable, except for sanidine. Sanidine would not be expected in the type of rocks examined and it was not found.

JG-1. Largely plagioclase (An_{54}), magnetite and altered ortho and clinopyroxene. Appears unsuitable for an age date.

JG-2. A modest amount of biotite along with major plagioclase (An_{50}), ortho and clinopyroxene and magnetite. Should supply an age date if a ferromagnesian concentrate is prepared. It is suggested that the biotite is due to hydrothermal activity, therefore the age obtained would be that of the hydrothermal activity instead of the date of original emplacement of the rock.

JG-3. Both minor biotite and hornblende, major plagioclase, ortho and clinopyroxene, and magnetite. The best rock of the group for age dating. Hydrothermal source of biotite and hornblende suspected.

JG-4. Modest biotite, major plagioclase, ortho and clinopyroxene, and magnetite. Appears suitable for age dating. Suspect a hydrothermal source for biotite.

JG-5. Plagioclase, ortho and clinopyroxene, and magnetite. An age date would depend upon pyroxene, not hopeful.

JG-6. Plagioclase, ortho and clinopyroxene, magnetite, not hopeful.

JG-7. Clinopyroxene altering to smectite?, plagioclase, and magnetite. Does not look suitable.

JG-8. Plagioclase, clinopyroxene, glass, and magnetite. Not suitable.

JG-9. Plagioclase, orthopyroxene, and magnetite. Not suitable.

JG-10. Largely plagioclase and opaques. Not suitable.

JG-11. Plagioclase, magnetite and altered phenocrysts, perhaps once pyroxene. The former phenocrysts not a mass of granular magnetite and corundum?

JG-12. Plagioclase and pyroxene. Pyroxene severly altered to granular magnetite, corundum? and smectite. Not suitable for an age date.

JG-13. Plagioclase, olivine clinopyroxene, glass and magnetite. Not suitable.

JG-14. Plagioclase, ortho and clinopyroxene and magnetite. Not suitable.

JG-15. Plagioclase, magnetite and clinopyroxene which is altering to magnetite and coarse smectite?. Not suitable.

JG-16. Plagioclase, ortho and clinopyroxene, glass and magnetite. Not suitable.

JG-17. Plagioclase, magnetite, ortho and clinopyroxene now altering to magnetite and smectite?. Not suitable.

Harold E. Enlows

Harold E. Enlows

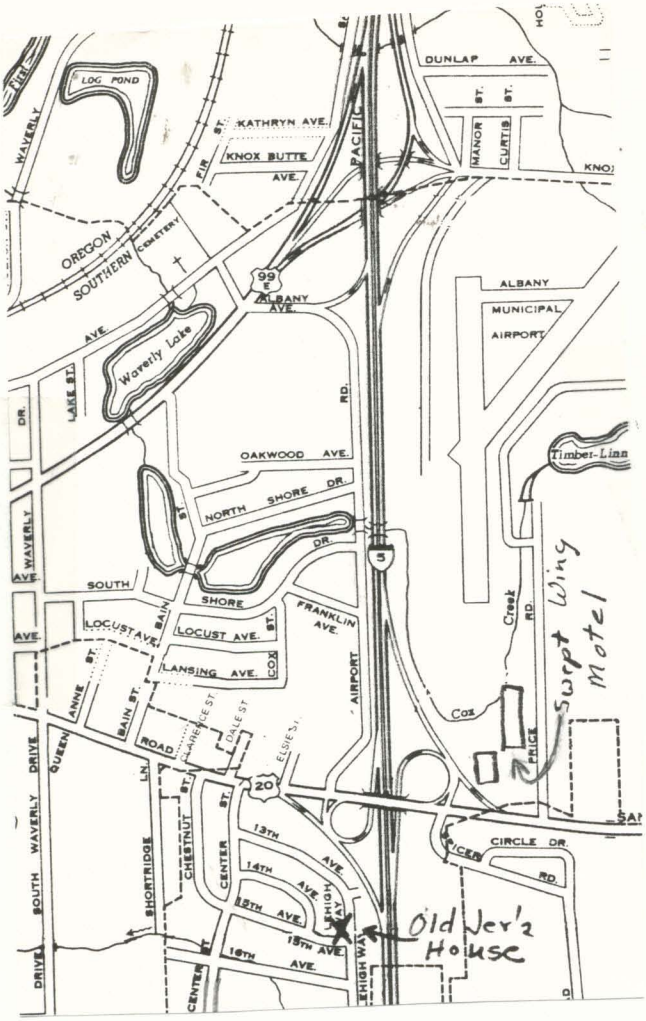
LOG POND
DUNLAP AVE.
KATHRYN AVE.
KNOX BUTTE AVE.
PACIFIC
MANOR
CURTIS
OREGON SOUTHERN
CEMETERY
99 E
ALBANY AVE.
ALBANY MUNICIPAL AIRPORT
Waverly Lake
LAKE ST.
OAKWOOD AVE.
NORTH SHORE DR.
SOUTH SHORE DR.
FRANKLIN AVE.
LOCUST AVE.
LANSING AVE.
COX
Timber-Linn
Swept Wing Motel
Cox Creek RD.
PRICE
CIRCLE DR.
PRICER
AIRPORT
WAVERLY DRIVE
QUEEN ANNE
MAIN ST.
CHESTNUT ST.
CENTER ST.
13TH AVE.
14TH AVE.
15TH AVE.
16TH AVE.
18TH AVE.
LEHIGH WAY
SHORTRIDGE
Old Jer's House

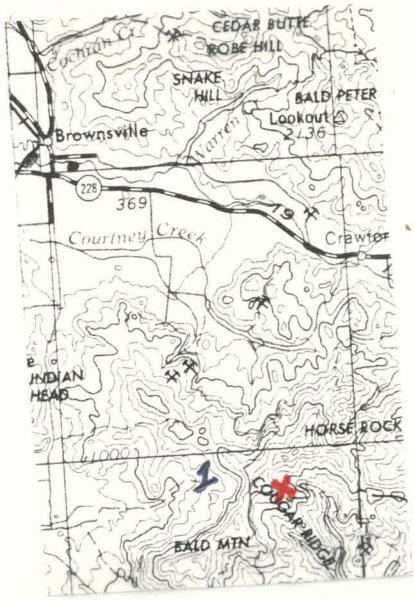
CEDAR BUTTE
ROBE HILL
SNAKE HILL
BALD PETER
Lookout
2,136
Brownsville
Courtney Creek
INDIAN HEAD
HORSE ROCK
BALD MTN
COUGAR RIDGE
1

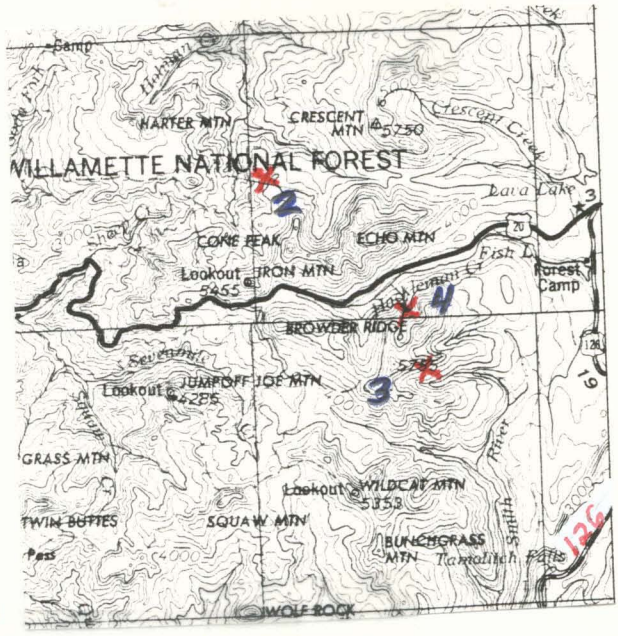
HARTER MTN
CRESCENT MTN
5750
Crescent Creek
MILLAMETTE NATIONAL FOREST
Lava Lake
COKE PEAK
ECHO MTN
Lookout
5455
IRON MTN
Forest Camp
BROWDER RIDGE
Lookout
4285
JUMPOFF JOE MTN
GRASS MTN
Lookout
5353
WILDCAT MTN
TWIN BUTTES
Pass
SQUAW MTN
BUNCHGRASS MTN
Tamolitch Falls
WOLF ROCK
2
3
4
5
6

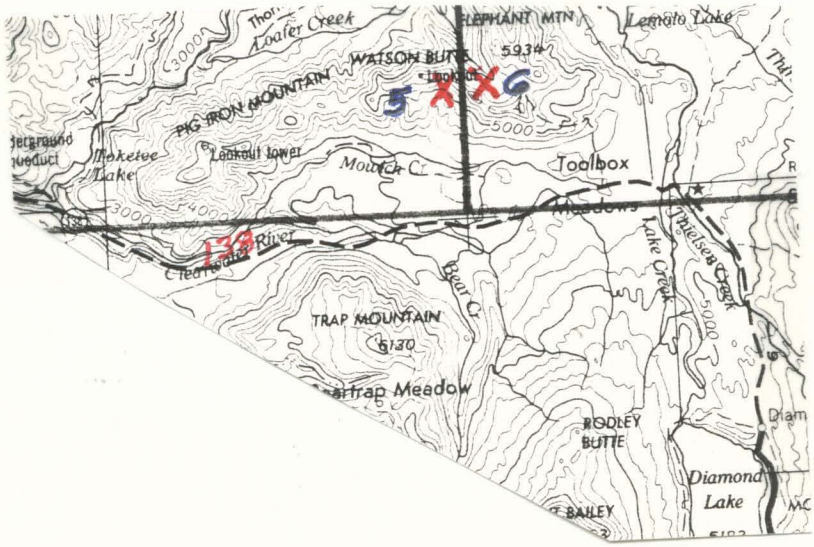
ELEPHANT MTN
5934
Lemolo Lake
WATSON BUTTE
Lookout
PIG IRON MOUNTAIN
Lookout Tower
Toketee Lake
Mouth Cr.
Toolbox Meadows
Thielsen Creek
Lake Creek
Clearwater River
Bear Cr.
TRAP MOUNTAIN
5130
Trap Meadow
RODLEY BUTTE
Diamond Lake
BAILEY
5
6

UNITED STATES
DEPARTMENT OF THE INTERIOR
BUREAU OF MINES

P. O. BOX 70
ALBANY, OREGON 97321

March 28, 1969

Mr. S. O. Agrell
Department of Geology and Geophysics
University of California
Berkeley, California 94720

Dear Mr. Agrell:

Re: Thin Sections of Contact Metamorphic Rocks

We examined your thin sections with considerable interest. It was refreshing to find some specimens that contain crystals large enough to identify optically.

I wish to thank you for the privilege of examining your thin sections. They are being returned under separate cover.

Sincerely yours,

Jack C. White
Geologist
Albany Metallurgy Research Center

cc: J. Gray

J. Gray

UNIVERSITY OF CALIFORNIA, BERKELEY

BERKELEY · DAVIS · IRVINE · LOS ANGELES · RIVERSIDE · SAN DIEGO · SAN FRANCISCO · SANTA BARBARA · SANTA CRUZ

UNIVERSITY OF CALIFORNIA 100 YEARS 1868 1968
A Tribute to the People of California

DEPARTMENT OF GEOLOGY AND GEOPHYSICS

BERKELEY, CALIFORNIA 94720

J. C. Gray
U S Dept. Interior
Bureau of Mines
P. O. Box 70.
Albany, oregon. 97321

Dear Mr Gray,

Thankyou for the samples of Emery-like rocks from W. C. Oregon, I've had sections made from them and find them most interesting, I'll send Mr White my comments early in April after I return from a field trip in S. California.

Meanwhile I'm sending him on loan a few thin sections of the Irish Rocks I described, that all I have here. When I return to Cambridge in the fall I will arrange for some samples to be sent to him.

yours sincerely

Stuart O. Agrell.

J.C. Gray
U.S. Dept. Interior
Bureau of Mines
P.O. Box 70
Albany, Oregon 97321

Dear Mr. Gray,

Thank you for the samples of emery-like rocks from W.C. Oregon. I've had sections made from them and find them most interesting. I'll send Mr. White my comments early in April after I return from a field trip in S. California.

Meanwhile I'm sending him on loan a few thin sections of the Irish rocks I described, that's all I have here. When I return to Cambridge in the fall I will arrange for some samples to be sent to him.

Yours sincerely,

Skaat O. Agrell

Agrell

February 26, 1969

Mr. S. O. Agrell
Department of Geology
University of California
Berkeley, California 94720

Dear Mr. Agrell:

We must apologize for being so late in answering your January 24 letter. We waited until some of the samples used in preparation of our report in the Ore Bin could be prepared and forwarded for your use.

Examination of these materials in thin sections is not of great value because of their extremely fine grain size. You may care to try oil immersion reflected light techniques on polished surfaces.

We thank you for your paper on similar rocks in N. E. Ireland and would like samples of them if possible. If you have technical questions of petrographic nature probably they should be directed to Jack White, Albany Metallurgy Research Center, P. O. Box 70, Albany, Oregon 97321.

If you are ever in the area we would like to discuss your study and ours. If we can be of further service please advise.

Sincerely yours,

Jerry J. Gray, Geologist
Albany Office of Mineral Resources

Enclosures

JJGray:js
CC:WAVogely
CWMerrill
MLWright
AOMR
DF
MF
JJG
JCWhite

Jerry Gray
1128

UNIVERSITY OF CALIFORNIA, BERKELEY

BERKELEY · DAVIS · IRVINE · LOS ANGELES · RIVERSIDE · SAN DIEGO · SAN FRANCISCO · SANTA BARBARA · SANTA CRUZ

UNIVERSITY OF CALIFORNIA 100 YEARS 1868 1968
A Tribute to the People of California

DEPARTMENT OF GEOLOGY AND GEOPHYSICS

BERKELEY, CALIFORNIA 94720

24th Jan. 1969

J. J. Gray.

Albany Office of Mineral Resources
Bureau of Mines
Albany, Oregon.

AOMR FEB 4 1969

NSP	Ret Chief
WNH	Editorial
PMc	Comment
FVC	File
GAK	Sec'y
JJG	Spec.
MAM	Cler.
CMH	Stat.

Dear Mr Gray,

I read with interest your paper in the November number of the 'Ore Bin' on 'Emery and Emery-like Rocks of the West Central Cascade Region'

Would it be possible to obtain cut-offs of some of your samples so that I could make thin sections of them for comparative study. I've worked on comparable rocks in N.E. Iceland and would like to see their similarities and differences and am at present working on some corundum-spinel etc rock in S. Utah some of which show affinities with metamorphosed laterites.

I enclose a Xerox copy of my [illegible] on the Irish Rocks which you can keep if you wish; and when I return in the fall to Cambridge I could send you some samples if you're interested.

Yours sincerely

Stuart O. Agrell

24th January, 1969

J.J. Gray
Albany Office of Mineral Resources
Bureau of Mines
Albany, Oregon

Dear Mr. Gray:

I read with interest your paper in the November number of the "Ore Bin" on "Emery and Emery-like Rocks of the West Central Cascade Region".

Would it be possible to obtain cut-offs of some of your samples so that I could make thin sections of them for comparative study. I've worked on comparable rocks in N.E. Ireland and would like to see their similarities and differences and am at present working on some corundum-spinel, etc., rock in S. Utah, some of which show affinities with metamorphosed laterites.

I enclose a Xerox copy of my paper on the Irish rocks which you can keep if you wish, and when I return in the fall to Cambridge, I could send you some samples if you are interested.

Yours sincerely,

Industrial Minerals

February 1990 No 269

- ABRASIVE MINERALS
  Taking the rough with the smooth
- NON-METALLIC MINERAL FLOTATION
  Reagent technology
- US GLASS INDUSTRY
  Overcapacity shadows strong demand
- IM CONGRESS, SYDNEY,
  between pp. 18 & 19

Abrasive minerals

Taking the rough with the smooth

by Bruce McMichael, *Assistant Editor*

Abrasive materials production, both natural and synthetic, is hostage to many and varied demands. Currently, these include new, tough environmental laws, declining natural resources, and changing fortunes in construction and automobile manufacture. The naturals — garnet, emery and diamonds — are performing well, particularly in the face of new legislation, while there is a new entrant to the synthetics club — Seeded Sol-Gel. This article outlines principal forces active in the market, technical developments, and highlights companies active in the field.

Abrasives — an overview

Credit for the discovery of man-made abrasives goes to Frank B. Norton founder of the now ubiquitous abrasives company Norton Co. of Worcester, Massachusetts, USA. Back in 1885 he manufactured the first vitrified man-made grinding wheel from emery grit and clay, firing it in his potter's kiln. Prior to this, emery was the only commercially available abrasive. The development of the fusing technology which resulted from the potter's kiln led to furnaces such as the Higgins, and Acheson furnace. Such furnaces required plentiful and cheap supplies of electricity and henee plants were constructed close to hydro-electric power sources, principally the Niagara Falls area in North America, but also in the Pyrennees Mountains, French Alps, southern Norway, and more recently in Venezuela and Brazil. The cost of energy can account for as much as 40% of the cost of final abrasive product.

The materials — ring out the old . . .

Well established abrasive materials are silicon carbide, the aluminium oxides, and diamond. The former two products have remained the two primary synthetic materials for much of this century. Synthetic industrial diamonds were first produced in 1955 and boosted the demand for diamond, both natural and synthetic industrial diamonds were first produced in 1955 and boosted the demand for diamond, both natural and synthetic, for inclusion in diamond tipped wheels. They are the only material hard enough and efficient enough to machine tungsten carbide and hard ceramics. Their applications are limited, however, to grinding or cutting non-ferrous materials, glass, plastic, and semi-conductor materials such as quartz and silicon. Necessity, as they say is the mother of invention. Thus, in 1959 cubic boron nitride (CBN) was introduced. Manufactured in a similar fashion to synthetic diamond, CBN proved to be as hard as synthetic diamond and is capable of grinding ferrous materials. The wear of CBN and aluminium oxide is significantly different. For example, in the grinding of a long slideway on a metalworking machine one pass of an aluminium oxide-based grinding wheel might result in a reduction of the diameter of the wheel by up to 0.005 inch (this produces an unacceptable taper), whereas wear on the CBN wheel could be as little as 0.0001 in. The former method would result in a grind wheel requiring regrinding whereas the latter CBN wheel could continue working.

The early 1970s saw the introduction, again by Norton, of the alumina-zirconia abrasives, which found immediate use in steel reconditioning and foundry fettling. They possess the advantages of self-sharpening grains and the ability to withstand long periods of high heat and pressure. New generations of advanced bonding resins were also contributory in its acceptance and now widespread usage.

Boron nitride is a development of the 1960s, rating 9.5 on Mohs' scale of hardness. Although not suitable for incorporation in grinding wheels it has found a place as a loose abrasive for lapping and polishing tungsten carbide, particularly wire drawing dies, and for the ultrasonic drilling of irregular shaped holes in hard ceramics such as used in the semi-conductor industry.

Natural abrasives are still available but have had market share taken away by the vast quantities of synthetic materials that are available as well as facing depleting stocks. Garnet is leading the way for the naturals in the light of environmental laws governing the emission of potentially harmful substances into the atmosphere, eg. free silica, and leachable heavy metals. Other abrasive minerals in the market place include olivine, tripoli, and staurolite.

. . . ring in the new

The most important technical breakthrough of recent times is that of the seeded gel (SG) range. Developed by Norton and announced in 1987, SG is a ceramic aluminium oxide. SG possesses a combination of properties from the more traditional materials. For example it has the toughness associated with regular brown fused alumina, while exceeding the sharpness of a friable white grain.

Markets

Technological improvements have reduced demand for abrasives. The foundry industry has lessened its demand for grinding wheels, due partly to lower output but also to the higher standards of finishing. This loss of demand from heavy industry has been partly offset by a growth in the precision end of the market. In the UK, this is seen for example, in the consumer boom for domestic DIY equipment such as sandpapers.

Blasting is an important market for abrasive materials, particularly brown aluminas, garnet, and olivine. Before health and environmental considerations surfaced concerning free silica, silica sand was the primary material used for blasting. However, its usage has been usurped by other materials which contains no free silica. Brown regular alumina is an efficient blasting agent utilising its strong, yet blocky shape to dig into and remove surface contamination, instead of merely denting and moving it from one place to another. In the blasting operation grains are fired at the surface using either compressed air or water, with suitable rust inhibitors. The latter method is known as wet or vapour blasting. Both wet and dry methods require high degrees of operator skill, manipulating grit size, nozzle size, blasting pressure, blasting angle, and distance between nozzle and work surface to achieve maximum benefit. Important markets for this process include cleaning of components such as turbine and impeller blades of gas turbine aero-engines, and etching glass.

Other markets for abrasives include lapping and polishing (often using diamond paste), through to non-slip surfaces such as flooring, boat decks, and airport runways. One unusual application is found in the mass catering industry. In this instance, potatoes are rapidly peeled by holding them against a rotating disc impregnated with an epoxy resin and brown fused alumina.

European abrasives associations

In common with all industries the abrasives sector has its federations and associations. Companies often belong to national associations whilst these national organisations belong to international groupings. The structure of the UK and European groups can be described as follows.

In the UK abrasives producers are affiliated to one of three associations. Manufacturers of loose grain or bonded material belong to the *Abrasive Industries Associations*. A second group belongs to the self-explanatory *Coating Abrasive Manufacturing Association*, and a third group involved in the manufacturing of industrial diamond abrasives belongs to the *Diamond Industry Producers Association*. These three associations in turn are affiliated to the European umbrella organisation located in Paris, *Federation of European Abrasive Producers (FEAP)*. Other national members of FEAP are France, West Germany, Spain, Italy, Austria, Ireland, Norway, Switzerland, Belgium, Luxembourg, the Netherlands, and Sweden.

Diamonds — hard sell

Industrial diamonds are not a girl's best friend, they are instead best friend to the stone cutter, roughneck oilwell driller, and pasta cutter — to mention a few of the material's more illustrious users. Varieties of industrial diamonds available include industrial stones (generally large stones but below gem quality) and small, irregular stones known as boart which are mostly used for drilling and grinding. Industrial diamonds are also available as grits or powders.

Australia — top producer

Australia is now the world's largest industrial diamond producer having usurped Zaire from that position in 1986. One operation is largely responsible for this change — *Argyle Diamond Mines Pty Ltd.* Ownership of the operation is split three ways. *CRA Ltd.* of Melbourne, Victoria has a majority holding of 56.8%, *Ashton Mining Ltd* has a 38.2% holding and the remaining 5% is held by *Western Australian Diamond Trust (WADT)*. The mine is located at Argyle, in the remote Kimberley Ranges of Western Australia. AK1, the principal kimberlite pipe, commenced operations in late 1985 on the basis of a proven ore reserve of 61m. tonnes and has a processing capacity of 25m. carats per annum. Argyle has also started alluvial mining following the discovery of a deposit in the lower reaches of the Smoke and Limestone Creeks that drain AK-1. This discovery has added an estimated 60m. carats to Argyle's resources. Current AK–1 pipe production is around 33m. carats per annum with treatment rates at about 4.9m. tpa recovering 6.7 carats per tonne. Expansion of the AK–1 processing plant is expected to be completed later this year. This will bring capacity up to 6m. tpa, holding diamond production levels steady in the face of an expected gradual decrease in grades.

Argyle's recent diamond production is as shown in the accompanying table. The break in time shown in the table results from a switch in reporting from calender years (1985, 1986, 1987) to fiscal years (1 July — 30 June). It is interesting to note that production of industrial diamonds is almost half the quantity of gem or near gem standard. This division can be quantified in the accompanying profile chart.

Diamond production at Argyle, *(m. carats)*

Year	*Industrial*	*Total*
1985	3.50	7.10
1986	16.10	29.20
1987	16.70	30.30
1987/88	16.44	19.72

Source: Australian BMR

Argyle diamonds are released to the market in the following way. *Argyle Diamond Sales (ADS)* markets 95% of total output, while the remaining 5% output belonging to WADT is sold through an independent rough dealer, *Arslanian*, in Antwerp, Belgium. In 1986, coinciding with the start of production from the main ore body, ADS entered into a five year contract with the *Central Selling Organisation (CSO)*. This agreement requires ADS to sell 75% of its near gem. 75% of its industrial diamond, and almost all of its gem-quality diamond to the CSO. The balance of near-gem and industrial diamonds are purchased through sales offices in Antwerp in association with *Horowitz Brothers*. The ADS/CSO sales agreement is up for renegotiation in 1991. This situation is unusual in that the CSO is not only ADS's major customer, it is also its major competitor.

Development of Argyle's Ellendale diamond resource, 400km south west of the main mine, is currently being re-examined following recent market studies and the increase in diamond prices early in 1989.

Argyle production profile *(%)*

			Impact on world supply	
Quality	*Volume*	*Value*	*Volume*	*Value*
Gem	5	50	8	3
Near-gem	45	45	25	10
Industrial	50	5	40	35
Total	100	100	30	5

Source: Australian Mining Review

Australia's second diamond mine is the Bow River alluvial operation. Production started in 1988 under the auspices of a joint venture between *Freeport-McMoRan Australia Inc.* and *Gem Exploration and Minerals Ltd.* Bow River is currently operated by Australian mining company *Poseidon Ltd* through its *Poseidon Exploration Ltd* subsidiary. This follows Poseidon's takeover of Freeport-McMoRan Australia in early 1989. Output from the mine was estimated to be about 10% industrial quality, 20% gem quality, and 70% near gem quality. Actual output in 1987/88 was put at 60,000 carats and 280,000 carats. Bow River is located 25km east-north-east of the Argyle mine.

Australia's domestic consumption of industrial diamonds is put at 3.5m. carats per annum, compared with a 1.8m. carat demand for gem and near gem diamonds. Production and import details of the Australian diamond industry can be seen in the accompanying table.

Australia's estimated diamond trade 1988/89 *(m. carats)*

	Total	*Gem/near gem*	*Industrial*
Production	36.30	16.30	20.00
Imports	1.70	0.15	1.50
Exports	32.60	14.60	18.00

Source: Australian BMR

There are at least 15 companies actively looking for diamonds in Australia. Further Australian activity in the sector can be seen by the companies active in overseas exploration. In Guinea, *Bridge Oil Ltd* through its involvement with Aredor Guinée SA is exploring, as is *Belgravia Resources. Afro-West Mining* is active in Sierra Leone, *Ashton, Acorn Securities*, and *Pelsort Resources* in Indonesia, and *City Resources* in China.

Other producing countries

In South Africa, *De Beers* has decided to proceed with investment to develop the Venetia diamond project. Venetia is located at Alldays, Northern Transvaal. The kimberlite pipe is similar in structure to De Beers' Premier diamond mine at Cullinan, near Pretoria. De Beers expects the capital outlay to be about R1,100m. Production is expected to commence in the latter half of this year, working up to capacity in 1993. At this stage the mine will recover some 4m. carats per annum, having treated 33m. tpa of ore. Mineral rights are owned by *Saturn Mining, Prospecting and Development* in which *Anglovaal* holds a 21.9% share and its 54% subsidiary, *Middle Witwatersrand* has a 65.5% holding. De Beers has a prospecting and mining agreement with Saturn which provides that after recoupment of the capital, plus an annual 12.5%, it will pay 50% on net mine earnings to the Anglovaal subsidiary.

Production data for individual mines in South Africa is classified. However, the country's total (industrial and gem quality) diamond output between 1984 and 1988 is shown below.

South African produces between 10 and 15% of the world's annual diamond output. Gem quality counts for around 11% of this output, the remaining quantity being near gem or industrial.

South African diamond output *(carats)*

Year	*Production*
1984	10,120,712
1985	10,205,936
1986	10,226,963
1987	9,050,855
1988	8,506,272

Source: South African Minerals Bureau

A growing interest has been expressed in the diamond-containing submarine gravels on the offshore coasts in the west. Exploration is proceeding at a number of locations. Botswana is the most significant producer of gem and quality diamond, offering 15m. carats per annum, valued at $1,000m. This compares with Australia's output of 35m. carats valued at $200m. In terms of value, South Africa follows Botswana, ahead of the USSR.

Joint-venture operation *De Beers Botswana Co. (Debswana)* (operated between De Beers and the government of Botswana) produced 15,229,359 carats in 1988. Other operations in Botswana include the Orapa, Letlhakane, and Jwaneng Mines.The Jwaneng Mine is currently building a recrushing plant to facilitate a planned output increase. The mine yielded a record 8,929,510 carats in 1988. Output in 1987 totalled 7,637,554 carats.

Diamond mining in the USSR mostly takes place in Yakutia. However, production is hampered by Arctic type weather conditions that prevail for much of the year. Diamond production was calculated to be 12m. carts in 1988.

Sierra Leone suffers from erratic production and smuggling. Output is estimated to be between 300,000 and 400,000 carats per year, although resources are rapidly being depleted. Interest has been shown in the reopening of *National Diamond Mining Co.'s* diamond-bearing kimberlite deposit at Kano. Production may restart later this year.

Zaire lost its crown in 1986 when Australia moved ahead in terms of industrial diamond production. The official figure (excluding smuggling) for total 1988 output was 18.2m. carats, valued at over $278m. *Société Minière de Bakwanga (Miba)*, the state-owned diamond mine, produced 8m. carats in 1988, valued at $72.3m.

Markets — a glittering prize

The USA is the largest consumer of industrial diamonds. The USBM estimates that apparent consumption in 1988 amounted to approximately 86m. carats. This is an increase of 19% when compared to 1987 figures. Between 1978 and 1988 average annual consumption was 55.7m. carats. Two distinct consumption trends have emerged. The years between 1979 and 1983 saw an average annual consumption of 37.5m. carats whereas the following four years' average consumption soared by 97% to 73.9m. carats. The boost to the industry was a direct result of the general resurgence of the economy and a switch to using industrial diamond in the major manufacturing sectors to take advantage of competitive prices.

The US Bureau of Census reports that in 1988 the average value of imported natural grit and powder was $0.82 per carat, synthetic grit and powder was $1.08, and industrial stones $9.31. Natural grit and powder has decreased in value since 1980, with the price in that year being 425% higher than 1988's. Natural grit and powder prices fell more than those of synthetic, making synthetic more valuable and natural more accessible to consumers.

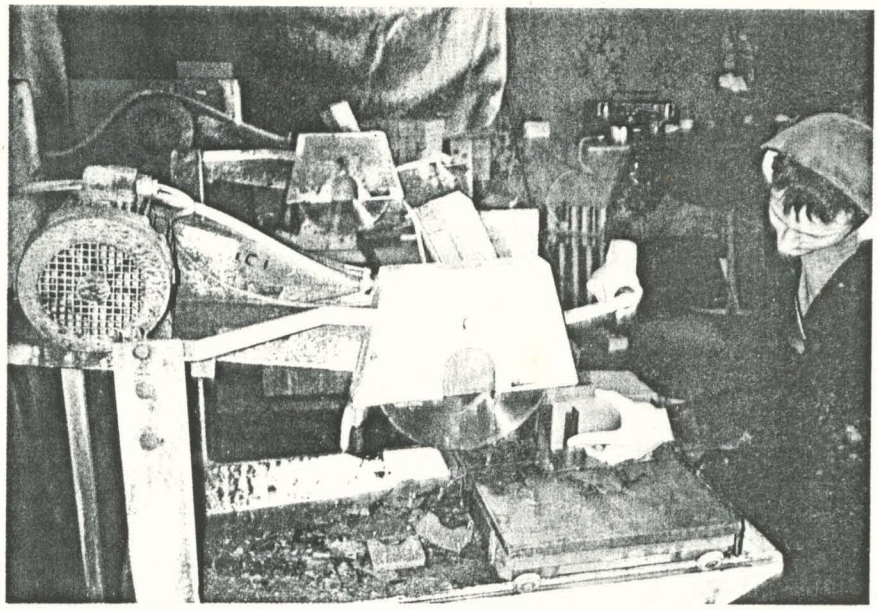

The construction industry is a major consumer of abrasives. This illustration shows an operator from Apex Brickcutters sawing a facing brick to specification with a 10 inch diameter diamond tipped blade. Running at 3,400rpm the blade can cut 20,000 bricks before replacement.

In Japan the high cost of natural diamonds has led to 95% of the market being taken by synthetics. Cutting saws and grinding wheels take the bulk of the material. In 1985 cutting saws accounted for 42.9% of industrial production, compared to 46.1% in 1987.

Japanese ID consumption *(%)*

Markets	*1985*	*1987*
Cutting saws	42.9	46.1
Grinding wheels	29.9	28.3
Trimmers	7.6	6.9
Dies	5.9	4.5
Drill bits*	4.1	4.1
Others	9.6	9.8

* Average value

Source: Materials Edge

The market for diamonds in Japan can be divided into nine groupings. At the end of 1987 the user breakdown was as follows — stone/road working (30%), construction (21%), electronics (12%), bearing machinery (12%), transport (8%), ceramics (7%), cable extrusion (4%), general machinery (4%), and watches (2%). The Japanese government has been involved in a massive public works and housing construction programme accounting for the overwhelming domination of those sectors as end consumers.

Estimates of diamond consumption in non-communist countries show a dramatic increase in the usage of both natural and synthetic diamonds since 1969, when consumption averaged 40m. carats per year. Since then production has trebled every ten years resulting in an estimated consumption in 1989 of 300m. carats, of which between 85% and 90% were synthetics. Two reasons account for this increasing usage — greater competitiveness between diamond producers leading to reduced units costs of tool materials and, secondly, the penetration of new market sectors.

Consumption

In terms of diamond type the fastest growth in consumption over the last ten years, expressed in carats, has been the 25% average increase in micron powders, used mainly for lapping and polishing. The electronics and semi-precious stone polishing industries have been important customers for this product. The other two main diamond types comprise the +60 US mesh product, used in sawing and drilling of natural stone and construction materials, and −60 US mesh size, used mostly for grinding of metals, ceramics, and tungsten carbide. These grades have shown average increases of 15% and 12% per year respectively, over the same period. Unit price erosion over the past decade has meant that market growth in monetary terms has been much lower than in caratage terms, since the larger sizes of diamond have a much higher unit price/carat. It is therefore, the increase in the +60 range of abrasives which has had the most significant effect upon the development of the diamond abrasives industry.

Industry estimates suggest that in 1989 some 120m. carats of +60 mesh diamond abrasives were consumed worldwide. Some

50% of these were used in the cutting of natural stone products, such as granite and marble, 40% in the construction industry for cutting of concrete and asphalt for roads and buildings, and 10% in other industries such as mining.

Garnet — a cutting edge

Garnet is very effective and efficient in several applications, particularly air blast abrasives, polishing, and water filtration. Industrial garnet of high quality is used as an abrasive powder and to manufacture coated abrasives. Lower quality garnet is used principally as hydro- or airblasting media, as well as a bedding material for water filtration equipment.

Consumption of garnet as a blasting medium has grown considerably, especially in line with the many and varied environmental laws that threaten some other abrasives. Garnet is a relatively low cost, silica free abrasive, which avoids the silicosis problem associated with silica sand blasting. Garnet is often compared with copper slag as a blasting media. Copper slag is often used as blasting media but has the inherent problem of leachable heavy metals. The US Navy uses copper and other metal slag airblasting techniques to clean its vessels. To avoid contamination in an open system, where the blasting media are not recycled and fall into the surrounding water, the Navy blends the original copper slag medium with other metal media in order to reduce the levels of contained leachable metals. However, twice as much garnet is required to achieve the same cleaning effect of slags. Garnet is also more expensive and transport costs are often higher. The rarity of garnet mines and the comparative abundance of slag sources make the relative transport costs from mine to end user unfavourable to the garnet supplier. Tonne for tonne garnet is more expensive than slags, but faster cleaning and lower consumption rates promote its competitiveness. Consequently its use as a recyclable abrasive has grown.

Hydro-jet cutting in the textile and plastics industries continue to be growing sectors for garnet. Other materials such as silicon carbide are often used as substitutes. Garnet is generally preferred because, although slightly more expensive it gives a cleaner cut and induces less wear on the spray nozzle.

Applications — cutting a dash

Several grades of garnet are available on the open market, with physical properties and sizing being of particular importance. High quality material is used for the lapping and grinding of glass, ceramics, and for coated and bonded products such as sandpaper, cloth, and abrasive wheels for grinding and finishing various metals, woods, rubber, and plastics. Lower quality material is used for cleaning and conditioning aluminium and other soft metals, particularly by aircraft and other transportation equipment manufacturers. Further applications for this grade include metal cleaning in structural steel fabrication.

Production — the top two

Production of abrasive grade garnet is dominated by Australia and the USA.

USA — and then there were three

There are three garnet producers in the USA. In the Pacific North West, *Emerald Creek Garnet Milling Co.* mines alluvial garnet deposits at Emerald Creek and Carpenter Creek, Benemah County, Idaho. Capacity is about 16,000 tpa mainly for sandblasting, non-skid applications, and water filtration. Emerald Creek Garnet's principal sales agents is *Myers Metals & Minerals* of Seattle. A further operation in New York state, in the town of Lewis, is that of the *NYCO Division of Processed Minerals Inc.*, which produces garnet as a by-product of wollastonite extraction. Current estimates of NYCO's reserves are between 1m. and 2m. tonnes. Capacity is rated at 500 short tpm with current extraction rates in the order of 200 short tpm. The company is set to expand operations this quarter and expects to increase output to near capacity. This plan will be carried out in the wake of constructing improved warehousing facilities and expanding markets. However, much of this increased output is destined for filtration markets, where Europe and south-central USA have increased demand. NYCO sells its garnet product through an agent, New Bern, North Carolina-based *International Garnet.*

Barton Mines Corp. of North Creek, New York operates a mine with capacity estimated to be about 20,000 tpa. Major markets served by the company are coated abrasives and colour television tube manufacture. *Canadian Pacific (US) Inc.*, is currently seeking a buyer for its wholly owned subsidiary, *Processed Minerals Inc.* of Syracuse, New York. Processed Minerals operates the NYCO wollastonite plant and *American Tripoli. Englehard Corp.* were involved in discussions with Canadian Pacific towards the end of last year, however the $110m. deal fell through in December for as yet undisclosed reasons. Canadian Pacific are seeking to divest itself of industrial mineral interests as they were no longer regarded as part of the core business. Thus Canadian Pacific is still seeking a buyer for its industrial mineral subsidiary.

One casualty of financial problems and land disputes is *Industrial Garnet Extractives Inc.* Operations ceased in April 1988 with a loss of 18,000 tpa to the market. The company sold primarily into the sandblasting and water filtration markets. Two mines were closed — in New York state and Rangeley in Maine. The latter plant was sold for salvage but there are no signs of a reopening of either operation. Taking up the slack in the market following Industrial Garnet's exit is *International Garnet Abrasives Inc.* which mines at Platsburgh, Clinton County.

Several preliminary investigations are being carried out in Canada on potentially garnet bearing deposits. One of the most promising sites is said to be at Crystal Peak, Vancouver.

Major US markets for garnet are abrasives and filtration media. Approximately 70–80% of output is sold into the domestic market (35% for filtration and 35–45% for abrasives), the remaining 20–30% is exported for filtration.

Production of crude garnet concentrates from 1978–1988 increased by about 11% in volume and 8% in value. For the same period, average annual production was 28,885 tonnes with a high of 42,498 tonnes in 1988 and a low of 19,265 tonnes in 1979. Consumption of garnet in the USA has been one of steady growth over the past decade with two exceptions. The years 1981 and 1984 saw 4% decreases in consumption. This downturn followed a general pattern observed throughout manufacturing industry. However the general trend has been an average growth of 8% compounded annually. New environment regulations have been responsible for this growth with garnet substituting for materials which contain leachable heavy metals and free silica.

Australia — major force

Australia is now a major producer and international supplier of garnet. *Garnet Millers Australia Pty Ltd,* a wholly-owned subsidiary of *Target Petroleum NL* mines and markets the mineral. The company has developed a garnet beach sand deposit near Port Gregory, Western Australia. A wet concentration plant is situated on the mine site, and damp garnet concentrate is trucked 100km south to either the port of Geraldton for shipment or its plant in Geraldton for further processing. Production for 1989 is estimated to be 20,000 tonnes. This compares with an output of 10,000 tonnes in 1986. The garnet is suitable for and hence sold heavily into, the following markets — powders and lapping compounds for polishing CRT glassware, single pass dry blasting media, and water filtration.

Prices have not altered over the past three years and remain at about $40 per tonne wet concentrate, FOB Geraldton, in bulk shipments and $1,000 per tonne for special products. Sales in Europe and North America are handled by London-and Toronto-based *Amalagamated Metals Corp.*, while Japan and other Asian markets are handled by *Sumitomo Corp.*

An unusual business arrangement was set up in Australia early in 1989 when US garnet producer Barton Mines and Australian operator Garnet Millers Australia Pty Ltd initiated a joint-venture company, *Garnet Millers Associates Pty Ltd.* In US markets, particularly on the east coast, Barton dominates the paper and coated abrasives market with a more round, smooth product derived from an alluvial deposit. On the west coast of the USA, however, the company has little market presence, especially for blasting products. The joint-venture agreement enables Barton to market Garnet Millers' blasting grade material and to cover eastern US markets. Meanwhile, Garnet Millers has access to Barton's paper abrasive grade products. However, the companies still compete for market share when supplying material to the polishing market.

Others — occasional entrants

India and China have extensive reserves which occasionally become available. However due to logistical difficulties and erratic quality this material has not made as much of an impact upon world markets as it might. Product from India is primarily derived from two beach sand mining operations located in the south-western area of Tamil Nadu state. Indian reserves have a reduced range and very few quantities of coarser grades. The major market for Indian product to date has been Japan. China is reported to have a large range of grades, with a predominance of the coarser grades.

World garnet capacity December 1988 *(tpa)*

Country	*Capacity*
USA	63,490
Australia	14,512
Norway	7,256
USSR	907
Turkey	635
China	18,140
India	27,210
Sri Lanka	91
Others	907
World total	133,140

Source: USBM Minerals Yearbook 1988

Values — stability rules

Prices of garnet in the USA have remained stable in the recent past. The average declared customs value per tonne in 1988 of crude garnet concentrates was $91. This compares with an average value for the period 1979–1988 off $76 per tonne. The average value was $64 per tonne in 1980 rising to a high of $93 in 1987 following a continued increase.

With the many grades of garnet supplied prices necessarily vary. Generally however, values are in the region of $240 and $472 per tonne. The average value per tonne of all grades sold in 1989 was $219, an increase of 23% over the 1987 average. An example of a price structure can be seen by looking at the five basic grades of garnet produced by NYCO (see accompanying table). Speciality grades are also produced.

NYCO garnet prices, January 1990 *(US$)*

Mesh size	*20,000–40,000 lbs*
8	200
12	200
16	200
25	190
36	195
50	200

Source: NYCO

Silicon carbide

The first recorded production of silicon carbide (SiC) was in the early 1890s, with first recorded production in 1901 at Niagara Falls, New York. It is synthesised by fusion in electric resistance furnaces, also known as Acheson furnaces, of silica and petroleum coke. Colouring varies from light green to black depending upon the quantity of trace elements present. Extensive use of the material for coated and bonded abrasives resulted from its extreme hardness combined with brittleness. Traditionally SiC has been utilised in metal and quartz finishing, sawing, and lapping.

The purest, green silicon carbide has a typical SiC content of over 99.5% and very low aluminium (<0.01%). More friable than black SiC, it breaks down on cutting to give fresh cutting edges. Black silicon carbide, containing 99% SiC, is more commonly used. Not only is it cheaper, it is also preferred in some applications because of its superior toughness. Lower purities of SiC find limited application in certain countries such as France, Italy, and Norway. Grading 98–99% SiC, this material is used for wire sawing of decorative industrial stones.

The bulk of consumption remains in the macrogrit size range, 8–220 mesh. However, microgrit production is being investigated, particularly in Europe. This market has expanded following increased demand for better finishes for certain metal parts. The price for finer grades is higher since production costs (for fine grinding) are higher than for macrogrit sizes, but competition is strong.

The last six years have seen significant changes in the silicon carbide industry, both in terms of declining market share and corporate changes. The industry has matured for several reasons. Primarily, as in the case of several other polishing and abrasive materials, a dramatic reduction in the finishing requirements of castings for heavy industries, such as in automobile manufacture, has been observed over the last ten years. Basically the foundry industry has increased efficiency and become better at making castings to near final shapes, thus reducing the amount of stock removal required in finishing. Another factor is the increasing substitution of plastics in many applications, again most notably in the automobile industry. For example, in the USA the weight of an average car fell by 573lbs over the ten year period to 1985. In that same period the use of plastic in cars increased from an average of 155lbs to 212.5lbs, whilst steel usage declined from 2,223lbs to 1,728lbs.

North America – an open and shut case

The silicon carbide industry, in common with other abrasive markets, in the early 1980s saw a decline in consumption resulting in the closure of several plants. *The Carborundum Co.* closed four plants at Vancouver, Jacksboro, Ammett, and Niagara Falls, and *Ferro Corp.* shut its one plant in Buffalo, New York.

Abrasive SiC production in North America
(tpa and $'000)

	Quantity	*Value*
1986	42,854	19,973
1987	49,521	23,128
1988	59,191	23,907

Source: USBM

However, output is now on the upswing. Starting with 43,241 tonnes in 1985 and averaging 6.5% growth per year through 1989, there is an expected growth of 8.9% in 1990 over 1989 as well as an increased demand into the 1990s of approximately 4.3% per annum. North America has seen a steady consolidation of operations over the past few years with major corporate restructuring, mergers, and capacity increases. The year 1986

saw industry pioneer, *The Carborundum Company*, sold to *Kennecott Copper Corp.* which itself was sold to *Sohio*. In November 1986 the company's SiC plant was operated under the auspices of its *Standard Oil Electro Minerals Division. Norton Co.*, now the world's largest producer of silicon carbide, then bought Sohio's US and Canadian operations including the 45,000 short tpa plant at Shawinigan. Quebec. During mid-1987 Norton purchased Norwegian producer *Arendal Smeltwerk A/S* from Standard Oil, adding a further 45,000 short tpa capacity to its potential stock.

In the face of declining markets, *Exolon-ESK Co.* is increasing capacity at its Hennepin, Illinois plant. Capacity will be raised by 30% taking it to 40–45,000 short tpa, an increase of 12,000 short tpa.

Europe — conquering pollution

Pollution problems affect most producers of silicon carbide. Removal of sulphur dioxide is a particularly difficult aspect of production. However, last December *Electroschmelzwerk Kempten GmbH (ESK)* of Munich, West Germany installed and commissioned a desulphurisation plant at its Delfzijl site in the Netherlands. The plant is operated by ESK's Dutch subsidiary *Electroschmelzwerk Delfzijl (ESD)*. Prior to installation of the new plant some 4,500 tpa of sulphur dioxide was emitted. The new unit will reduce emissions by 90%, and the local fertilser industry will buy 2,000 tpa of the resultant liquid sulphur. The new plant is in line with objectives laid down by the Dutch Government regarding the National Environmental Policy Plan. The production process for silicon carbon manufacture requires the material to be fused in a furnace for seven days at temperatures reaching 2,500°C. ESD operates its own power station to produce the necessary electrical power to feed the operation and it is here that the sulphur emissions are to be cut. The facility was designed, engineered, and constructed by *KTI BV* of Zoetermeer and consists of the following units — a gas scrubber, reactor for the removal of oxygen, hydroylsis reactor, Lo-cat reactor under licence from *ARI Technologies Inc.*, and a sulphur/separator section. Delfzijl has a capacity of 50,000 tpa SiC. Sorting of the grits is, however, undertaken at two sites in West Germany — Grefath, near Cologne (fabrication of microgrits) and Kempten (micro- and macro-grits).

North & South American SiC capacity 1990 *('000 tonnes)*

Operator	*Site location*	*Capacity*
North America		
Norton Co.	Shawinigan, Qu	38.1
	Cap de Madeleine, Qu	25.0
General/Sterling	Niagara Falls, Ont	20.1
Exolon-ESK	Hennepin, Il	40.8
	Thorold, Ont	10.9
South America		
Carbometal SAIC	Argentina	1.5
Fabri Casale	Argentina	3.6
Carborundum SA	Brazil	15.0
Casil SA	Brazil	18.0
Electrometalurgia de Veracruz	Mexico	20.1
Other		16.3
Total		**209.4**

Norwegian producer, Arendal Smeltwerk A/S was sold to Norton Co. three years ago. The company was previously a subsidiary of Standard Oil. Two plants are operated by Norton, at Arendal and Lillesand. Both plants are currently operating at full capacity with Arendal producing 45,000 tpa and Lillesand 24,000 tpa. Capacity increases were achieved following debottle necking and realisation, through pushing output to the limit, of

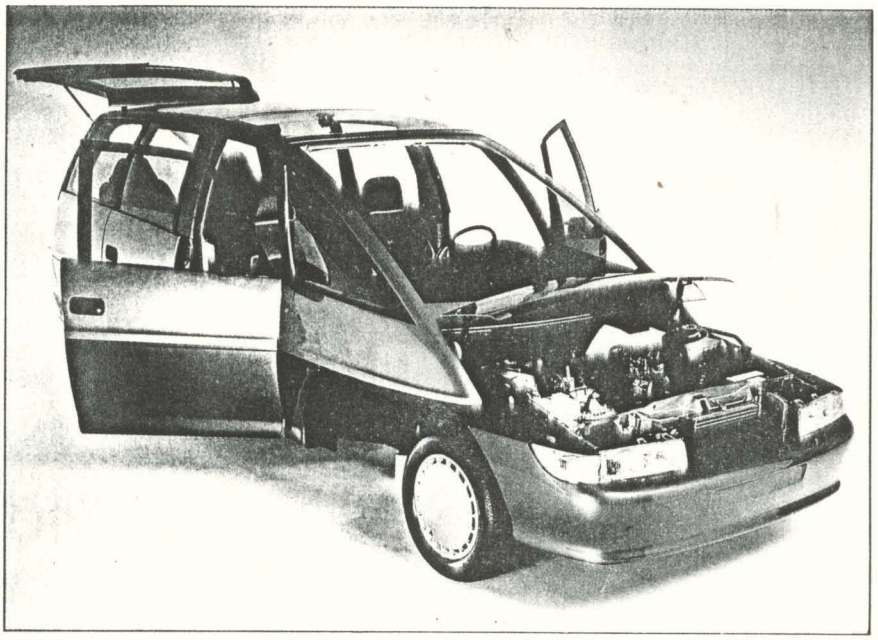

This prototype car, built by Du Pont at a cost of DM1m., highlights the many hundreds of plastic or polymer components that are available today. The introduction of such materials to the auto and aerospace industries has greatly reduced the demand for abrasive minerals.

Source: Du Pont

what output is actually possible. Although the group's output of abrasive grains is across the whole range, microgrits and green grade of SiC are the major products. Sales of abrasive grains rose 20% in 1989 over 1988 with strong markets being in the Far East, primarily Japan, Taiwan, and South Korea.

Silicon carbide capacity 1988 (tpa)

Country	*Capacity*
North America	126,527
Mexico	22,675
Brazil	12,698
West Germany	36,280
France	16,362
Italy	36,280
Netherlands	45,350
Norway	73,921
Spain	18,140
Total	226,297
Czechoslovakia, USSR	
Poland, Yugoslavia	158,725
China	145,120
India	13,605
Japan	86,165
Total	244,890
World total	791,891

Source: USBM

Sol-gel — new kid in town

Norton Co. released its Seeded Sol-Gel abrasives range onto the North America and European markets in 1988. Seeded gel (SG) abrasives are ceramic aluminium oxide abrasives developed in the USA and are intended to be the next generation of abrasives. Targeted end markets are in particularly demanding sectors, for example the aerospace industry and in situations where a particularly hard abrasive is required. They are expensive to manufacture with end products costing up to 2–3 times as much as conventional fused alumina abrasives. SG is particularly suited too hard or difficult to grind materials and, in the workshop, will compete with white or pink fused alumina products.

SG abrasive is not a fused material, but rather an aluminium oxide ceramic material. The starting material is alumina-gel, a by-product of the Ziegler process. Crystal seeding of the gels is undertaken through a process of heterogeneous nucleation (an advanced form of crystalisation). Extremely fine alpha-alumina seeds are dehydrated and sintered, thus forming a progression of alumina polymorphs in which the last transformation is the formation of alpha-alumina. In time this reaction leads to the growth of abrasive grains or seeds.

While the introduction of this new abrasive in vitrified bonded grinding wheels required the development of new bonds and manufacturing systems, conventional equipment and processes can be used for coated abrasive products. One grain of 60-grit abrasive grain, for example, will contain billions of these sub-micron particles, resulting in sub-micron sized cutting points on each grain.

Potential markets for SG abrasives

Market	*Application*	*Material*
Primary automotive	Disc grinding	Carbon steel
Metal fabrication	Weld grinding	Mild/carbon steels
Investment foundry	Dressing & deburring	Ni/stainless steels
Ferrous & non-ferrous foundries & forges	Dressing & deburring	Cast iron/steel/alloys
Aerospace	Dimensioning/grinding	Ni alloys & steels
Hand tools	Grinding	Forged tool steels
Garden tools	Offhand dressing	Carbon steels
Friction materials	Brake linings & pads	

Source: Norton Co.

The more traditional abrasives such as fused alumina are disadvantaged in similar markets due to the fracturing that occurs when the grain is put under pressure. Alumina oxide grains blunt after use causing friction and resultant metallurgical damage. SG is utilised on belts and fibre discs. Norton's range of R984 belts uses a 'Y' heavyweight, woven, polyester cloth backing which is single flexed and butt jointed with a Sheldahl patch giving optimum performance when applied in medium to heavy pressure applications. Norton's range of SG fibre disc — F944 — uses a 0.75mm thick fibre backing and is used with hard to medium back-up pads in situations where moderate to high pressures are applied. These products use grit sizes of 24 to 120 mesh. As yet

SG is only available from Norton on its in-house manufactured products. Crude material will not be available to abrasive wheel manufacturers for the foreseeable future.

Alumina-zirconia

Alumina-zirconia (AZ) was first introduced to the abrasives market in the early 1970s. It was developed by *Norton Co.* in the USA and is now produced at the company's Huntsville, Alabama, USA and Niagara, Ontario, Canada plants.

Manufacture of these abrasives is achieved by fusion of baddeleyite or zircon sand with alumina. An unconventional cooling effect is employed to give the grain a dendritic microcrystaline intergrowth, which confers a distinctive sharpening property to the material. This enhanced cleaving or self-sharpening property is of major importance to the success of the product. Other abrasives blunt during use, through prolonged exposure to heat and pressure. However alumina-zirconia products break at cleavage planes when transmitted heat from the surface reaches a critical level. The work needed to cleave AZ is directly proportional to the amount of contained zirconia.

AZ and NZ — different percentages

Two types of alumina-zirconia abrasives are manufactured by this process, and are branded by the quantity of contained zirconia in the blend. The AZ group contains 25% zirconia, compared to the 40% zirconia in the NZ group. A further division of the AZ group is made — ZS or ZF, depending on end use. ZS abrasives are employed mainly for steel conditioning. During initial treatment the grains are dry panned thus achieving a rounded edge and higher packing density. A major use of AZ is in foundries where, because they can withstand higher speed and pressure of working, they are used to smooth down steel billets. The ZF group, still containing 25% zirconia, is utilised in foundry wheel applications.

The NZ, or 40% zirconia containing material, is used in small diameter wheels, for instance in cutting-off marble and stone slabs, and expansion grooves in motorways. The NZ group can itself be further divided into two groups — E347 and E349. E347 alumina-zirconia is utilised as bonded abrasives, whilst E349 is put to use in coated abrasives. The essential difference is in the crushing technique used to produce a blocky shape for E349 and a more elongated particle shape for E347.

Norton can expect some competition from other producers in the near future with respect to producing crude alumina-zirconia abrasives. Patents for the production of this material are soon to expire or have already done so. In the UK for example, the patent for the NZ abrasive expired this month, to be followed by the expiry of the ZF and ZS patents in June 1992. Patents in the USA expire in June 1992 (ZF and SZ) and August 1992 (NZ). In Canada patents expired in 1988, whilst in Italy and Spain they cease in 1994.

Prices

Popular grades of ZF abrasives are currently fetching average prices (del. UK for one tonne lots) of around $2.89 per kg. For commonly used grain sizes of the ZS family of abrasives an average price is $3.42 per kg. Bonded abrasives of 40% zirconia variety are priced at $3.60 per kg, compared with coated abrasives which fetch an average of $5.70 per kg. *Norton Materials UK* are responsible for marketing the products to industry in the UK.

Emery — losing to synthetics

Emery is a natural mixture of corundum and magnetite or haematite, containing magnesium-aluminium silicates and titania impurities. Top quality material comes from Turkey, but even this material is highly variable in consistency. Synthetic materials have eclipsed emery in many applications but the latter still finds a favour in metal polishing and non-abrasive applications, as an abrasive aggregate for non-skid, wear resistant floors, pavements, and stair treads, as tumbling or deburring media, and in the manufacture of coated abrasives. Emery's fortunes are thus increasingly dependent upon the vagaries the construction industry, in particular public works spending where much of the non-skid flooring is applied. Much US emery has been used as a concret strengthener, notably in concrete toppings of 0.5–1 in. thickness.

Production — group of three

World output of emery is largely limited to the USA, Turkey, and Greece.

USA — gone west

Recent developments in the US emery industry have left just one producer, *Oregon Emery Co.* Other companies that have ceased production were located in the state of New York. Small scale selective mining was conducted by *De Luca Emery Mine* and *John Leardi Emery Mine.* Each operation sold its products to a single customer. De Luca sold material to *Washington Mill Abrasive Co.* of North Grafton, Massachusetts whilst John Leardi sold material to *Emeri-Crete Inc.* of New Castle, New Hampshire. John Leardi shut down operations in 1988, when the mine site was acquired by a housing corporation. Closure of east coast mining operations was somewhat hastened even though reserve exhaustion was approaching. Mine sites were close to residential areas and consequent tightening of environmental controls covering drilling and blasting speeded the shutdowns. The De Luca mine ceased operating several years ago.

Extensive market research and evaluation conducted by Oregon Emery has indicated that the business climate is now suitable for a major new producer in the market. The company, located in Albany, mid-western Oregon owns four emery deposits, first identified in the late sixties. Reserves of emery are extensive, with one deposit reported to contain over 5m. short tons of marketable material. Oregon emery is dark grey in colour, possessing an aluminium oxide content up to 65% and a resulting Mohs hardness of 8–9. The material contains corundum and magnetite, together with hercynite, cordierite, silimanite, mullite, magnesia, and silica. The high hardness and toughness are enhanced by the corundum content and a very fine interlocking grain structure. These properties rank Oregon emery above the east coast material and close behind the Turkish product.

Oregon emery — chemical and physical properties

Al_2O_3	up to 67%
SiO_2	28%
Fe_3O_4	20%
TiO_2	2%
Colour	grey to black
Mohs' hardness	8–9
SG	3.2–3.7
MP	approx 1,700°C
Sodium sulphate soundness test	0.27%
LA abrasion test	6.00–9.35%

Source: Oregon Emery Co.

Turkey — high corundum content

Production of emery in Turkey is mainly controlled by Etibank. Total production capacity is currently 20,000 tpa at Mugla-Glk. The chemical composition of the emery is — Al_2O_3 57% min, SiO_2

24–26%, TiO_2 2–3%, CaO 1.5–2%, LOI 7–9%. Etibank's production is sold to markets in Europe and the USA. Turkish emery has the highest corundum content of all sources.

Greece — state controlled

Greece has an annual production of some 10,000 tpa centred on the island of Naxos. Deposits are the property of the Greek state but are actually worked by local villagers who then supply a centralised depot. Some 50% of the output is exported in lump form, with the remaining material shipped to the mainland for further processing. *Icon Mining & Commercial Co. SA* at Votanikos, close to Athens, crushes and classifies emery into a range of sizes which are then sold for use as grinding wheels, millstones, coated abrasives, grinding and polising pastes, wire sawing grits, and non-skid surfaces. *Hellenic Corundum Ltd* at Elefinsa crushes and classifies emery, mainly for use in non-skid flooring.

Other abrasives — a selection

Other natural minerals tripoli, staurolite, and olivine are known for their abrasive properties as are certain fused and sintered material such as alumina-magnesia spinel abrasives.

Tripoli

Tripoli is a loose geological term, covering material generally microcrystalline in nature, soft, friable, and porous with a silica content averaging 98–99% with minor amounts of alumina, titania, and iron oxide. The USA is the only country with a significant output of the mineral, with Arkansas being the major supplier.

Individual grains of tripoli lack distinct edges and corners, restricting them to use only as mild abrasives. Major markets for the material, although still small, are in toothpaste, industrial soaps, or as a buffing and polishing compound in lacquer finishing, and in the automobile industry. Its usage as an abrasive is declining. However, an expanding market for the mineral is being found as a filler and extender, particularly for paint but also for rubber, plastic, and enamel.

Production of tripoli in the USA, in parallel with the coutry's consumption, decreased for the fifth successive yéar in 1988. The average annual production for the previous ten years was 105,527 tonnes, with a high of 115,985 tonnes in 1979, and a 1981 low of 973,478 tonnes. Production recorded in the USA in 1988 totalled 99,908 tonnes. Between 1978 and 1988 the average annual consumption of tripoli in the USA declined by 34,206 tonnes. The country consumed 48,615 tonnes in 1979 compared with 26,371 in 1988. This latter figure was the lowest recorded since the 22,675 tonnes of 1953.

There are six major producers of tripoli in the USA, mostly based in central or mid-western states. *Malvern Minerals Co.* of Garland County, Arkansas produces both crude and finished material. *American Tripoli Co.* produces crude material in Ottawa County, Oklahoma in addition to finished material in Newton County, Montana. *Illinois Minerals Co.* and *Tammsco Inc.*, both operate in Alexander County, Illinois and produce crude and finished amorphous (microcrystalline) silica. Finally, *Keystone Filler and Manufacturing Co.* in Northumberland County, Pennsylvania process rottenstone, a decomposed fine grained siliceous shale.

Staurolite

The major use of staurolite, as an abrasive, is for impact finishing of metals and sandblasting of buildings. Industrial grade material is mined primarily by one company, *E. I. du Pont de Nemours & Co.* Production of staurolite is as a by-product of the company's heavy mineral sands operations in Clay County, north central Florida. Staurolite is a naturally occurring complex, hydrated iron aluminosilicate with a variable composition. Most often occurring as opaque, reddish-brown to black crystals with specific gravity between 3.74 and 3.83, staurolite has a Mohs' hardness of 7–8. Du Pont's material has a nominal composition of 45% aluminium oxide (minimum), 18% ferric oxide (maximum), 5% silica (max), 3% silica (max), and 3% zirconium dioxide.

Staurolite is marketed as an abrasive medium under at least two trade names — Starblast (80 mesh), and Siasill (90 mesh). These products similarly to garnet, are finding increased favour following the introduction of tougher environmental laws, relating to free silica.

Olivine — environmentally friendly

The current market for olivine abrasives in the UK is about 5,000 tpa. This figure is expected to grow considerably in the near future in line with new Government legislation. Last October the Health & Safety Commission introduced the *Control of Substances Hazardous to Health Regulations 1988 (COSHH).* COSHH regulation 4(1) prohibits the use of sand or other substance containing free silica as an abrasive for blasting articles in any blasting apparatus. Blasting apparatus is defined as the "apparatus for cleaning, smoothing, roughening, or removing of part of the surface of any article by the use of an abrasive jet of sand, metal shot or steam or by a wheel". Silica sand is now banned in the UK, although some operators have continued to use it.

Olivine is suitable for blasting applications for several reasons. It has less than 1% free silica, contains no free metals, has a Mohs' hardness of 6.5–7.5, and has a high specific gravity of 3.3 ensuring that particles impacting the work surface have a higher energy facilitating dirt and scale removal. Olivine is thus particularly suited to bridge or building cleaning, and for similar situations where slag abrasives are unsuitable. The UK is a consumer of olivine as a blasting agent particularly where the use of slag abrasives might cause environmental problems.

Prices

Several olivine blasting grades are available with *Scangrit* being a major supplier to the UK market. Prices have been steady over the past year with the UK's Scangrit offering, on a basis of ex-works per tonne, the following — AFS20 grade (1.7–0.355mm) at £59, AFS30 grade (1.0–0.18mm) £55, and AFS60 grade (0.5–0.125mm) £75.

Production

Olivine is sourced from Norway, Italy, Austria, the USA, Mexico, Japan, and Spain although not all produce blasting grade material. *A/S Olivin,* the state-owned Norwegian company, is the world's largest producer of olivine. The company produces 2.1m. tpa, although of this only about 150,000 tpa is fully dried and sold into blasting, foundry, and selected refractory markets.

In Italy *Nouva Cives SpA* quarries ore from two operations in Vidracco, near Turin. Nouva Cives began exploitation of its second deposit in 1988. Located between the municipalities of Vidracco, Baldissero, Canavasse, and Castellamonte, it has olivine and magnesite reserves estimated to be about 100m. tonnes. The company has an annual production capacity of 200,000 tonnes of a variety of grades. Of the total annual production 30% is used in sand blasting, bituminous products, and abrasives.

Production of olivine in the USA is concentrated between *Olivine Corporation* and *Applied Industrial Materials Corp. (Aimcor).* Olivine Corp. sources its olivine from the Bellingham surface mine in Washington State. The company, however, is keen to concentrate on refractory grade products and a range of olivine-containing refractory incinerators. However, it sells around 75,000 short tonnes of olivine to Aimcor for processing at its Hamilton, Washington facility. Here Aimcor produces ten different grades, including aggregate, for blasting, refractory, and blast furnace applications.

Sintered abrasives

The first large-scale commercially available sintered abrasives were produced by milling calcined bauxite. This process required the milling of calcined bauxite to a fine grained size, forming into abrasive grit size, before finally being fired at 1,500°C thus forming strong, hard, tough pellets, of polycrystalline alumina. More recently, however, abrasive grits consisting of alumina and magnesia spinel have become available. These materials are manufactured by sintering dried alumina gel particles at about 1,400°C. High density alumina (or alumina containing) materials can also be produced by firing a dried alumina gel made from alpha-alumina monohydrate (boehmite) or by hot pressing dried powders from such gels.

Bonded and coated abrasives

Bonded abrasives

Forms of bonded abrasives include wheels, segments, bricks, sticks, and sharpening stones. The common characteristic that holds this group together is that each is made of abrasive particles held together by a bonding material and two or three minor components. Commonly used bonds are clay or glass-based vitrified bonds, resin, shellac, and rubber. Bonds utilised in smaller quantities include silicates and oxychlorides, the former in cutlery grinding, the latter for grinding the ends of springs.

The aspect differentiating bonded abrasives from coated abrasives is that the latter products are cemented on a backing without any significant adhesion between grains. Like their coated counterparts, bonded abrasives generally employ aluminium oxide or silicon carbide. Cutting efficiency is an important factor. Hardness, toughness, grain size, and grain friability are others. Further considerations include the relative proportions of grain and bond, type of bond, and the method of dressing.

With so many variables involved ie. abrasive type, grain size, grade, structure (open to dense spacing of grains), and bond type the total number of variations can run into hundreds of thousands. However there are estimated to be some 16,000 types of bonded abrasives which are in common use.

Coated abrasives

Three elements make up the structure of coated abrasives — the abrasive grain, bond, and backing. The grain is the actual tool, the backing is the tool holder, and the bond is the agent to bind tool and tool holder together. Coated abrasives were developed to polish or finish, and to form or remove stock from metal, ceramics, plastics, rubber, wood, stone, and other materials.

Factors influencing the use of abrasive grains are many and varied. However, the three principal ones are type of material to be machined, requirements, and type of machining to be done. Similarly characteristics of grains which influence the use of abrasives are grain hardness, toughness, heat resistance, and particle shape. There are five types of backings — paper, cloth, fibre, papercloth, and cloth fibre. Fibre backings are made of vulcanised rubber which is particularly suited to stock removal operations due to its inherent heavy weight. Paper cloth backings are employed on flat surfaces because they are fairly inflexible. Abrasive grits are drawn electrostatically to the paper, and then bonded with either water-soluble glues (animal hide glue suffers at high temperatures and is only used on household application papers), waterproof resin-on-resin, or resin-on-glue types.

The abrasive products industry is beginning to adopt standards to encourage a user friendly attitude. An example of this is the colour of backing material. Woodworking paper generally uses white alumina and, for ease of recognition, is set on yellow paper, whilst brown alumina generally associated with metal working papers is set on brown paper ■

An Investigation of Ball-on-Ball Impact

by George Laird II

ABSTRACT—The Bureau of Mines, U.S. Department of the Interior, has used a shock accelerometer to measure deceleration in ball-on-ball impact. The accelerometer signal was analyzed by a fast-Fourier-transform (FFT) technique, and signal components were identified from the accelerometer characteristics, solid mechanics, and finite-element modal and spectral analysis. Following frequency-domain digital filtering to remove extraneous frequencies, the remaining signal was reconstituted by an inverse FFT. Supporting Hertzian quasistatic and elastic and elastic-plastic dynamic finite-element calculations were carried out. All calculations predicted similar peak decelerations and contact times. The former agreed well with experiment. However, stress-wave effects make it difficult to use deceleration measurements to define contact times, even at an impact velocity of 8 ms^{-1}. Such an impact must be analyzed as dynamic rather than static.

Introduction

Impact wear is one of the most severe forms of wear in the mining and mineral-processing industries. The Bureau of Mines, U.S. Department of the Interior, has for many years been investigating the mechanisms of such wear in those ferrous alloys used by these industries. To this end, the Bureau developed the ball-on-ball impact machine shown in Fig. 1.[1] As each ball drops, numerous impacts of varying magnitude are produced. These simulate the inconsistent loading often encountered in mining and mineral processing. The Bureau has tested many alloys and ranked them by resistance to impact failure.[2,3] To understand better the mechanisms of impact failure in these alloys, and to model these mechanisms by finite-element analysis, it was desired to determine the impact acceleration as a function of time from first impact.

Several methods of measuring the acceleration were considered. Due to the severity of the impact, piezoelectric transducers and surface-mounted strain gages were ruled impractical;[4,5] high-speed photography[6] was eliminated because of the expense and time involved. A shock accelerometer was chosen for its rapid response characteristics, broad frequency spectrum, ruggedness, and easily analyzed output signal.[7]

Steel (and other hard) objects are known to resonate when impulse loaded or otherwise excited at frequencies near their harmonics.[8] In addition, other research has shown the important effects of stress waves on impacts between ferrous materials.[4,5,9] If the harmonic frequencies of the target and/or the frequencies of the stress waves generated by the impact are within a factor $\simeq 2\times$ of the resonant frequency of the transducer, then transducer ringing is yet a further complication.[8] Once these spurious effects were identified, they were deleted from the shock accelerometer signal by frequency-domain digital filtering using a fast-Fourier-transform (FFT) method.[10,11] The amplitude and frequency of the digitally filtered waveform were compared with the peak acceleration and the (inverse of the) time of contact predicted by the Hertzian theory of quasistatic elastic impact[12] and by elastic and elastic-plastic dynamic finite-element analyses.

George Laird II is Mechanical Engineer, Albany Research Center, Bureau of Mines, 1450 SW Queens Avenue, Albany, OR 97321.

Original manuscript submitted: September 20, 1988. Final manuscript received: March 14, 1989.

Experimental Procedure

For a steel* ball dropped onto a stationary NiHard 4 (white cast iron) ball† from the drop height (3.28 m) used in the ball-on-ball impact test, Hertzian quasistatic analysis yields (see Appendix) a peak deceleration of -93.5×10^3 ms^{-2} and a contact time (frequency) of 150 μs (6670 Hz). These values and the need to limit cable noise led to the decision to use a charge-amplified, single axis, shock accelerometer. The accelerometer selected had a full-scale rise time of 5 μs over a frequency range of 0.25-8000 Hz at a peak measurement of 500×10^3 ms^{-2} with an accuracy of ± 5 percent using an output voltage of 0.0905 mVg^{-1}. Its resonant frequency was 65 kHz.

This shock accelerometer was threaded onto a 7.87-cm diameter steel ball as shown in Fig. 2. This ball was fitted with polyethylene guides to minimize friction as it slid down the 8.25-cm diameter drop tube and to constrain the accelerometer axis normal to the impact area. Figure 3 shows the experimental configuration at impact. Twenty-two 7.62-cm diameter NiHard 4 balls are aligned within the 8.25-cm diameter J-shaped tube and are free to move during the impact. After impact, it is usual for one or two balls to pop gently out of the end of the J tube. The impacting ball is observed not to rebound after impact.

The shock accelerometer signal was recorded, analyzed, and transformed into its Fourier components by an

**AISI 1080 steel hardened to a Brinell hardness of 7.31 GPa*

†NiHard 4, approximate composition 9 wt pct (percent) Cr, 6-percent Ni, 3.0-percent C, 1.5-percent Si, and balance Fe, hardened to a Brinell hardness of 6.98 GPa

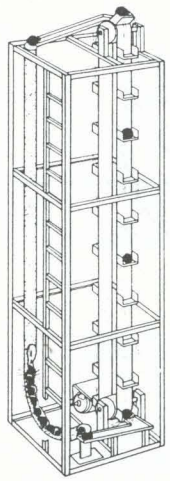

Fig. 1—Ball-on-ball impact machine

J. Exp. Mechanics

Assuming that the absolute maximum value of π_{ij} is 10.0×10^{-13} m²/N, the maximum induced stress is equal to the breaking strength of 5.5×10^{8} N/m² (Ref. 16) and n_0 is 3.52, we obtain the value of eq (29) to be 0.02. Consequently, the maximum light-path difference $e_{max} = t \tan \theta_{max}$ after the transmission becomes 0.08 mm. This value is small enough for the photoelasticity.

Conclusion

The general stress-optic law for a single crystal plate under a plane stress state is developed. It is proved by experiments on silicon beams in pure bending. It is found that, in order to determine the stress distributions in the single crystal plate by using the shear difference method, there must be an optical condition for piezo-optical coefficients with respect to the model coordinates. If the condition is not satisfied, a relation with regard to the stress components other than the general stress-optic law is required.

It can be expected that the plates cut from the single crystal have various elastic constants depending on the crystallographic direction. If the single crystal plate satisfies the optical condition mentioned above, it is a useful photo-anisotropic material for the study of anisotropic elasticity. Alkali halide and garnet as well as silicon and gallium arsenide are considered as photo-anisotropic materials.

TABLE 2—ELASTIC COMPLIANCE COEFFICIENTS AND ELASTIC CONSTANTS OF SILICON BEAM

Beam	A	B	C	D	E
Compliance $\times 10^{-11}$ m² N⁻¹					
s_{11}'	0.768	0.592	0.655	0.592	0.592
s_{22}'	0.768	0.592	0.655	0.592	0.592
s_{12}'	−0.214	−0.038	−0 101	−0.155	−0.155
s_{66}'	1.260	1.964	1.711	1.495	1.495
s_{16}'	0	0	−0.169	0	0
s_{26}'	0	0	0.169	0	0
s_{31}'	−0.214	−0.214	−0.214	−0.097	−0.097
s_{32}'	−0.214	−0.214	−0.214	−0.097	−0.097
s_{36}'	0	0	0	0	0
s_{41}'	0	0	0	−0.166	0
s_{42}'	0	0	0	0.166	0
s_{46}'	0	0	0	0	−0.332
s_{51}'	0	0	0	0	0.166
s_{52}'	0	0	0	0	−0.166
s_{56}'	0	0	0	−0.332	0
Elastic constant $\times 10^{11}$ Nm⁻²					
E_1'	1.302	1.689	1.527	1.689	1.689
E_2'	1.302	1.689	1.527	1.689	1.689
ν_1'	0.279	0.064	0.154	0.262	0.262
ν_2'	0.279	0.064	0.154	0.262	0.262
G'	0.794	0.509	0.584	0.669	0.669

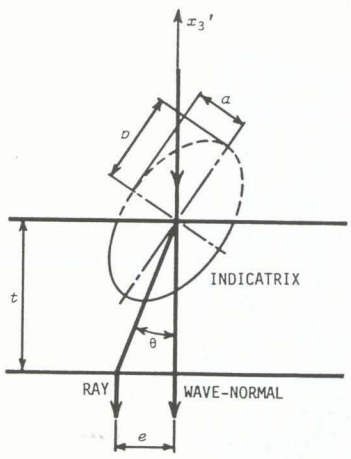

Fig. 4—Light pass inclined normal to surface of the plate

Acknowledgment

The authors wish to thank Shinetsu-handoutai Co. Ltd. for presentation of the silicon beams. The authors also wish to thank Nagoya University Computation Center for numerical calculations. This work was supported by the Grant-in-Aid for Scientific Research from the Ministry of Education.

References

1. Cloud, G.L. and Pindera, J.T., "Techniques in Infrared Photoelasticity," EXPERIMENTAL MECHANICS, **8** (5), 193-201 (May 1968).
2. Redner, S., "Photoelastic Data Acquisition in Infrared," VDI-Berichte, 313, 57-62 (1978).
3. DeNicola, R.O. and Tauber, R.N., "Effect of Growth Parameters on the Residual Stress and Dislocation Density of Czochralski-Grown Silicon Crystals," J. Appl. Phys., **42** (11), 4262-4270 (1971).
4. Shimaoka, M., et al., "Measurement of Stress in Silicon Chip by Infrared Photoelasticity," J. N.D.I. (in Japanese), **36** (12), 901-907 (Dec. 1987).
5. Kotake, H. and Takasu, Shin., "Quantitative Measurement of Stress in Silicon by Photoelasticity and Its Application," J. Electrochemical Soc., **127** (1), 179-184 (Jan. 1980).
6. Kotake, H., et al., "Quantitative Photoelastic Measurement of Residual Stress in LEC Grown GaP Crystals," J. Crystal Growth, **50**, 743-751 (1980).
7. Chaturvedi, S.K., "Fundamental Concepts of Photoelasticity for Anisotropic Composite Materials," Int. J. Eng. Sci., **20** (1), 145-157 (1982).
8. Chaturvedi, S.K., "A Rational Theory of Oblique Incidence and Its Extension to Stress-Separation in Birefringent Composites," EXPERIMENTAL MECHANICS, **23** (1), 36-41 (1983).
9. Yamada, M., "Quantitative Photoelastic Measurement of Residual Strains in Undoped Semi-insulating Gallium Arsenide," Appl. Phys. Lett., **47** (4), 365-367 (Aug. 15, 1985).
10. Sampson, R.C., "A Stress-Optic Law for Photoelastic Analysis of Orthotropic Composites," EXPERIMENTAL MECHANICS, **10**, 210-215 (May 1970).
11. Knight, C.E. and Pih, H., "Orthotropic Stress-Optic Law for Plane Stress Photoelasticity of Composite Materials," Fibre Sci. and Tech., **9**, 297-313 (1976).
12. Nye, J.F., Physical Properties of Crystals, Clarendon Oxford (1972).
13. Love, A.E.H., Mathematical Theory of Elasticity, 4th Ed., Cambridge (1927).
14. Narasimhamurty, T.S., Photoelastic and Electro-Optic Properties of Crystals, Plenum Press (1981).
15. Hetenyi, M., Handbook of Experimental Stress Analysis, John Wiley & Sons (1950).
16. Runyan, W.R., Silicon Semiconductor Technology, McGraw-Hill (1972).
17. Briggs, H.B., "Optical Effects in Bulk Silicon and Germanium," Phys. Rev., **77**, 287 (1950).
18. Brantley, W.A., "Calculated Elastic Constants for Stress Problems Associated with Semiconductor Devices," J. Appl. Phys., **44** (1), 534-535 (Jan. 1973).
19. Giardini, A.A., "Piezobirefringence in Silicon," The American Mineralogist, **43**, 249-262 (1958).
20. Hornstra, J. and Penning, P., "Birefringence Due to Residual Stress in Silicon," Philips Res. Rep., **14**, 237-249 (1959).

Analogic Inc. Model Data 6000A digital waveform analyzer.* This analyzer is powered by a 16-bit, 8-MHz central processing unit with 16-bit precision and thus provides an analog to digital conversion with a theoretical accuracy of one part in two.[15] The accelerometer signal was sampled at a rate of 1 MHz until 8192 data points were obtained. The analyzer had a bandwidth (−3 db) of 250 kHz. With the frequency of interest around 7 kHz, Nyquist's rule was well satisfied and anti-aliasing was ensured during the subsequent FFT analysis.[11,13]

A rectangular (boxcar, or nonwindowing) window option was employed. The accelerometer signal was subsequently converted by FFT into amplitude and phase components as a function of frequency. To remove unwanted frequency components or to filter the waveform digitally, the amplitudes of such components were set to zero. The remaining amplitude and phase components were then reconstituted by carrying out an inverse FFT.

To verify the accuracy of the FFT algorithm, several representative impact waveforms were recorded, transformed, and reconstituted without making use of digital domain filtering. This showed that the FFT algorithm attenuated the peak voltage of the signal by only $\simeq 0.01$ percent.

Three steps were taken to identify Fourier components of the recorded impact waveform. First, the finite-element model shown in Fig. 4 was used to perform a modal (eigenvalue) analysis of the steel ball, using the Householder solution method.[14] The model comprises 50, six-node, isoparametric triangular elements and has 220 degrees of freedom (DOF). The material properties used are the elastic moduli and density of steel (see Appendix). To increase computational efficiency, the Guyan reduction[15] was used to reduce the number of DOF to 45 master DOF. This technique retains the exact potential energy of the system but modifies the kinetic energy to some extent.[15] Thirty-six master DOF in the y-axis direction (shown as arrows in Fig. 4) were selected to model accurately the mass distribution of the steel ball and to correspond with those longitudinal modes that most influence the accelerometer signal. The remaining nine master DOF were selected automatically to correspond to the lowest ratios of stiffness to mass.[16]

Reference to a specific product does not imply endorsement by the Bureau of Mines.

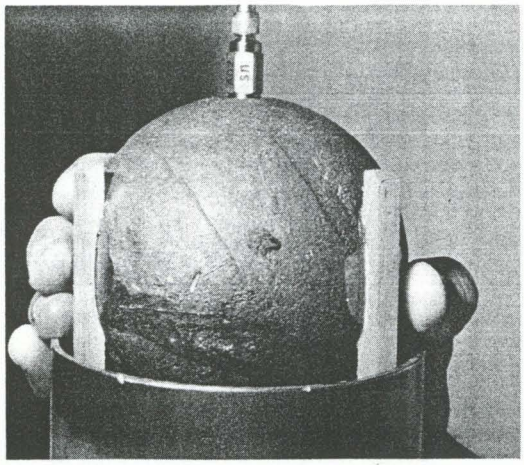

Fig. 2—Instrumented steel ball at lip of drop tube

To complement the modal analysis, a mode superposition spectral analysis was performed using the same finite-element model with the addition of a sinusodal force $F = F_0 \sin(2\pi t/f)$, where $F_0 = 4.48$ N, $f = 1 - 100$ kHz, and t = time. The force F was applied parallel to the axis of impact at the accelerometer position,[16] i.e., diametrically across the ball from the point of contact. The mode superposition technique uses the same eigenvalues, eigenvectors, and reduced stiffness and mass matrices in its solution. Damping was not used; consequently, the driving force and the resultant displacement remained in phase.

The second technique employed to identify spurious Fourier components of the impact waveform was solid-mechanics analysis. Owning to the shape of the ball, the stress waves produced during impact are reflected and/or refracted in several different directions. The dominant stress wave created by normal impact is initially a compression wave. Such a wave travels in steel at 5.118 ms^{-1} and therefore travels twice the diameter of the ball (0.157 m) in 31 μs. Thus the frequency of propagation of this wave is approximately 32.5 kHz.

The third source of information about spurious Fourier components was the accelerometer calibration data which identified a resonant frequency at 65 kHz.

Dynamic Finite-element Modeling

The dynamic elastic (linear) and elastic-plastic (nonlinear) finite-element models of ball-on-ball impact took as their input the same geometry, mechanical properties,

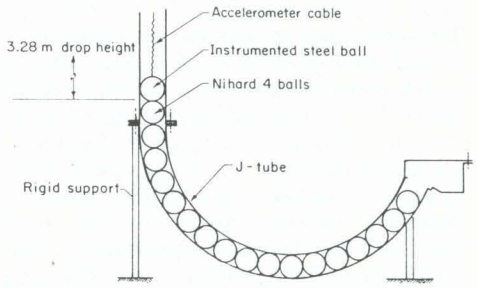

Fig. 3—Experimental configuration at impact

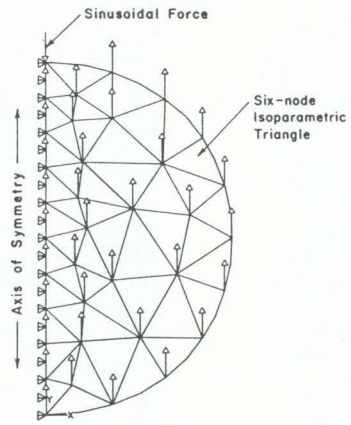

Fig. 4—Axisymmetric finite-element model of steel ball

and initial conditions as used in the Hertzian quasistatic analysis. The nonlinear analysis used a von Mises yield criterion with a bilinear kinematic hardening rule. This constitutive relationship required as input the elastic moduli, the yield stresses, and the work-hardening rates (tangent moduli) of the steel and NiHard 4 balls. The yield stresses of the two balls were estimated (see Appendix) from their Brinell hardnesses as 2.62 GPa (steel ball) and 2.50 GPa (NiHard 4 ball). The tangent modulus for the steel ball was obtained from published data[17] for carbon steels as 4.817 GPa. For the NiHard 4 ball, work hardening data were unavailable. The default value of five percent of the elastic modulus ($\simeq$10 GPa) recommended by the finite-element code was therefore used.[16]

The axisymmetric finite-element model used in the dynamic analyses is shown in Fig. 5. In these analyses the top ball is first given a velocity of -8.02 ms^{-1} by displacing each of its nodes a distance of -8.02×10^{-6} m in the y direction during the first load step ($\Delta t = 1\,\mu$s). After this load step the y displacements of the nodes are set free and the balls are in contact with an approach velocity of 8.02 ms^{-1}. The top and bottom spheres contact via eight gap elements.[16] Each gap element has a unique gap opening calculated as the sum of the separation of the surfaces of the two balls plus 8.02×10^{-6} m. The stiffness of each gap was set to 2,100 GPa, a value approximately one order of magnitude greater than Young's modulus of either ball.[16] Note that the purpose of the gap elements is to transfer forces across the interface between the top and bottom balls. Therefore, a high gap stiffness is used to limit unrealistic displacement of the surface of either ball.

The model contained two types of solid element, a four-node linear isoparametric quadrilateral and the six-node isoparametric triangle described previously. The four-node element was chosen primarily to improve the overall accuracy of the calculation. The gain in accuracy comes about because the quadrilateral element permits the use of 2×2 Gaussian integration, which is more accurate than the three-point Gaussian integration used with the triangular element. The quadrilateral element also made it easier to obtain a well-defined mesh in the region of maximum Hertzian contact stresses. In all, the model contained 160 four-node quadrilateral and 240 six-node triangular elements, with a total of 666 nodes.

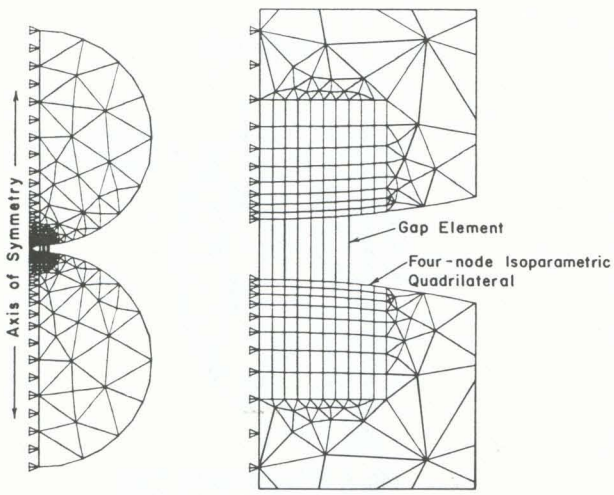

Fig. 5—Finite-element model of ball-on-ball impact

By its nature, dynamic finite-element analysis approximates a continuous event as a series of discrete steps. In such an analysis, the equations of motion of the nodes are formulated in terms of the mass, damping, and stiffness coefficients. These equations are then solved at discrete times by a Newmark direct integration technique.[16] To determine the integration time step (ITS) necessary to model the contact of two balls impacting at 8.02 ms^{-1} with sufficient accuracy, the stiffness of the gaps and the primary frequency to be resolved ($\simeq$7 kHz) must both be considered. Using equations provided in Ref. 16, a minimum ITS of 1 μs was calculated. From Hertzian theory the contact time was calculated as 150 μs. Thus for both dynamic analyses (linear and nonlinear) a total of 175 iterations was specified, for an elapsed time of 175 μs. The additional 25 μs allows a steady-state condition to be reached in which the steel ball is at rest and the NiHard 4 ball is moving off at nearly 0.8 ms^{-1}.

Damping was incorporated into both dynamic analyses through the Rayleigh or proportional damping method.[18] This sets

$$[C] = \beta[K] + \alpha[m]$$

where β and α are constants and C, K, and m are the damping, stiffness, and mass matrices, respectively. In the present situation α can be set to zero and β is taken as $\frac{\xi}{\pi f}$, where ξ is the damping ratio or loss coefficient and is the frequency of interest. For ferrous materials Lazan[19] shows ξ to range from 0.1 to 3 percent; and in this analysis the frequency of interest is the impact frequency of $\simeq$7 kHz. Hence, to limit stress-wave effects in the dynamic analysis a value of $\xi = 2.5$ percent or $\beta = 1.137 \times 10^{-6}$ was used.

Results and Discussion

Figure 6 shows a typical accelerometer signal as recorded by the waveform analyzer. It exhibits a maximum of 1.923 V, implying that the instrumented ball experienced a maximum deceleration during impact of -2.08×10^5 ms^{-2}, and a minimum of -0.645 V, implying that the ball experienced an acceleration of 0.709×10^5 ms^{-2}. Such an acceleration is physically unreasonable and is one indication of the presence of spurious components in the waveform. Another such indication is the demonstration by Deresiewicz[20] and Macmillan and Laird[21] that a quasi-

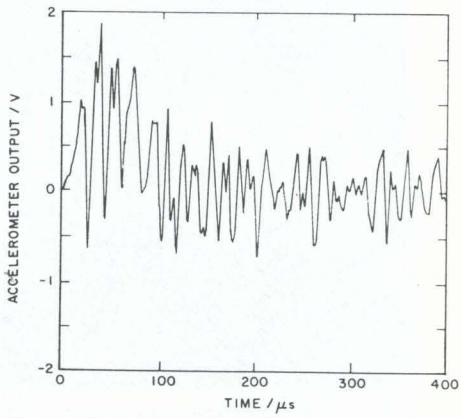

Fig. 6—Raw accelerometer output signal

static Hertzian impact produces a waveform which varies with time t very nearly as $\sin^{1.5} t$. A further troubling feature of Fig. 6 is that Hertzian quasistatic theory (see Appendix) predicts a maximum deceleration of -91.9×10^3 ms^{-2}, or only about 55 percent of the value measured. Finally, it should be cautioned that the sharp fluctuations in voltage exhibited in Fig. 6 may not represent precisely corresponding fluctuations in the force acting on the accelerometer because the accuracy of the accelerometer falls progressively with rise in frequency above 8 kHz.

To decipher the complex waveform of Fig. 6, the signal was in turn digitized, Fourier transformed, filtered, and reconstituted. The transform of the waveform seen in Fig. 6 is presented in Fig. 7 as plots of amplitude (a) and phase (b) versus frequency. Peak amplitudes occur between frequencies from 0 to 18 kHz and at frequencies of 33.9, 50.7, 67.1, and 80.1 kHz. Study of many such waveforms reveals that the peaks from 0 to 18 kHz and the sharp peaks at about 67 and 80 kHz occur reproducibly. The peak at 39 kHz also occurs in each spectrum, although it is not always as sharp as in the example presented in Fig. 7(a); the peak at 50.7 kHz also occurs frequently. In addition smaller peaks occur more or less reproducibly at frequencies greater than 100 kHz. The amplitudes of these peaks are underestimated by an unknown amount because the accuracy of the accelerometer deteriorates at frequencies ≥ 8 kHz.

Hertzian quasistatic theory shows that the impact frequency is $\simeq 7$ kHz. Consequently, it is plausible that the impact waveform is the source of the frequencies from 0 to 18 kHz, and that the higher frequencies derive from the ball harmonics, stress waves, and accelerometer ringing.

The natural frequencies below 100 kHz computed from the finite-element modal analysis are 35, 49, 55, 71, 72, 74, and 91 kHz. Results from the spectral analysis are shown in Fig. 8. They indicate the amplitude of the accelerometer displacement versus the frequency of the sinusoidal forcing function. Note that the forcing function does not evoke a significant response at the natural frequencies of 49, 71, 72 and 91 kHz. Hence these frequencies can be discarded when reconstituting the waveform. Comparison of Figs. 7 and 8 shows that the remaining natural frequencies of 35, 55, and 74 kHz correlate fairly well with the peak amplitudes observed in the FFT signal at 33.9, 50.7 and 80.1 kHz. Consequently, these peaks are evidence of activation of these three natural frequencies. Higher frequency components were not investigated for several reasons: (1) the accuracy of the accelerometer decreases at frequencies ≥ 8 kHz, (2) such high frequency components are damped out more rapidly, and (3) such frequencies are far removed from the impact frequency.

As reported above, the longitudinal wave frequency was calculated to be about 32.5 kHz. Hence, the peak shown in Fig. 7 at 33.9 kHz is attributed to activation of the lowest natural frequency by the impact event.

Shock accelerometers are designed for fast response and as such employ minimal damping in their construction. They are therefore especially prone to transducer ringing. The peaks shown in Fig. 7 at 33.9 and 50.7 kHz are close enough in frequency (i.e., within a factor $\simeq 2\times$) to the accelerometer resonant frequency (65 kHz) to cause ringing, and so the sharp peak at 67.1 kHz in Fig. 7 is attributed to accelerometer ringing.

Since the peaks at 33.9, 50.7, 67.1, and 80.1 kHz result from ball harmonics, stress waves, and accelerometer ringing, these spurious frequencies were all removed from the FFT output prior to reconstituting the impact waveform. Figure 9 shows the FFT output after such deletion, with only the frequencies from 0 to 18 kHz left intact. An inverse FFT was applied to this modified spectrum. The resultant waveform is shown in Fig. 10.

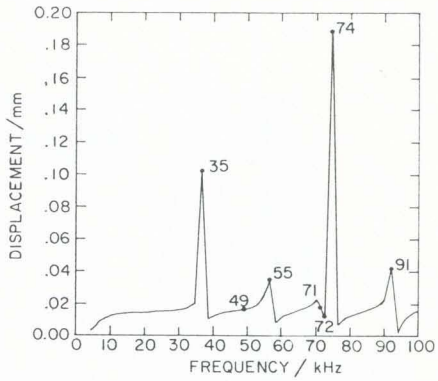

Fig. 8—Results of finite-element analysis of spectral response of steel ball

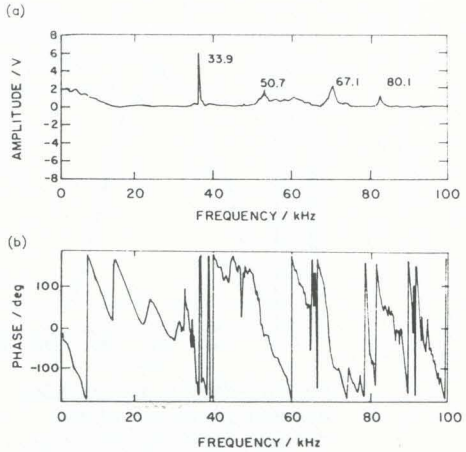

Fig. 7—Components of impact waveform identified by fast-Fourier transformation

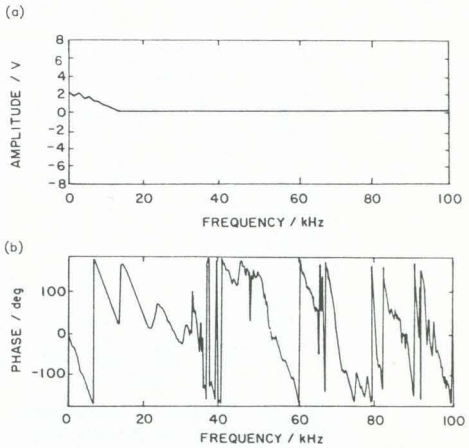

Fig. 9—Components of impact waveform after frequency domain digital filtering

An average of 10 measurements processed in this fashion gave a peak deceleration of -84.2×10^3 ms^{-2} $\pm 6.9 \times 10^3$ ms^{-2} and an apparent contact time of 101 μs ± 8 μs. These values differ from the predictions of Hertzian quasistatic theory (see Appendix) by -8.4 percent and -32.6 percent, respectively.

Figure 11 shows the results of the dynamic linear finite-element prediction of the deceleration during impact of the point on the steel ball at which the accelerometer is attached. The peak deceleration is -92.7×10^3 ms^{-2} and there is measurable deceleration for $\simeq 150$ μs. Direct calculation gave a contact time of $\simeq 153$ μs. These values are in very close agreement with the peak deceleration and the contact time predicted by the Hertzian quasistatic theory. Note, however, that it takes 10 to 20 μs before the impact deceleration starts to rise steeply. This is because the compressive stress wave generated at the contact interface at first contact takes about this time to traverse the diameter of the steel ball and affect the motion of the accelerometer. Note also the shoulder on the left side of the peak in Fig. 11 at 35 to 40 μs after first contact. The decrease in slope terminating in this shoulder is caused by the reflection of the primary longitudinal compression wave as a tensile wave. This tensile wave is then reflected again at the contact interface as a compression wave; correspondingly, the deceleration again rises steeply. Further reflections and/or refractions of stress waves are undoubtedly responsible for the double maximum exhibited in Fig. 11. Similarly the 10 μs or longer 'tail' seen on the extreme right of this figure is the result of residual-stress-wave decay at the end of the impact event.

The existence of such hard to define transients at each end of the impact event makes it difficult to define the contact time from such a plot. Figure 11 indicates why an experimental determination of contact time by means of an accelerometer can be some tens of microseconds different under dynamic conditions than under quasistatic conditions. The linear dynamic finite calculation may in fact be in much better agreement with experiment than is at first apparent.

Figure 12 is the analog of Fig. 11 obtained from the nonlinear (elastic-plastic) dynamic finite-element analysis. The striking feature is the close similarity between the two plots. The peak deceleration is reduced -4 percent, to -88.6×10^3 ms^{-2}, and the time during which there is measurable deceleration is reduced -3 percent, to 145 μs. Direct calculation gave a contact time of 148 μs. The stress wave effects seen in Fig. 11 at the beginning, 35 to 40 μs into, and at the end of the impact event are all faithfully reproduced. The results of incorporating plastic flow into the model are threefold. First, the discrepancy between the measured and the calculated peak deceleration is reduced to 4 percent; second, the calculated contact time is reduced by $\simeq 3$ percent, probably bringing it into slightly better agreement with experiment; and third, a shoulder is introduced into the plot of deceleration versus time immediately prior to peak deceleration.

Figure 13 is a plot of the contours of shear stress in both balls at the moment of peak deceleration. The maximum shear stress is about 1.37 GPa in both balls. For the steel ball the shear yield stress is 1.31 GPa and the tangent modulus is 4.82 GPa. Thus the contour labeled A, which is the locus of points at which the shear stress is 1.3 GPa, provides an accurate delineation of the plastic zone; and in this zone the plastic strain rises to nearly 0.02. In the case of the NiHard 4 ball, which has a shear yield stress of 1.25 GPa and an assumed tangent modulus of 10 GPa, the corresponding contour **A** slightly underestimates the extent of the plastic zone. In this ball the maximum plastic strain is nearly 0.02 also. The contact radius in Fig. 12 is approximately 3.5 mm, and the point of maximum shear stress occurs in each ball at a depth of 1.3 mm, which is 37 percent of this contact radius. Under elastic quasistatic conditions, the contact radius is calculated as 2.85 mm, with the point of

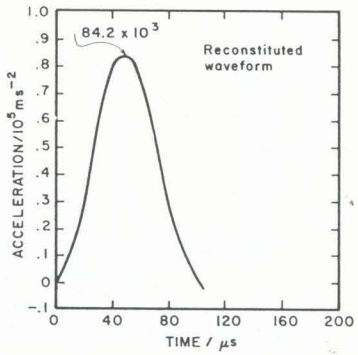

Fig. 10—Reconstituted waveform

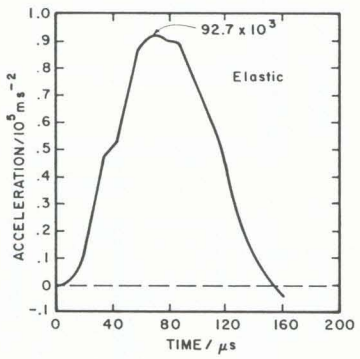

Fig. 11—Elastic finite-element calculation of the deceleration of the steel ball during impact against the NiHard 4 ball

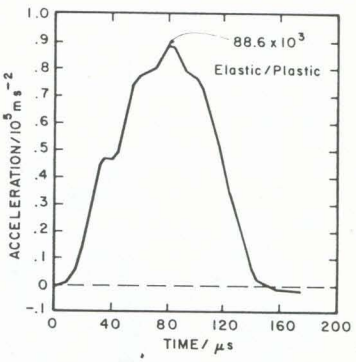

Fig. 12—Elastic-plastic finite-element calculation of the deceleration of the steel ball during impact against the NiHard 4 ball

maximum shear stress occurring at a depth of 1.3 mm, or 47.5 percent of the contact radius. Evidently, plastic flow in the impacting balls increases the contact radius. The good agreement of the location of the maximum shear stress is reasonable since the elastic shear stress is much greater than the increment of shear stress introduced by plastic deformation.

Summary and Conclusions

Ball-on-ball impact has been studied experimentally by use of a shock accelerometer and theoretically by Hertzian quasistatic theory and dynamic linear and nonlinear finite-element techniques.

It is demonstrated that, when the effects of ball harmonics, stress waves, and accelerometer ringing are removed from the accelerometer output by digital filtering techniques, the measured peak deceleration is only four percent less than the value predicted by a nonlinear finite-element calculation and only eight percent less than the values obtained from Hertzian quasistatic theory and from a linear finite-element calculation.

The experimental studies reveal further that the time during which deceleration is measured with an accelerometer (mounted on the falling ball diametrically across from the point of contact) is only about two-thirds of the contact time predicted by Hertzian quasistatic theory and linear and nonlinear dynamic finite-element analysis. Part of this discrepancy arises from the accelerometer having a finite rise time, but the dynamic finite-element analyses identify an even larger source of discrepancy. In particular, they demonstrate that the accelerometer does not detect contact until some 10 to 20 μs after it first occurs. This is because the stress wave created by the impact takes this length of time to traverse the diameter of the falling ball. The same calculations also reveal that the finite rate of decay of the impact stress waves and of reflections and/or refractions of these waves makes it difficult for the accelerometer to detect the separation of the two balls. Acceleration is thus a poor measure of contact time when dynamic conditions exist. It is evident both from the present experiments and from the accompanying linear and nonlinear analyses that measurement of ball-on-ball impact is heavily influenced by dynamic phenomena and that an impact at even 8 ms^{-1} must be considered as a dynamic rather than a quasistatic event.

Comparison of the linear and nonlinear dynamic finite-element analyses reveals that the onset of even quite small amounts of plastic flow significantly reduces both the peak deceleration and the time during which deceleration is calculated. It is not clear whether this latter decrease represents a true decrease in contact time or merely a more rapid decay of the impact stress waves. Onset of plastic flow also significantly increases the contact radius.

From the finite-element modeling it can be concluded that the contact time in a ball-on-ball impact lies closer to the calculated Hertzian quasistatic value of 150 μs than to the experimental value of 101 μs derived from the output of a shock accelerometer. Nevertheless, a shock accelerometer can provide an accurate estimate of the peak deceleration when its output is properly processed to eliminate the effects of ball harmonics, stress waves, and accelerometer ringing.

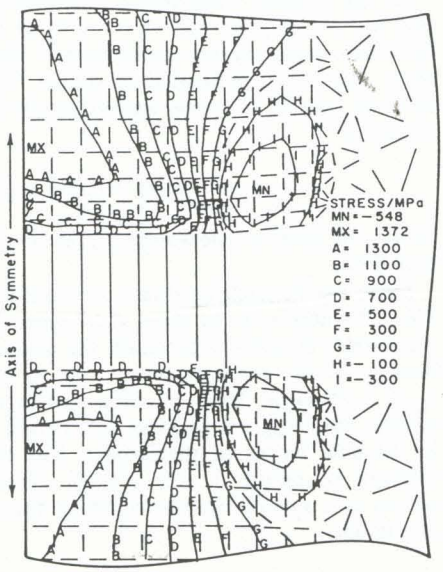

Fig. 13—Elastic-plastic shear stresses in both balls at peak deceleration (steel ball) and peak acceleration (NiHard 4 ball)

Acknowledgment

The author wishes to thank Dr. Norman H. Macmillan for his review of this work, Dr. Clarence Calder of Oregon State University for his contributions to the experimental analysis, and Mr. A.D. Hartman of the Bureau of Mines for his assistance in performing the FFT analyses.

References

1. *Blickensderfer, R. and Tylczak, J.H., "A Large-Scale Impact Spalling Test," Wear,* **84**, *361-373 (1983).*
2. *Blickensderfer, R. and Tylczak, J.H., "Laboratory Tests of Spalling, Breaking, and Abrasion of Wear-Resistant Alloys Used in Mining and Mineral Processing," Bureau of Mines R.I.8968 (1985).*
3. *Blickensderfer, R., et al., "The Effect of Heat Treatment on Spalling of a Cr-Mo White Cast Iron," Wear of Materials 1983, ed. K.C. Ludema, ASME, New York, 471-476 (1983).*
4. *Crook, A.W., "A Study of Some Impacts Between Metal Bodies by a Piezo-Electric Method," Proc. Roy. Soc.,* **A212**, *377-389 (1952).*
5. *Goodier, J.N., Jahsman, W.E. and Ripperger, E.A., "An Experimental Surface-Wave Method for Recording Force-Time Curves in Elastic Impacts," ASME J. Appl. Mech.,* **26**, *3-7 (1959).*
6. *Veillette, P. and Simard, D., "Electric Arc Characterization Using High-Speed Cinematography and Spectroscopy," Proc. 42nd Electric Furnace Conf., AIME, Warrendale, PA, 173-182 (1984).*
7. *Holman, J.P., "Experimental Methods for Engineers," 3rd Ed., McGraw-Hill, New York, 151-158 (1978).*
8. *Thomson, W.T., "Theory of Vibration with Applications," 2nd Ed., Prentice-Hall, Englewood Cliffs, NJ, 48-103 (1981).*
9. *Hunter, S.C., "Energy Absorbed by Elastic Waves During Impact," J. Mech. Phys. Sol.,* **5**, *162-171 (1957).*
10. *deSilva, C.W., "The Digital Processing Acceleration Measurements for Modal Analysis," Shock & Vib. Dig.,* **18** *(10), 3-10 (1986).*
11. *Mitchell, L.D., "Signal Processing and the Fast-Fourier-Transform (FFT) Analyzer,"* EXPERIMENTAL TECHNIQUES, **9** *(10), 3s-15s (1985).*
12. *Timoshenko, S.P. and Goodier, J.N., "Theory of Elasticity," 3rd Ed., McGraw-Hill, New York, 420-422 (1970).*
13. *Kelley, R.D. and Richman, G., "Principles and Techniques of Shock Data Analysis," AD 726219, Shock & Vib. Inf. Center, Naval Res. Lab, Washington, DC, 1-122 (1969).*
14. *Cook, R.D., "Concepts and Applications of Finite Element Analysis," 2nd Ed., John Wiley and Sons, New York, 302-325 (1981).*
15. *Guyan, R.J., "Reduction of Stiffness and Mass Matrices," AIAA J.,* **3**, *380 (1965).*
16. *DeSalvo, G.J. and Gorman, R.W., "ANSYS-Engineering Analysis Systems User's Manual," Revision 4.3, Swanson Analysis Systems, Houston, PA (1987).*
17. *Hauck, J.E., ed., "Materials Selector 74," Metal Progress,* **78** *(4), 22-68 (1974).*

18. Clough, R.W. and Penzien, J., "Dynamics of Structures," McGraw-Hill, New York (1975).
19. Lazan, B.J., "Damping of Materials and Members in Structural Mechanics," Pergamon Press, New York, 79-84 (1968).
20. Deresiewicz, H., "A Note on Hertz's Theory of Impact," Acta Mech., 6, 110-112 (1968).
21. Macmillan, N.H. and Laird II, G., "An Approximate Description of the Temporal Evolution of a Hertzian Impact," Mat. Sci. Eng. A108, 1.1-1.3 (1989).
22. McGannon, H.E., ed., "The Making, Shaping, and Treating of Steel," 9th Ed., US Steel Corp., Pittsburgh, 1202 (1970).
23. Kelly, A. and Macmillan, N.H., "Strong Solids," 3rd Ed., Oxford Univ. Press, 392 (1986).
24. Crepeau, P.N., Antolovich, S.D. and Calboreau, G.A., "Modeling Fracture Toughness in High Chromium White Cast Iron," AFS Trans., 88, 503-510 (1986).
25. Macmillan, N.H., "The Influence of Poisson's Ratio on Hertzian Contact Stress," submitted to J. Mat. Sci. Let. (1988).
26. Tabor, D., "Hardness of Metals," Oxford Univ. Press, 19-94 (1951).

APPENDIX

The Hertzian theory of elastic contact provides a description of the stresses and strains generated in the vicinity of the region of contact between two curved bodies when (1) the dimensions of the contact region are small compared to the principal relative radii of curvature of the bodies and (2) there is no friction at the contact interface. Consider, therefore, the case of two spheres, of radii R_1 and R_2, masses m_1 and m_2, elastic moduli E_1 and E_2, and Poisson's ratios ν_1 and ν_2 impacting along their line of centers with relative velocity V. If sphere 2 is initially stationary relative to some coordinate y, the peak deceleration $\ddot{y}_1$ experienced by sphere 1 is given in the same coordinates by

$$\ddot{y}_1 = \frac{1}{m_1} F_m$$

where F_m is the peak force generated. The Hertzian theory provides

$$F_m = -\left(\frac{5\sqrt{5}}{6}\right)^{2/5} V^{6/5}(m_r)^{3/5}(R_r)^{1/5}(E_r)^{2/5}$$

where

$$\frac{1}{E_r} = \left(\frac{1-\nu_1^2}{E_1} + \frac{1-\nu_2^2}{E_2}\right)$$

$$R_r = \frac{R_1 R_2}{R_1 + R_2}$$

and

$$m_r = \frac{m_1 m_2}{m_1 + m_2}$$

In addition, the contact time t_m is given by

$$t_m = \frac{4\, y_m}{5\, V}\, \beta^{(2/5,\,1/2)}$$

where the complete beta function $\beta^{(2/5,\,1/2)} = 3.5318$ and

$$y_m = \left(\frac{15}{16}\right)^{2/5} V^{4/5}\,(m_r)^{2/5}\left(\frac{1}{R_r}\right)^{1/5}(E_r)^{-2/5}$$

In the present experiments

$$R_1 = 0.03937 \text{ m and } R_2 = 0.0381 \text{ m}$$

$$m_1 = 2.02 \text{ kg and } m_2 = 1.90 \text{ kg}$$

$$E_1 = 207 \text{ GPa}^{22}$$

$$\nu_1 = .28^{23}$$

$$E_2 = 215 \text{ GPa}^{24}$$

$$\nu_2 = .28^{23}$$

Further, the impact velocity V was calculated as 8.02 ms^{-1} from the expression

$$V = (2gh)^{1/2}$$

where g is the acceleration due to gravity (9.806 ms^{-2}) and h is the drop height (3.28 m). Thus, if the motion of ball 2 during the impact is not constrained by the J tube and the other balls within it,

$$F_m = -188.9 \text{ kN},$$

$$\ddot{y}_1 = -91.9 \times 10^3 \text{ ms}^{-2}$$

$$t_m = 150.0\ \mu\text{s}$$

To find the peak values of the stresses generated inside either sphere in the vicinity of the contact region requires knowledge of both the radius a_m of the contact circle and the force F_m acting across this circle at the moment of peak deceleration. The Hertzian quasistatic theory provides

$$a_m = \left(\frac{15}{16}\right)^{1/5} V^{2/5}\,(m_r)^{1/5}\,(R_r)^{2/5}\,(E_r)^{-1/5}$$

and F_m is given above. The maximum compressive stress P_0, which acts at the center of the circle of contact, is then obtained as

$$P_0 = -\frac{3}{2}\frac{F_m}{\pi a_m^2}$$

$$= -\frac{30^{1/5}}{\pi} V^{2/5}\,(m_r)^{1/5}\left(\frac{1}{R_r}\right)^{3/5}(E_r)^{4/5}$$

In the present experiments, therefore, it is predicted that $a_m = 2.85$ mm and $P_0 = -10.88$ GPa. Further, it has been demonstrated numerically[25] that the maximum shear stress τ_{max} generated in sphere i ($i = 1,2$) during such an impact is given approximately by the Hertzian theory as

$$\tau_{max} = |(0.383 - 0.233\ \nu_i) P_0|$$

Hence, in both of the spheres used in this work $\tau_{max} = 3.43$ GPa.

Since the Brinnell hardness of a solid is approximately $5.6\tau_y$,[26] where τ_y is the shear yield stress (i.e., one half the yield stress in uniaxial tension), the quasistatic shear yield stresses of the present spheres are $\tau_{y_1} = 1.31$ GPa and $\tau_{y_2} = 1.25$ GPa. Both of these values are considerably smaller than τ_{max}, suggesting that plastic flow may occur in the later stages of the impact. The first such flow is difficult to detect in this contact geometry because it occurs at a point below the center of the circle of contact, at a depth

$$z = (0.382 + 0.333\,\nu_i) a_\gamma = 0.475 a_\gamma$$

where a_γ is the current radius of the circle of contact.[25]

A Portable Slurry Wear Test for the Field

B. W. Madsen
Bureau of Mines,
U.S. Department of the Interior,
Albany, OR 97321-2198

A new portable slurry wear test apparatus developed by the Bureau of Mines, U.S. Department of the Interior, makes it possible to gather materials wear and corrosion data at a mineral processing site. The portable wear cell is identical in design to a laboratory cell reported previously. It allows simultaneous evaluation of 16 specimens in a continuous flow of fresh slurry. Data obtained from selected metals and polymers showed high-chromium white cast irons to perform particularly well in tests with an aqueous lead-zinc sulfide ore slurry. However, ultra-high-molecular-weight polyethylene that exhibited superior wear resistance in comparable laboratory tests with an aqueous slurry of silica sand did not perform as well in field tests. Such results show how misleading it can be to use laboratory data to predict relative rates of wear in industrial slurries, even under nominally identical flow conditions. Field testing is therefore needed. In situ electrochemical corrosion measurements on a low-alloy steel showed that the field and laboratory slurries were similarly corrosive.

Introduction

The Bureau of Mines is conducting research aimed at reducing the wear and corrosion of mining and mineral processing equipment. Moving minerals in a slurry is an efficient means of transporting them and is used in many mineral processing operations. However, the movement of such slurries can cause significant erosion and corrosion. Erosion is caused by the solid particles striking a container, and corrosion can occur if the liquid reacts chemically with the container. Several studies have been made of erosion-corrosion phenomena (Jackson, 1974; Hoey et al., 1975; Liu and Hoey, 1975; Bass, 1977; Hocke and Wilkinson, 1978; Lebedev et al., 1980; Elkholy, 1983; Moroz, 1983; Singleton and Blickensderfer, 1985), using a variety of experimental methods (Postlethwaite et al., 1974; Postlethwaite, 1981; Tsai et al., 1981; Pitt and Chang, 1985, 1986a, b; Spencer and Sagues, 1987). However, few quantitative measurements have been made in industrial environments. The present author developed a flow-through laboratory apparatus (Madsen, 1985, 1987a; Madsen and Blickensderfer, 1987) that yields constant rates of wear because worn particles are not recycled. This apparatus also permits corrosion measurements to be made during erosion. Such measurements have demonstrated that large synergistic effects can develop between erosion and corrosion (Madsen, 1987b, 1988).

The present study extends the author's work to an industrial mineral processing environment. For this purpose a portable version of the slurry wear apparatus was constructed. The erosion and corrosion of 17 metals and 3 polymers were compared under nominally identical flow conditions in slurries of complex sulfides in mill water and of silica sand in tap water. The new apparatus can be tapped into an industrial slurry flow and left to run for long periods of time. This makes it possible to test at the low velocities of flow (1 to 5 $m \cdot s^{-1}$) often encountered in industrial situations.

Apparatus, Materials, and Procedures

Apparatus. The portable slurry wear test apparatus consists of the cell shown in Figs. 1 and 2 plus a pump, a motor

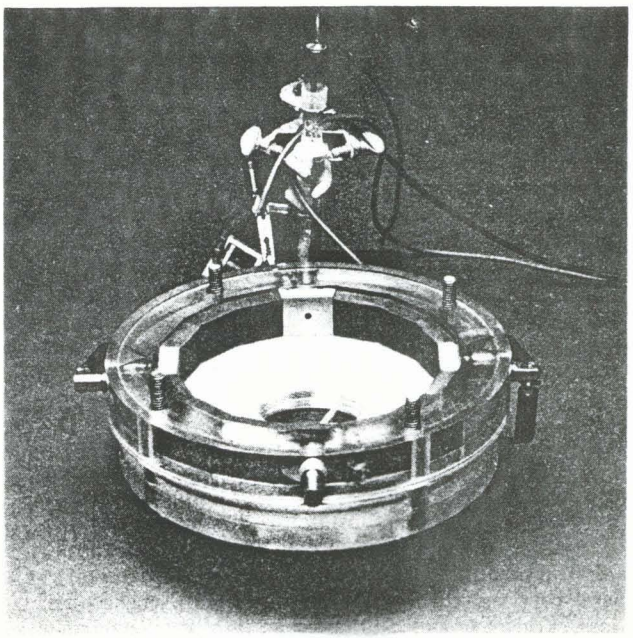

Fig. 1 The wear cell configured for making corrosion measurements

Contributed by the Fluids Engineering Division and presented at the Winter Annual Meeting, Chicago, Ill., November 27-December 1, 1988 of THE AMERICAN SOCIETY OF MECHANICAL ENGINEERS. Manuscript received by the Fluids Engineering Division January 4, 1989.

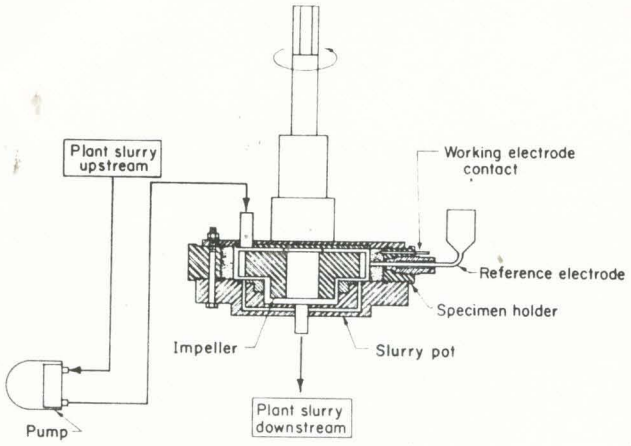

Fig. 2 Schematic diagram of the wear cell

to drive the impeller, a speed controller and velocity indicator, a pH meter, a thermometer, and a strip chart recorder, all mounted on a portable cart as shown in Fig. 3. This cart is equipped with leveling bolts and a lifting eye. To permit electrochemical testing, a potentiostat-galvanostat (EG&G Princeton Applied Research Model 273[1]) and an IBM[1] compatible microcomputer equipped with a National Instruments IEEE-248[1] interface board are also provided. Together, these control the potential applied to the working electrode and measure the resulting current through it. Both the voltage and current are recorded in digital form on magnetic discs for later processing. The potentiostat and the computer are compact and readily portable to facilitate setting up experiments in field environments. The strip chart recorder provides a continuous record of temperature and pH.

Figure 1 shows the wear cell in the configuration used when making corrosion measurements. This cell is common to both the portable and the laboratory versions of the apparatus. During both wear and corrosion testing an impeller moves a continuous stream of fresh slurry past 16 specimens set into the rim. The slurry enters the cell at its perimeter from the top and exits via four radial channels and a central hole in the bottom, Fig. 2. Each specimen is a 10-mm thick plate beveled to fit its neighbors and has a wear surface of 6.66 cm^2 (23.8 mm × 28 mm). Each of the 16 specimens can be a different material. Metal specimens are coated on their nonwearing surfaces with an insulating layer of nylon. Figure 1 also shows the saturated calomel electrode (SCE) used as the reference electrode in the corrosion studies and the Luggin probe connecting it to the slurry through the center of the specimen serving as the working electrode. The cross-sectional area of the Luggin probe is 0.12 cm^2, leaving the area of the working electrode as 6.54 cm^2. The two specimens serving as counter electrodes and their connections are also visible in the photograph. A514 type B steel was chosen for these electrodes because it is a freely corroding material that allows an electric current to pass with little or no resistance. Although some iron

[1]Reference to a specific product does not imply endorsement by the Bureau of Mines.

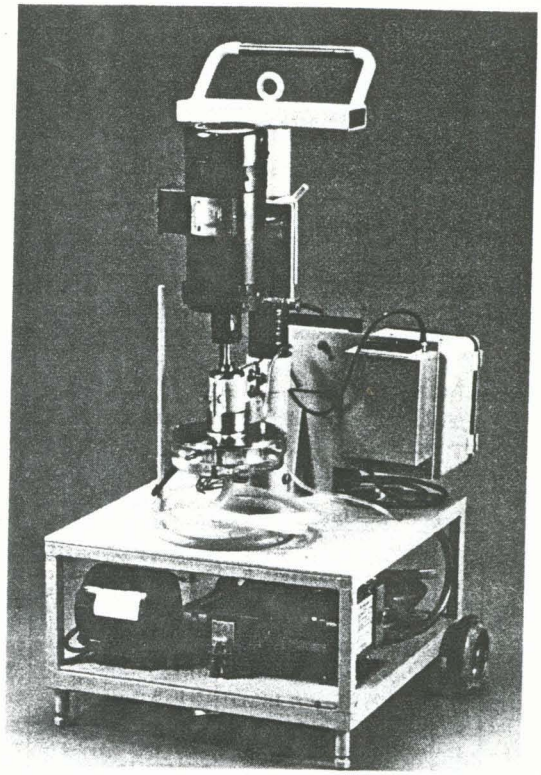

Fig. 3 Portable slurry wear test apparatus

enters the slurry when these electrodes are anodically polarized, the high rate of flow of the slurry minimizes the concentration that can accumulate. The remaining 13 spaces are filled with nonconducting polymeric spacers.

Materials

Specimens. Table 1 summarizes the phase and chemical compositions of all the metals used in the tests. Also included are their Brinell harnesses, as measured using a load of 3 × 10^4 N. Six of the 17 metals tested (Nos. 1, 2a–c, 3, and 4) were white cast irons. These ranged in Cr content from 2 to 20 wt pct. They were variously heat-treated to produce different distributions of carbides in austenitic and/or variously tempered martensitic matrices. Two other cast irons (Nos. 5 and 6) contained no Cr. The alloys containing Cr consisted of flakes of graphite in a pearlitic matrix and those containing no Cr consisted of graphite nodules in a matrix containing both pearlite and cementite. The other six metals (Nos. 7–12) were low alloy steels that were heat-treated to produce variously tempered martensites. In one case (No. 10) the alloy contained a dispersion of fine carbide particles. The final three metals were two high Cr-content austenitic stainless steels (Nos. 13 and 14) and an age-hardened Al alloy (No. 15).

Table 2 lists the some of the properties of the three polymers used. These were a high-density, extra-high-molecular-weight polyethylene (HDPE, No. 16), an ultra-high-molecular-weight polyethylene (UHMWPE, No. 17), and a chlorinated polyvinyl chloride (No. 18).

Nomenclature

A = ampere
K = degree Kelvin
g = gram
h = hour
L = liter
mA = milliampere
min = minute
mL = milliliter
mm = millimeter
mm^3 = cubic millimeter
mV = millivolt
μm = micrometer
μS = microsiemen
pct = percent
s = second
Ω = ohm

Table 1 Phase and chemical compositions and Brinell hardness of the alloys tested

No.	Material	Phase Composition	HB[1], Gpa	Density, g/cm^3	Composition, wt pct								Heat Treatment
					C	Cr	Ni	Mn	Si	Mo	Cu	Al	
	WHITE CAST IRONS												
1	20-2-1 White cast iron	Austenite + M_7C_3 carbides (rod & blade)	6.82	7.76	2.8	20.0	1.00	0.7	0.70	2.0	ND	ND	1285 K, 8h; AC; 815 K, 4h; AC
2a	18-1 White cast iron	Tempered martensite + M_7C_3 carbides (rod & blade)	7.45	7.68	3.43	17.6	0.34	0.86	0.21	1.07	ND	ND	1285 K, 4h; AC; 785 K, 12 h; AC
2b	18-1 White cast iron	Austenite + M_7C_3 carbides (rod & blade)	5.08	7.75	3.43	17.6	0.34	0.86	0.21	1.07	ND	ND	As cast
2c	18-1 White cast iron	Tempered martensite + M_7C_3 carbides (rod & blade)	5.38	7.68	3.43	17.6	0.34	0.86	0.21	1.07	ND	ND	920 K, 12h; AC;
3	Modified NiHard 4	Martensite + M_7C_3 carbides (coarse, dendritic)	5.82	7.72	3.7	9.42	5.31	2.01	1.12	0.66	ND	ND	1050 K, 6h; AC
4	NiHard 1	Austenite + fine globular M_7C_3 carbides	6.53	7.78	3.16	1.36	3.70	0.56	0.25	0.04	ND	ND	720 K, 4h; AC; 550 K, 4h; AC
	OTHER CAST IRONS												
5	Pearlitic high-C cast iron	Pearlite + C flakes	4.40	7.45	3.1	ND	ND	0.70	0.60	ND	ND	ND	1310 K, 2h; WQ
6	Nodular cast iron, 0.45 S	Pearlite + cementite + C nodules	2.85	7.23	2.85	ND	0.4	0.2	1.2	0.1	ND	ND	As cast
	LOW ALLOY STEELS												
7	Abrasion-resistant A	Tempered martensite	4.76	7.84	0.33	0.98	0.14	0.61	0.38	0.20	0.16	0.03	Proprietary
8	Abrasion-resistant B	Tempered martensite	5.34	7.86	0.31	1.84	0.26	0.99	1.64	0.37	ND	ND	Proprietary
9	Low-alloy experimental	Tempered martensite	4.61	7.89	0.23	2.0	0.24	0.45	0.05	0.06	0.29	0.06	1175 K, 1h; WQ; 370 K, 1h; AC
10	AISI 1095	Tempered martensite	4.44	7.86	1.07	<0.1	<0.1	0.30	0.20	<0.1	<0.04	0.04	1175 K, 1h; WC; 370 K, 1h; AC
11	AISI 52100	Lightly tempered martensite + fine M_7C_3 carbides	6.70	7.84	1.05	1.39	0.13	0.34	0.26	<.1	0.12	<0.02	1130 K, 1h; OQ; 370 K, 1h; AC
12	ASTM A514 type B	Heavily tempered martensite	2.69	7.84	0.19	0.50	0.10	0.90	0.30	0.10	0.02	0.03	As received
	OTHER ALLOYS												
13	316 Stainless steel, wrought	Austenite	1.40	8.03	0.04	17.2	12.4	1.6	0.40	2.3	ND	ND	As received
14	Mn-N Stainless steel, (NP599), forged	Austenite	2.29	7.91	0.09	16.4	2.16	8.71	0.41	0.21	0.31	ND	AC from 1470 K
15	6061 - T651 Al alloy (1 Mg)	Al solid solution + Mg_2Si precipitate	0.92	2.67	ND	0.20	ND	ND	0.6	ND	0.28	>97	SHT & aged

[1]HB- Brinell hardness with load of 3 X 10^4 N (3000 kg force)
ND - Not determined; FC - Furnace cooled; AC - Air cooled; WQ - Water quenched; OQ - Oil quenched; SHT - solution heat-treated

Table 2 Properties of the polymers studied

Property	HDPE (No. 16)	UHMWPE (No. 17)	CPVC (No. 18)
Chemical formula	$(CH_2)n$	$(CH_2)n$	$(CH_2\ CHCl)n$
Molecular weight	330,000	$3\times10^6-5\times10^6$	-----
Density, g/cm3	0.933	0.923	1.67
Shore D hardness	63	67	85
Tensile strength at yield, MPa	23	24	45-48*
Ultimate tensile strength, MPa	31	39	55
Young's modulus, MPa	827	760	2480
Flexural modulus, MPa	965	900*	2860
Elongation at yield, pct	5-10*	25	1-5*
Elongation to failure, pct	800	470	2-40*
Fracture toughness, MPa m ½	2-5*	1-2*	2-4*

*Data generic to the class of polymer.

Specimens of both classes of materials were prepared by abrading on dry SiC papers down to 400 grit (38 μm), cleaning ultrasonically in water containing a standard laboratory detergent, and rinsing successively in water and ethanol. They were then dryed in a hot air stream and weighed to the nearest 0.1 mg. Specimens were used several times without re-preparing their surfaces. Previous work (Madsen 1985; 1987a, b; Madsen and Blickensderfer, 1987) has shown that small changes in surface topography do not affect their rates of wear. Corrosion measurements were made only on A514 type B steel specimens. These were prepared in the same fashion as the wear test specimens, except that a hole was drilled in the center of each to provide access for the Luggin probe.

Slurries

The industrial slurry came from a grinding-flotation mill in the Cascade Mountains near Lyons, OR. The particles were smaller than 600 μm and contained chlorite and other clays, calcite and other carbonates, quartz, ferromagnesian silicates, sphalerite, galena, chalcopyrite, pyrite, hematite, and organic matter. The clays accounted for one-third to one-half of the total mass, the harder quartz and ferromagnesian silicates for about one quarter, and the sulfides for about 10 to 20 pct. More than half of the total mass was in the minus 325-mesh size fraction, and less than 1 percent was coarser than 50 mesh. The pH varied between 7.36 and 7.8 and the specific conductance was $\sim 65\ \mu S \cdot m^{-1}$. The solids content of the slurry varied no more than 1 wt pct during any one test. Between tests, however, this parameter varied from 19 to 25 wt pct. In general, the particles in this slurry exhibited sharper edges and corners and a more angular shape than did the silica sand particles in the laboratory slurry. This latter slurry consisted of 2 wt pct of 212- to 300-μm (minus 50- to plus 70-mesh) American Foundryman's Society (AFS) silica sand in tap water.

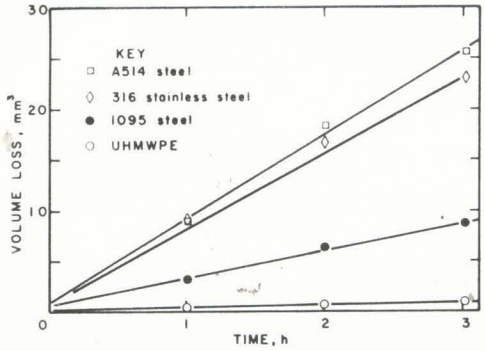

Fig. 4 Typical data from a laboratory wear test conducted at 294 K using an impeller tip speed of 12 m•s^{-1}. The slurry was 2 wt pct AFS silica sand in tap water.

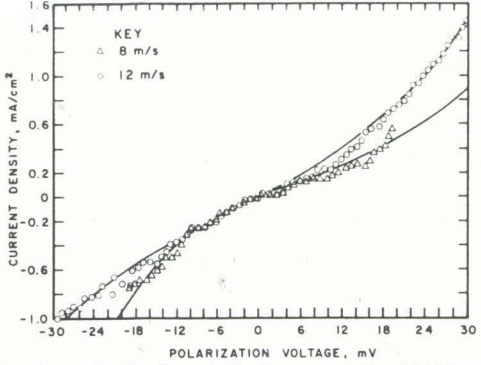

Fig. 5 Anodic and cathodic polarization curves for A514 type B steel exposed to the field slurry at impeller tip speeds of 8 and 12 m•s^{-1}

When making electrochemical corrosion measurements in the laboratory slurry, 0.06M Na_2SO_4 was used instead of tap water. The specific conductance was thereby raised to ~50 μS•m^{-1}, reducing the drop in potential through the slurry. Previous work (Madsen, 1987b) has shown that the use of this low concentration of sodium sulfate does not affect wear rates.

Procedures

Wear Testing. Both the field and the laboratory tests were conducted at 294 K at a flow rate of 4500 mL•min^{-1}. This rate was controlled by the slurry feed pump and was independent of the motion of the impeller. At this flow rate the retention time of the slurry in the wear cell was ~2 s. In both environments, tests were conducted at impeller tip speeds of 8 m•s^{-1} and 12 m•s^{-1}. Field test A lasted for 208 min and used the lower speed and a slurry containing 25 wt pct solids. Field test B, which used a slurry containing 19 wt pct of solids, was run for 98 min at the higher speed. All laboratory tests lasted for 3 h and were interrupted at 1 h intervals to monitor mass loss. Before reweighing, worn laboratory test specimens were cleaned and dried in the same fashion as they were initially. The worn field test specimens were dried at the test site with a paper towel. They were then returned to the laboratory for cleaning, drying, and weighing according to the standard protocol. Wear rates were expressed conventionally as volume loss per unit time. This was calculated for the field tests as the ratio of total volume loss to test time, and for the laboratory tests as the slope of a plot of volume loss versus test time. This slope was determined by linear regression. Two or three A514 type B steel specimens were included in each test to provide an indication of experimental scatter.

Corrosion Testing

Polarization scans were made in both field and laboratory slurries. The field slurry contained 15 wt pct of solids and the laboratory slurry 2 wt pct. Impeller tip speeds ranged from 4 to 14 m•s^{-1}. The scanning rate was always 1 mV•s^{-1} and the range of potential scanned was from about −30 mV to +30 mV relative to the open circuit corrosion potential (E_c). At each current density ($j = I/A$, where I is the current and A the area of the working electrode), the polarization voltage ϕ was calculated from the measured voltage by subtracting the product IR. R is the resistance of the path through the solution between the reference and working electrodes. Previous work (Madsen, 1987a, b) has shown it to remain constant at ~1 Ω over the narrow range of potential involved. The corrosion current (I_c) and current density ($j_c = I_c/A$) at the corrosion potential (i.e., when $\phi = 0$) were then calculated by using nonlinear regression (Mansfeld, 1973; Gerchakov et al., 1981; Rocchini, 1987; Madsen, 1988) to fit the polarization data to the equation

$$I = I_c\,[\exp(2.303\,\phi/B_a) - \exp(-2.303\,\phi/B_c)], \qquad (1)$$

where B_a and B_c are the anodic and cathodic Tafel slopes, respectively.

Results

Wear. The results of the field tests are summarized in Table 3, with the specimens ranked according to increasing wear rate. Note that a somewhat different partial suite of materials was used at each impeller tip speed, and that a white cast iron is at the top of the list. Increasing the impeller tip speed from 8 to 12 m•s^{-1} and the solids content of the slurry from 19 to 25 wt pct increased the rates of wear of the polymers by a factor of 2 to 4X. A514 type B steel was the only metal field-tested at both speeds, and for this material the increase in speed and solids content resulted in a 3.7-fold increase in wear rate.

Figure 4 shows typical data obtained in laboratory tests conducted at 12 m•s^{-1}. Note the linearity of the data for each material. Table 3 presents wear rates obtained for the full complement of 20 materials from experiments conducted at impeller tip speeds of 8 and 12 m•s^{-1} in laboratory slurries which did not contain sodium sulphate. Where more than one specimen of any given material was tested, the wear rate is quoted as the mean plus and minus one standard deviation. Note that raising the impeller tip speed from 8 to 12 m•s^{-1} increases the wear rates of the polymers by 2 to 4X and those of the metals by 4 to 9X. As a result, the change in impeller tip speed changes the ranking of the test materials. Note also the excellent performance of ultra-high molecular weight polyethylene at both speeds.

Corrosion. Figure 5 shows the experimental data obtained from the polarization scans and the curves fitted to these via equation (1). Average values of B_a and B_c were 68 and 66 mV per decade of current in the field tests and 54 and 100 mV per decade of current in the laboratory tests, respectively. Table 4 summarizes the corresponding values of E_c and corrosion rate. The latter values were obtained by using Faraday's law to convert j_c to units of mm^3•h^{-1} as described in the Discussion section. Note that increasing the impeller tip speed shifts E_c to a more negative value in both slurries, that E_c is slightly more negative in the field test slurry than in the laboratory slurry at low impeller tip speeds, and that the corrosion rate does not vary much at impeller tip speeds greater than 4 m•s^{-1}.

Discussion

The results reported in Table 3 exhibit two striking features. The first is the order of magnitude higher wear rate exhibited by the polymers in the field tests than in the laboratory tests. The percentage increase is comparable for all three polymers at both 8 and 12 m•s^{-1}, although the lower speed field test was conducted in a significantly less dense slurry than was the

Table 3 Wear rates measured in field and laboratory tests

No.	Material	Wear rate, $mm^3 \cdot h^{-1}$		
		Field Test A, 25 wt pct solids, 8 $m \cdot s^{-1}$	Laboratory tests @ 2 wt pct solids	
			8 $m \cdot s^{-1}$	12 $m \cdot s^{-1}$
2b	18-1 White cast iron	0.33	0.17	0.70
2a	18-1 White cast iron	0.56	0.14	0.85
4	NiHard 1	0.79	0.35	1.36
2c	18-1 White cast iron	0.82	0.22	0.89
14	Mn-N Stainless steel	0.95	1.67	7.82
9	Low-alloy experimental steel	1.01	1.33	5.39
7	Abrasion resistant steel A	1.10	1.00	4.07
17	UHMWPE	1.11	0.07 ± 0.07	0.18 ± 0.12
12	A514 type B steel	1.73 ± 0.03	1.93 ± 0.19	8.44 ± 0.46
6	Nodular cast iron	1.84	1.58	6.64
16	HDPE	2.63	0.30 ± 0.11	1.01 ± 0.25
18	CPVC	12.0	1.66 ± 0.45	6.56 ± 1.90
		Field Test B, 19 wt pct solids, 12 $m \cdot s^{-1}$		
1	20-2-1 White cast iron	1.39	0.08	0.75
3	Modified NiHard 4	1.97	0.11	0.98
17	UHMWPE	2.63	0.07 ± 0.07	0.18 ± 0.12
11	AISI 52100 steel	2.98	0.36	2.21
10	AISI 1095 steel	3.40	0.53	2.68
8	Abrasion resistant steel B	4.11	0.60	3.58
5	Pearlitic high C cast iron	4.36	0.43	2.74
13	316 Stainless steel	5.55	1.30	6.96
12	A514 type B steel	6.44 ± 0.28	1.46 ± 0.06	8.40 ± 0.55
16	HDPE	8.56	0.30 ± 0.11	1.01 ± 0.25
15	6061-T651 Al	32.8	6.44	31.31
18	CPVC	47.4	1.66 ± 0.45	6.56 ± 1.90

Table 4 Corrosion potentials and rates for A514 type B steel as function of slurry type and impeller tip speed. Values given for E_c are within 1 mV unless otherwise stated.

Impeller tip speed, $m \cdot s^{-1}$	E_c, mV vs SCE		Corrosion rate, $mm^3 \cdot h^{-1}$	
	Field slurry	Laboratory slurry	Field slurry	Laboratory slurry
0*	< −600	< −600	ND	0.053 ± 0.037
4	−494	−470	<0.148	0.282 ± 0.093
8	−494	−475	0.218 ± 0.121	0.138 ± 0.065
12	−515	−492	0.208 ± 0.040	0.130 ± 0.014
14	−515	−515	0.211 ± 0.062	0.212 ± 0.003
16	ND	−525	ND	0.155 ± 0.050

ND Not determined
*With slurry feed pump and impeller shut off. The value of E_c drifted under these conditions between −600 and −630 mV versus SCE.

higher speed field test. Evidently, the wear rates of the polymers are not markedly dependent on solids content in such dense slurries. In contrast to the polymers, the metals exhibited smaller and less consistent changes in wear rate in response to the same change in slurry. Those high-chromium, high-carbon content materials containing large volume fractions of carbide particles—the white cast irons, NiHard I and modified NiHard 4—wore about twice as fast in the field tests as in the laboratory tests at both 8 and 12 $m \cdot s^{-1}$. In contrast, both the high-chromium, low-carbon, austenitic materials (316 stainless steel and the Mn-N stainless steel) and the low-chromium cast irons and steels showed less variation in wear rate with change in slurry. Indeed, both A514 type B steel and the low-alloy experimental steel exhibited less wear in the field test slurry than in the laboratory slurry when tested at 8 $m \cdot s^{-1}$. 316 stainless steel did the same when tested at 12 $m \cdot s^{-1}$. The 6061-T 651 Al alloy also showed little change of wear rate with slurry type.

The polymers do not corrode in either the field or the laboratory tests. Therefore, their order-of-magnitude-higher wear rate in the former suggests that the two kinds of slurry particles lead to different mechanisms of erosion. Examination of the eroded surfaces revealed the presence of fine shavings on the surfaces of the polymeric specimens used in the field tests. This suggests that the more angular particles present in the field slurry cause more micromachining (type II cutting) and less plowing and/or type I cutting than do the rounder AFS sand particles (Finnie, 1958; Hutchings, 1979).

From Faraday's law, the density of A514 type B steel (7.86 × 10^3 $kg \cdot m^{-3}$), and the area (A) of the working electrode (6.54 cm^2), it follows that a corrosion current density of 1 $mA \cdot cm^{-2}$ is equivalent to a volume loss rate of 0.86 $mm^3 \cdot h^{-1}$. In all of the present experiments the oxygen content of the slurry was close to the solubility limit of ~9 × 10^{-6} $g \cdot g^{-1}$ (Dean, 1973). At the chosen flow rate of 4500 $mL \cdot min^{-1}$ this is enough to sustain a corrosion current density of ~1270 $mA \cdot cm^{-2}$ (~1090 $mm^3 \cdot h^{-1}$). Thus the measured corrosion rates reported in Table 4 suggest that ≤0.02 percent of the available oxygen was ever consumed.

The lack of any systematic variation of corrosion rate with increase in impeller tip speed above 4 $m \cdot s^{-1}$ suggests that in both slurries the corrosion reaction is under activation control (Fontana and Greene, 1978). In contrast, the rate of corrosion of A514 type B steel in stationary, near-neutral aqueous solutions is cathodically controlled by the rate of diffusion of oxygen to the corroding surface (Fontana and Greene, 1978). The observation that E_c never shifts far enough in the positive direction for passivation to occur (Wranglen, 1985) is also consistent with the suggestion that the present reaction is under

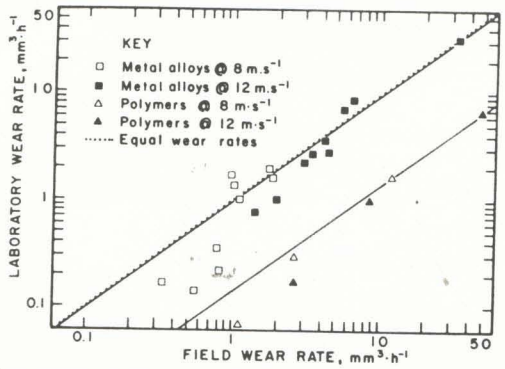

Fig. 6 Comparison of the wear rates measured in the field and laboratory tests

activation control. However, it is not clear why E_c becomes more negative at the highest impeller tip speeds. Perhaps erosion-induced surface roughening increases either the anodic and/or the cathodic exchange current density, leading to reduced activation polarization of either or both electrode processes (Fontana and Greene, 1978). Alternatively, the shift may have a hydrodynamic origin, perhaps related to increased turbulence at higher impeller tip speeds.

Comparison of the appropriate data from Tables 3 and 4 also suggests that, in the case of A514 type B steel, corrosion accounted for no more than 10 percent of the volume loss measured in either slurry at an impeller tip speed of 8 $m \cdot s^{-1}$ and for only 2–3 percent of that measured at 12 $m \cdot s^{-1}$. However, previous cathodic protection studies carried out in the laboratory slurry (Madsen, 1987b) show that passing a positive current through the slurry from the counter electrodes to the working electrode reduces the wear rate. For example, passing a positive current of density ≥ 25 $mA \cdot cm^{-2}$ reduces the rate of wear of A514 type B steel from 28 to 19 $mm^3 \cdot h^{-1}$ at an impeller tip speed of 15.6 $m \cdot s^{-1}$. Thus corrosion appears to have a much bigger effect on erosion than does erosion on corrosion.

The mechanism(s) responsible for this synergism is (are) as yet far from clear. Nevertheless, the results obtained to date do lead to two conclusions. First, similar values of the corrosion rates were measured in slurries containing insulating quartz sand particles and slurries containing semiconducting sulfide ore particles. This shows that the net effect of any galvanic corrosion processes occurring during contact of slurry particles with the working electrode is small. Second, 0.06*M* Na_2SO_4 does not affect wear rates (Madsen, 1987b). This shows that any precipitation of iron sulfate at or near the surface of the working electrode is likewise unimportant.

To end on a more practical note, attention is drawn to the plot of wear rates in the laboratory tests (y) versus wear rates in the field tests (x) presented in Fig. 6. The dotted line represents equal rates of wear in the two tests ($y = x$) and the two solid lines were drawn by using the least squares technique to fit separate equations of the form $y = ax$ to the data obtained from the metallic and polymeric specimens. It is clear that there is a better correlation between the two rates at the higher impeller tip speed. Figure 6 also emphasizes the much greater variation of wear rate with slurry type exhibited by the polymers as compared to the metals: the line fitted to the data obtained from the polymers lies much farther from the dotted line than does the line fitted to the data obtained from the metals.

Conclusions

Field testing remains a necessary part of the reliable selection of materials to resist the combined effects of slurry erosion and corrosion. The advantage of the present, portable apparatus is that it permits the erosive and corrosive effects of industrial slurries to be determined at the flow velocities of greatest interest under reproducible flow conditions. This is done without having to transport large quantities of such slurries to a distant laboratory. The disadvantage is that the test does not, in general, duplicate the flow conditions characteristic of the industrial application. For this reason it may fail to predict correctly the relative service lives of different materials. However, since the actual slurry of interest is used, the predictions made are likely to be better than those obtained in tests with a substitute slurry.

Acknowledgments

The author wishes to thank his colleagues for their support and encouragement. He gives special thanks to Darrell P. Hoskins, physical science technician, for his sustained efforts in conducting the slurry wear tests. He is also grateful to the owners and operators of the Shiny Rock Mining Company, in particular George Atiyeh and Joe Webber, for the use of their grinding-flotation mill facilities near Lyons, OR.

References

Bass, M. L., 1977, "Erosion-Corrosion of Cast Pump Alloys," presented at Pacific Northwest Metals and Minerals Conf., Seattle, WA. 24 pp. Available from BuMines, Albany Research Center, 1450 Queen Avenue SW, Albany, OR 97321, USA.

Dean, J. A. (ed.)., 1973, *Lange's Handbook of Chemistry*, 11th Edition, McGraw-Hill, New York, NY, pp. 10–7.

Elkholy, A., 1983, "Prediction of Abrasion Wear for Slurry Pump Materials," *Wear*, Vol. 84, pp. 39–49.

Finnie, I., 1958, "The Mechanism of Erosion of Ductile Metals," *Proc. 3rd U.S. National Congress of Applied Mechanics*, ed. by R. M. Haythornthwaite, ASME, New York, NY, pp. 527–532.

Fontana, M. G., and Greene, N. D., 1978, *Corrosion Engineering*, McGraw-Hill, New York, NY.

Gerchakov, S. L., Udey, L. R., and Mansfeld, F., 1981, "An Improved Method for Analysis of Polarization Resistance Data," *Corrosion*, Vol. 37, p. 696.

Hocke, H., and Wilkinson, H. N., 1978, "Testing Abrasion Resistance of Slurry Pipeline Materials," *Tribology Int.*, Vol. 5, pp. 289–294.

Hoey, G. R., Dingley, W., and Freeman, C., 1975, "Corrosion Inhibitors Reduce Ball Wear in Grinding Sulfide Ore," *CIM Bull.*, Vol. 68, pp. 120–123.

Hutchings, I. M., 1979, "Mechanisms of the Erosion of Metals by Solids Particles," *Erosion: Prevention and Useful Applications*, ASTM STP 664, ed. by W. F. Adler, ASTM, Philadelphia, PA, pp. 59–76.

Jackson, L. D. A., 1974, "Controlling Abrasion in Slo (sic) Slurry Pipeline Systems," *Can. Min. J.*, Vol. 95, pp. 42–45.

Lebedev, A. N., Shchyerbakov, O. B., and Balashov, G. V., 1980, "Corrosive and Erosive Wear of Steel in Ore Milling Equipment," *Zashch. Met.*, Vol. 16, pp. 327–330.

Liu, A. W., and Hoey, G. R., 1975, "Mechanisms of Corrosive Wear of Steel Balls in Grinding Hematite Ore," *Can. Met. Quart.*, Vol. 14, pp. 281–285.

Madsen, B. W., 1985, "A Study of Parameters Using a New Constant-Wear-Rate Slurry Test," *Wear of Materials 1985*, ed. by K. C. Ludema, ASME, New York, NY, pp. 345–354.

Madsen, B. W., 1987a, "Measurement of Wear and Corrosion Rates Using a Novel Slurry Wear Test Apparatus," *Materials Performance*, Vol. 26, No. 1, pp. 21–28.

Madsen, B. W., 1987b, "Measurement of Erosion-Corrosion Synergism With a Slurry Wear Test Apparatus," *Wear of Materials*, 1987, ed. by R. C. Ludema, ASME, New York, NY, pp. 777–786.

Madsen, B. W., 1988, "Synergism Between Electrochemical Corrosion and Slurry Wear," *Proc. 43rd NACE Annual Conf.*, NACE, Houston, TX, Vol. 3, pp. 242/1–242/15.

Madsen, B. W., and Blickensderfer, R., 1987, "A New Flow-Through Slurry Erosion Wear Test," *Slurry Erosion: Uses, Applications, and Test Methods*, ASTM STP 946, ed. by J. E. Miller and F. E. Schmidt, Jr., ASTM, Philadelphia, PA, pp. 169–184.

Mansfeld, F., 1973, "Tafel Slopes and Corrosion Rates From Polarization Resistance Measurements," *Corrosion*, Vol. 29, p. 397.

Moroz, P., 1983, "Wear Mechanisms in Steel and White Iron Grinding Balls in Wet Ore Grinding Applications," presented at Post Deadline Session, Int. Conf. on Wear of Materials, Reston, VA.

Pitt, C. H., and Chang, Y. M., 1985, "Electrochemical Determination of Erosive Wear of High Carbon Steel Grinding Balls," *Min. and Met. Proc.*, Vol. 2, pp. 166–173.

Pitt, C. H., and Chang, Y. M., 1986a, "Corrosive-Erosive Wear of Grinding Ball Metals at High Jet Velocities," *Proc. 41st NACE Annual Conf.*, NACE, Houston, TX, Vol. 3, pp. 232/1–232/15.

Pitt, C. H., and Chang, Y. M., 1986b, "Jet Slurry Corrosive Wear of High-Chromium Cast Iron and High-Carbon Steel Grinding Ball Alloys," *Corrosion*, Vol. 42, pp. 312.

Postlethwaite, J., 1981, "Direct Measurement of the Corrosion Current for Oxygen-Reduction Corrosion," *Electrochemical Corrosion Testing*, ASTM STP 727, ed. by F. Mansfeld and U. Bertocci, ASTM, Philadelphia, PA, pp. 290–302.

Postlethwaite, J., Tinker, E. B., and Hawrylak, M. W., 1974, "Erosion-Corrosion in Slurry Pipelines," *Corrosion*, Vol. 30, pp. 285–290.

Rocchini, G., 1987, "A Computerized Tool for Corrosion Rate Monitoring," *Corrosion*, Vol. 43, p. 326.

Singleton, D. J., and Blickensderfer, R., 1985, "Wear and Corrosion of 12 Alloys During Laboratory Milling of Phosphate Rock in Phosphoric Acid Waste Water," RI 8919, U.S. Bureau of Mines, Washington, DC.

Spencer, D. K., and Sagues, A. A., 1987, "Erosion by Sand and Coal Slurries," *Corrosion-Erosion Wear of Materials at Elevated Temperatures*, ed. by A. V. Levy, NACE, Houston, TX, pp. 367–385.

Tsai, W., Humphrey, J. A. C., Cornet, I., and Levy, A. L., 1981, "Experimental Measurement of Accelerated Erosion in a Slurry Pot Tester," *Wear*, Vol. 68, pp. 289–303.

Wranglen, G., 1985, *An Introduction to the Corrosion and Protection of Metals*, Chapman and Hall, London, England.

88 312

Concentration of Silicon Carbide with a Density Separation Process

Johan M. Versteegen and Wijnand L. Dalmijn

Delft University of Technology
Department of Raw Materials Processing
P.O. Box 5028
2600 GA Delft
The Netherlands

During the production of silicon carbide a by-product is generated, which contains a mixture of crystalline and amorphous silicon carbide. Utilizing the difference in density, shape and surface properties of the crystalline and amorphous silicon carbide, separation tests were carried out with gravity concentration and flotation equipment. The flotation results of the fine fraction of the silicon carbide mixture were not encouraging. The processing of the coarse fraction of the silicon carbide mixture by jigs resulted in a high grade crystalline SiC concentrate with the desired specifications. The separation was largely influenced by the shape factor. An IHC-jig with a newly designed hydraulic drive was used to carry out the test program.

INTRODUCTION

Silicon carbide has a large field of technical applications, because of its outstanding chemical, physical and mechanical properties. For this reason it is an important material for abrasive, conductive and refractory materials and ceramics. The production of silicon carbide is carried out by electrical heating of a mixture of sand and petroleum coke in a modified Acheson furnace (figure 1) according to the following reaction:

$$SiO_2 + 3\,C \longrightarrow SiC + 2\,CO$$

Due to the temperature gradient inside the furnace two silicon carbide products are generated. A crystalline product, called SiC, which consists of about 96% α-SiC and 4% β-SiC, and an amorphous silicon carbide material, called Asg (Amorph schwarz grun), consisting mainly of β-SiC, with minor inclusions of α-SiC. The SiC product has wider industrial applications than Asg and is more valuable. During the recovery of the furnace product via shovels and hydraulic hammers these products are partly mixed, because of the irregular interface between both products. This mixture can only be sold as low grade material for metallurgical purpose. Extraction of the SiC fraction would be advantageous. Elektroschmelzwerk Delfzijl B.V., The Netherlands, a manufacturer of silicon carbide, produces annually 20.000 ton of this low grade mixture. At Delft University of Technology tests were carried out, to extract the high grade SiC product out of this mixture.

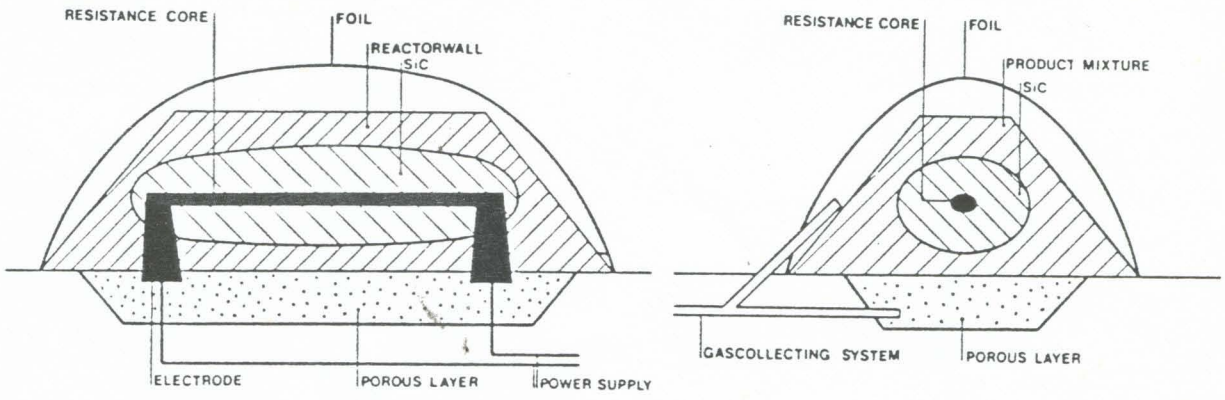

Figure 1. Cut through silicon carbide furnace.

Product analysis

The recovery of the furnace product is based on the clearly visible difference in appearance between SiC and Asg. The SiC is transported to West-Germany, where after leaching, grinding and screening a quality control by fire treatment is carried out on testing bars of SiC, in order to reveal contaminations such as iron. Incidentally the SiC is analysed by XRD, in order to determine the content of α-SiC. The Asg, which is crushed in Delfzijl is analysed on the chemical content of silicon carbide, in behalve of the customer's specifications.

A reliable quantitative analysis is important for the interpretation of the testwork. Since both SiC and Asg have the same chemical formula, a

chemical or XRF analysis is not possible. B. Ziemer (1979) developed a new method, in which reflection intensity combinations of XRD are measured. A function of these intensity combinations was reported as linear, and only depending on the SiC content. In our analitical testwork a clear influence of texture and structural faults of SiC was found. The analysis of SiC was additionally handicapped by contamination of wolfram carbide of the grinding apparatus. For these reasons it was decided to use handsorting as the only practical method left to determine the SiC content. All reported values were detemined in this way.

Product quality

The crystalline SiC after separation can only be sold as high grade product if it meets the specifications required by the customer. First of all the minimum content of crystalline SiC has to be 96% . Material from the furnace walls or crust must be avoided because this grey-white crustmaterial will cause weak spots in the end products, e.g., abrasive wheels or heat conductors. The density of this material does not differ significantly from SiC and Asg and has to be removed by handsorting during production before the gravity separation process. The remaining contamination may consist of silicon dioxide and graphite, which can be removed by leaching. The end product is also sensitive for contamination by metals such as iron.

SEPARATION

As the furnace is emptied large fragments of 30-40 cm are generated. The crystalline SiC is directly transported to West-Germany, where it is leached to remove the silicon dioxide and graphite. For all the various applications the SiC has to be ground and screened to a size less than a few mm. The mixture of Asg and SiC is further processed in Delfzijl. First the product is crushed to a maximum size of 20 mm by a jaw crusher. The next size reduction depends on the customer's specifications. Figure 2 shows the present size distribution after the jaw crusher. The low grade mixture contains both fine and very coarse particles. Due to the fact that this material is only saleable if strict size specifications are met, it is not recommended to grind for the separation process all the material to a smaller more uniform size range. For this reason different methods of separation are to be considered. The physical properties of silicon carbide, such as electrical and magnetic, do not permit a separation based on them. Since the surface of SiC consists of a thin layer of silicon dioxide, flotation of the SiC is possible, using collectors that are used for quartz flotation. The flotation was a feasable option (ESD, 1982). A closer study of the results and the method of analysis, however, showed that the applied chemical analysis was inadequate for an evaluation of the obtained results. For this reason new flotation tests were carried out. The results of these new tests were not encouraging. Despite the clearly visible optical difference in surface structure at the different particles, no significant separation of SiC and Asg was found with the flotation process. Also the measurement of the zeta-potentials indicated that separation would be very difficult, since all obtained values of the zeta-potential of SiC and Asg lay between -20 and -80 mV. Tests with a heavy medium cyclone circuit (ESD, 1980), based on difference in density, showed that the separation of Asg and SiC was very well possible. Unfortunately, the FeSi of the applied heavy medium caused an intolerable iron contamination of the SiC product, which could not be removed by thorough and repeated washing. For this reason the testwork had to be concentrated on the gravity separation of the coarse fraction by jigging.

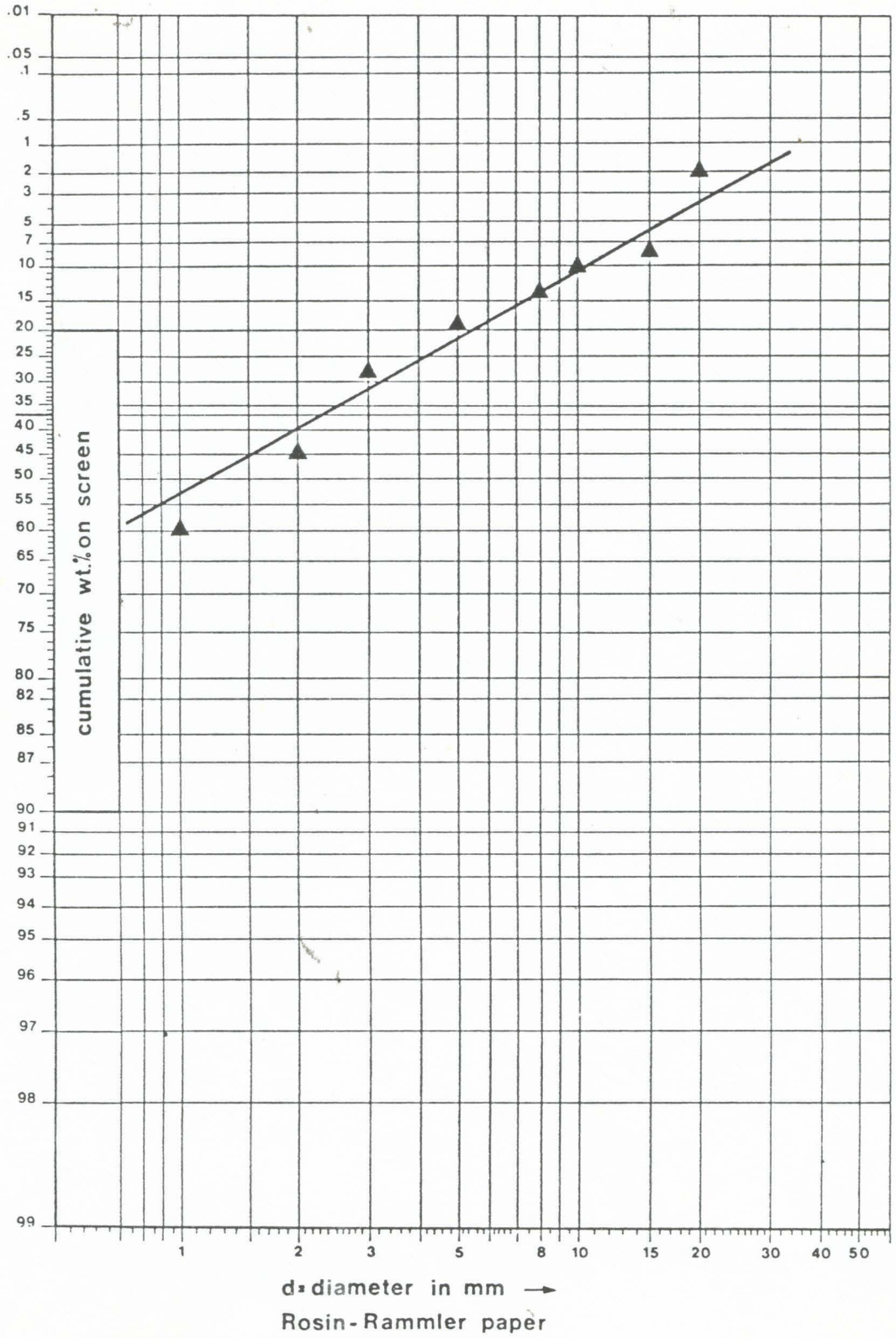

Figure 2. Size distribution of SiC/Asg-mixture after jaw crushing.

Tests and results

Gravity separation is based on the difference in density, shape and size between the materials. The testmaterial had a density of 3.14-3.22 g/cm^3 for SiC and 2.66-2.99 g/cm^3 for Asg, which is in agreement with values given by Wecht (1977). All tests were carried out in an IHC-jig with a newly designed hydraulic drive, shown in figure 3. The jig, which has a bed surface of 50 x 50 cm^2, was operated in a batch mode to limit wear of the piping and pumps.

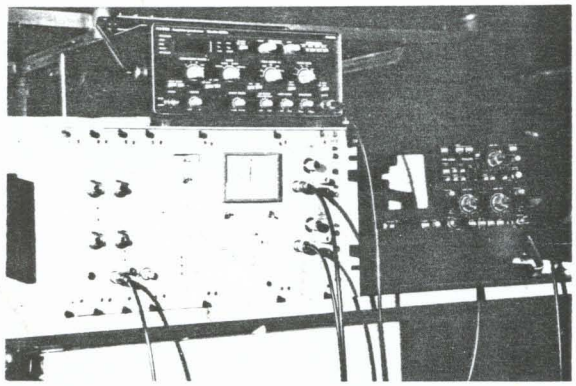

Figure 3[a]. (above)
Control equipment for hydraulic drive.

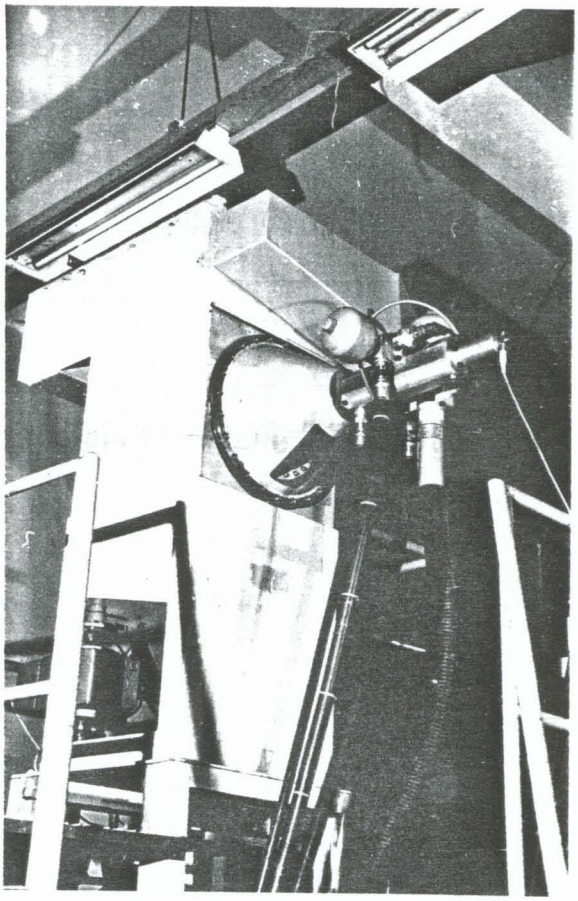

Figure 3[b]. (right)
IHC-Jig and hydraulic drive.

The hydraulic drive made an accurate setting of the stroke, frequency and waveform possible. This permits a high reproducebility of the tests. Apart from the generally used sinus wave, other waveforms as block or saw-tooth can be generated by this drive. The stroke can be varied from 0 to 5 cm and the frequency from 0 to 100 Hz, although at frequencies higher than 1.67 Hz the stroke is restricted to prevent damage of the jig membrane.

The jiggability of a material mixture is according to Schubert (1978) represented by the quotient q:

$$q = \frac{D_h - D_m}{D_l - D_m}$$

In which: D_h = density of heavy material
D_l = density of light material
D_m = density of medium (water)

At values of q < 1.5 the jigging becomes more difficult and a lower limit of 1.25 has been indicated (Schubert, 1978). The q value of the testmaterial was approximately 1.3. This means that jigging is difficult. Moreover, the shape factor of the material further aggrevated the jiggability. For this reason jigging tests were carried out with a small size interval of 3-8 mm as feed, which contained about 70% crystalline SiC. The hydraulic drive was, in accordance with Schubert (1978) and Uhlig (1974), set for a sinus wave with a frequency of 2.67 Hz and a stroke of 23 mm. The hutch water amounted to 0.37 liter per second. The thickness of the jigbed amounted to 30-32 mm. After 4 minutes of jigging the jigbed was divided in a top and bottom product, each with about the same mass.

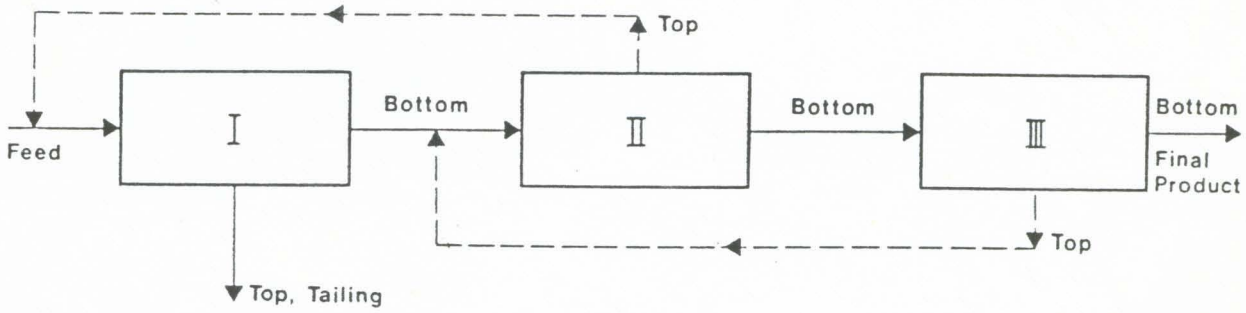

Figure 4. Flowsheet of the process in the computer simulation.

This was repeated until enough bottom product was obtained for further jigging. Figure 4 shows the scheme of the testwork. The bottom product of the third step was the final concentrate. To simulate recirculation of the top product, a computer program was written. This is shown by the dotted lines of figure 4. The simulation gave a final concentrate with a crystalline SiC content of 96.6% and a recovery of 40%. This product met the required specifications. The chemical analysis of the feed, high grade crystaline SiC and jigged final concentrate are shown in table 1, confirming that the final conctrate closely approaches the crystalline SiC. It should be kept in mind that the percentages in table 1 only represent the chemical content of silicon carbide and do not distinguish α- and β-SiC.

During the first tests it became clear that the separation result, and thus the maximum grade, strongly depended on the shape factor of the particles, and further studies were carried out to include the shape factor. The length/width ratio of the particles, shown in figure 5, was chosen as parameter for the comparison between top and bottom of the jigbed. This l/w-ratio was determined by a Joyce Loebl Magiscan Image Analyser. The particles were glued on glass plates and scanned with the help of a video camera. The analogue signal of this image is digitalized and the obtained data is in

Table 1. Chemical analysis of feed, crystalline SiC and jigged concentrate

product	% silicon carbide	% free carbon
feed	87.77	5.83
concentrate	95.58	0.78
crystalline SiC	96.48	0.37

convolution models processed by the computer, using the x-, y-axis and grey value of the particles as main parameters.

The length/width ratio of the SiC varied over the height of the bed, whereas the Asg had a constant average value of 1.32. Figure 6 shows the change of the l/w-ratio after 4 minutes jigging. The jigging causes an increase of the percentage of the SiC particles with small l/w-ratio in the bottom of the bed. This means that SiC with a high l/w-ratio has moved to the top of the bed.

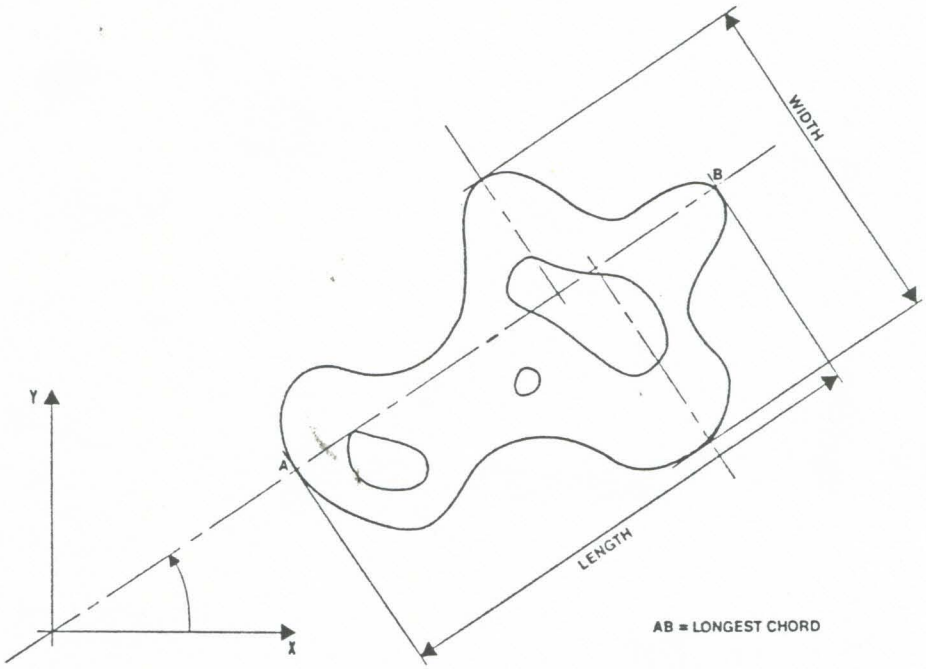

Figure 5. Definition of particle shape.

The l/w-ratios of the feed are expected to lay between the values of top and bottom product, and the intersection of feed, top and bottom has to be in one single point. The deviations from these ideal curves are caused by sample preparation and prefered orientation of the particles on the glass plates. Samples taken from the bottom of the bed were screened at 2, 3, 4 and 6 mm, and analysed by handsorting. After three jigsteps at 4, 8 and 12 minutes, three extra tests were carried out under the same conditions, at 2, 3 and 5

minutes. In table 2 are given the mass percentage of each screened fraction of SiC and the corresponding l/w-ratio. With these percentages and intervals of the l/w-ratio of SiC of 1.5-1.8, 1.8-2.0 and 2.0-2.2 a mass balance over the bed can be made. With this mass balance the percentage of the feed which has gone to the top of the bed is calculated for each interval of l/w-ratio. These calculated percentages are shown in figure 7 as a function of the jigtime.

It was obvious that a linear relation did not fit in figure 7. According to Mayer (1964) and Neese (1966), there is an exponential relation between the grade of concentration in the jigbed and the jig time. The curve of the Asg in figure 7 agrees well with an exponential function. In order to compare the SiC fractions with both Asg and between each other, it was assumed that this exponential relation is valid for all particles. The values in the graph have a relative deviation of 10-20 percent, which could be improved if the interface of the top and bottom fractions is better defined, and prefered orientation of the particles on the glass plates is mimimized.

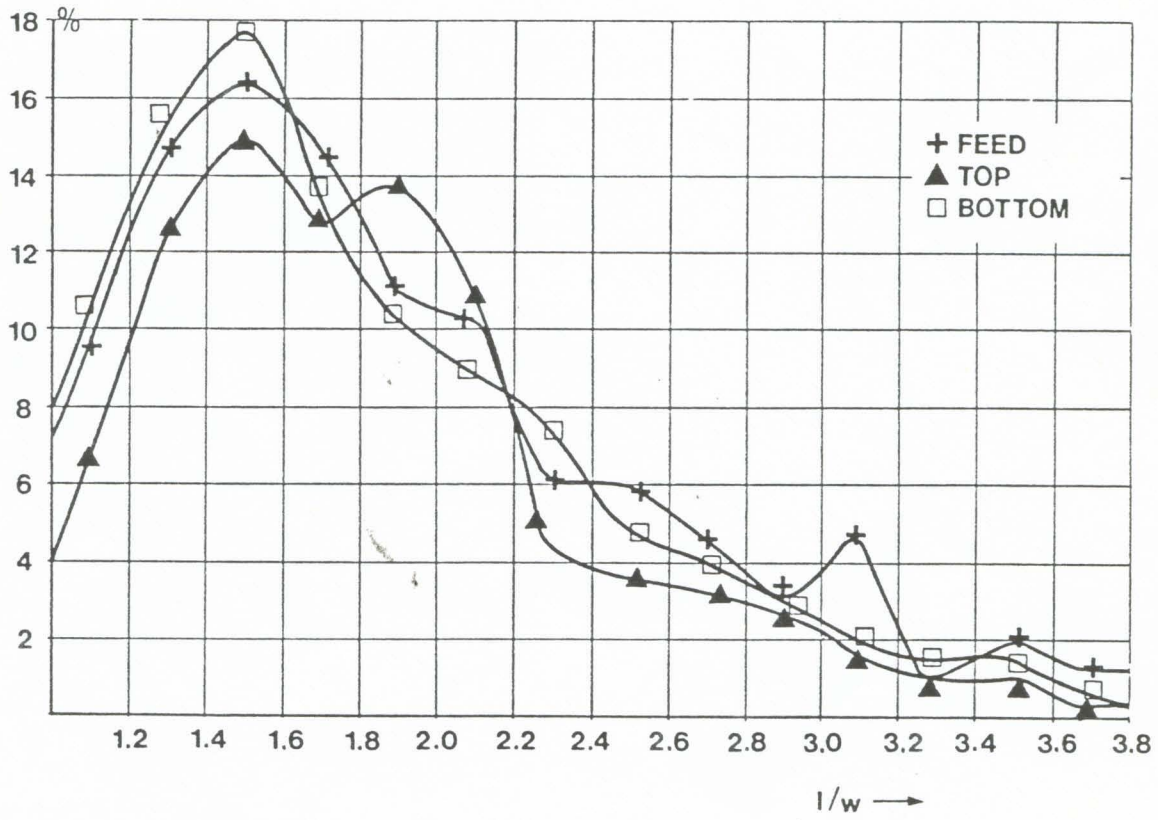

Figure 6. l/w-values after 4 minutes jigging.

Figure 7 shows that the fraction with l/w-ratio 2.0-2.2 goes faster to the top of the bed than all other fractions, including the Asg fraction. Comparison of the curves of the fractions with various intervals of l/w-ratio demonstrates that the time, during which the fractions go to the top of the bed decreases if the l/w-ratio increases. This can be explained by the fact that the oblong particles disturb the ideal packing in a bed of round

particles, thereby creating a larger porosity around themselves. Due to this difference in porosity around the particles the apparent density of the particles decreases (Mayer 1964). Since the difference in density is already small, the effect of this decrease will be substantial. The oblong particles (high l/w-ratio) will migrate to the top of the bed.

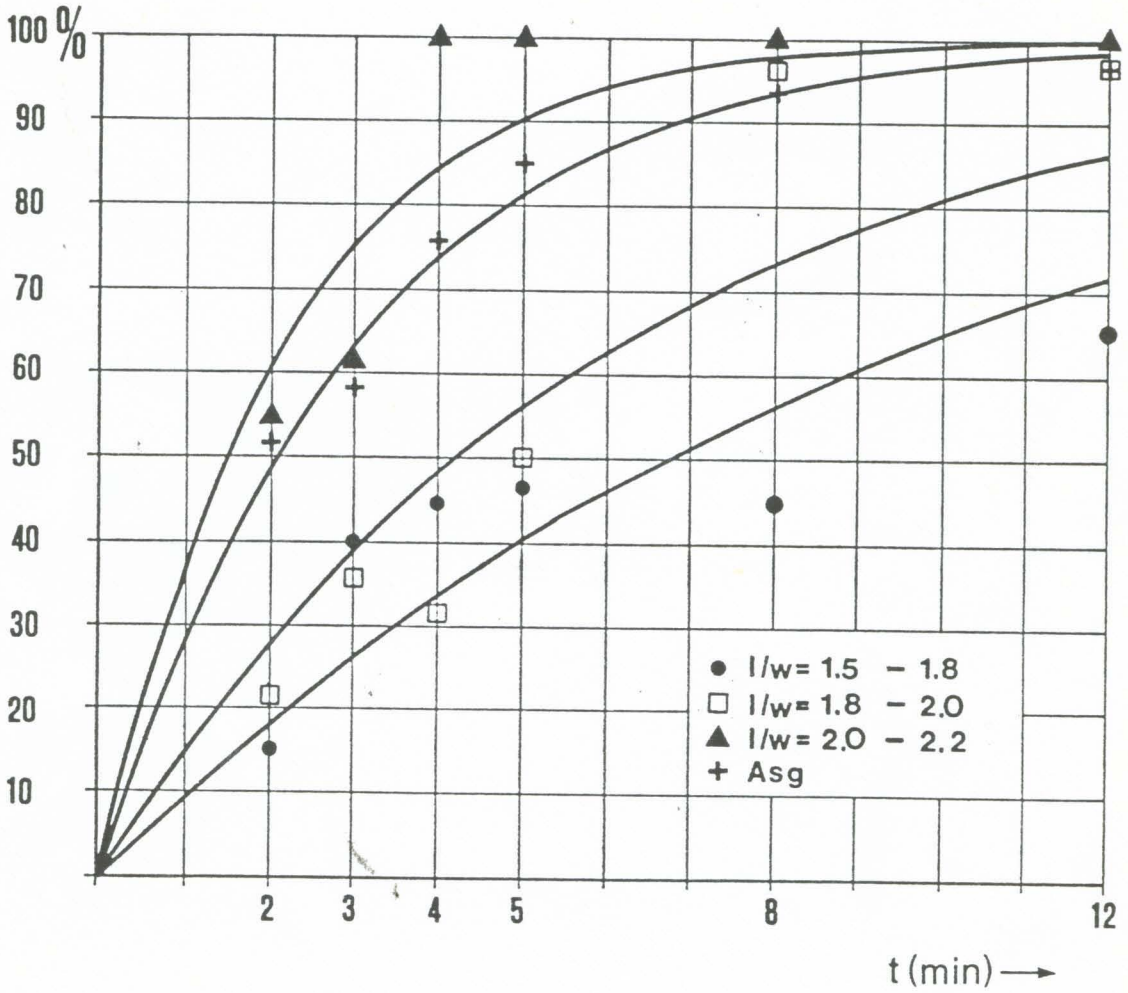

Figure 7. Recovery of different fractions in the top of the jigbed.

The relation between the time, during which the various fractions go to the top of the bed and the l/w-ratio has not been quantified. It is however clear that if the l/w-ratio increases, the separation of the Asg becomes more difficult or for a high recovery of SiC even impossible. For this reason the recovery has to be low for a high grade SiC product. With increasing jig time more SiC will move to the top, because in the last stage of the demixing process the separation will take place based on the difference in shape of the particles.

ECONOMICS

The 3-8 mm fraction of the jaw crusher product contains, according to figure 2, 20 wt percent of the total Asg/SiC mixture. With 70% SiC in the feed and 40% recovery, 1100 ton SiC can be extracted by jigging. According to the German mothercompany of Elektroschmelzwerk Delfzijl B.V., the nett extra value of the jigged concentrate would amount to Dfl. 700 per ton, at 1986 prices. At that time there was a market for minimal 4000 ton concentrate per year. By changing the setting of the jaw crusher and grinding the oversize, it is possible to increase the feed of the jig to extract 4000 ton SiC concentrate. This would give a total annual revenue of Dfl. 2.8 million. A concentration plant for 4000 ton concentrate per year would cost in the order of Dfl. 700,000.

Table 2. Mass distribution and l/w-ratio of different size fractions of SiC in the bottom of the bed

jig time (min)	Asg content (%)	minimum size (mm)	mass distribution (%)	l/w-ratio
0	30.47	6	18.75	1.62
		4	23.20	1.66
		3	25.57	1.89
		2	2.02	2.10
2	20.48	6	21.53	1.58
		4	28.60	1.62
		3	28.12	1.94
		2	1.27	2.12
3	22.28	6	18.11	1.60
		4	26.81	1.65
		3	32.23	1.86
		2	1.35	2.08
4	16.03	6	20.17	1.61
		4	27.84	1.65
		3	33.45	1.87
		2	2.52	1.93
5	11.28	6	25.10	1.55
		4	31.38	1.62
		3	29.49	1.82
		2	2.75	1.95
8	7.66	6	18.49	1.52
		4	32.00	1.54
		3	38.72	1.75
		2	3.14	1.93
12	5.49	6	23.23	1.47
		4	31.04	1.53
		3	36.78	1.75
		2	3.46	1.92

CONCLUSION

A mixture of amorphous and crystalline silicon carbide can be upgraded by jigging. For this upgraded product a market exists. Due to the oblong form of the particles, the recovery in the jig process of the crystalline SiC has to be low. Concentration of the crystalline SiC by three times jigging and recirculation of the middling product will result in a maximum recovery of approximately 40% . The jigging of the mixture has good economical prospects. Flotation results of the fine fraction were not encouraging.

REFERENCES

Benecke, T., 1981, "Metallurgisches Siliciumcarbid in Elektro- und Kupolofen", Giesserei, Vol. 68, No. 12, jun., pp. 344-349.

Elektroschmelzwerk Delfzijl B.V., 1980, Internal report.

Elektroschmelzwerk Delfzijl B.V., 1982, Internal report.

Fichtner, H., 1975, "Untersuchungen uber die Aussagefahigkeit der rontgenografischen Pulvermethode zur Bestimmung der Polytypie in SiC-materialen", Jahresabschlussbericht, AdW der DDR.

Gmelin Handbook, 1957, Si suppl,. Vol.B.

Heinicke, G., et. al., 1973, "Einfluss von Tribosorption und Tribochemisch Prozessen auf grenzflachenmechanische Verhalten von Siliciumcarbid", Kristal und Technik, No. 8, pp. 379-391.

Mayer, F. W., 1964, "Fundamentals of a potential Theory of the jigging process", 7th International Mineral Processing Congress.

Neesse, T., 1966, "Der aufbereitungstechnische Setzvorgang als statischer Prozess", Wissenschaftliche Zeitliche Zeitschrift der Hochschule fur Architectur und Bauwesen, Vol. 13, No.5, Weimar.

Ney, P., 1973, "Zetapotentialen und Flotierbarkeit von Mineralen", Applied Mineralogy, Springer, Wien.

Schubert, 1978, Aufbereitung festmineralischen Rohstoffe, Vol. II, VEB Deutscher Verlag fur Grondstoffindustrie, Leipzig.

Uhlig, D., 1974, "Zur theorie und Praxis der Setzbarkeit und Nassmagnetscheidung", Freiberger Forschungshefte A522, VEB Deutscher Verlag fur Grundstoffindustrie, Leipzig.

Wecht, E. H. P., 1977, "Feuerfest Siliciumcarbid", Applied Mineralogy, Vol 11, Springer, Wien-New York.

Ziemer, B., 1979, "Eine neue Variante zur α/β Analyse in SiC Formkorpern" Silikatechnik, Vol. 30, No. 3, pp. 75-78.

Pyroprocessing techniques

The fiery world of industrial minerals

by Bruce McMichael, *Assistant Editor*

As with any review of technical processing the thermal or heat treatment of industrial minerals is replete with specific terms and jargon often only intelligible to the initiated. This article will attempt to provide an overview of the major techniques used for a selection of minerals and, at the same time, throw light upon such terms as calcination, shaft kilns, sintering, and exfoliation.

Thermal treatment of minerals can take a variety of forms ranging from merely drying the mineral to actually initiating a chemical or physical change in its make-up. However, drying excess water from the surface of the mineral will not be covered in this review nor will the firing of ceramics be discussed. Whilst mentioning various companies in connection with certain processes, the article is not intended to provide an exhaustive review or market analysis of suppliers or users involved in the industry, or the end markets for the products obtained. For this information the reader is referred to other, more specific Industrial Minerals articles. The article aims to familiarise readers with the whys and wherefores of pyro-processing techniques using specific mineral examples.

Fire and heat have both fascinated us and kept us alive. Fire was given to Mankind, according to Greek legend, by the Titan Prometheus. He was punished severely for the crime having stolen the flame from the home of the gods' Mount Olympus. Chained to a mountain top, his liver was torn at and eaten daily by an eagle whilst at night it regrew. He suffered until another great hero, Hercules, broke his chains and freed him. The gift of fire was then used by Hannibal of Carthage to clear boulders from his path as he crossed the Alps. He set fires under boulders and shattered them by dousing them with cold water. This could be, albeit tenuously, the first recorded usage of a heat source working for man in an industrial minerals context. Heat sources were used in antiquity to smelt metals, fire clays and glasses but controlling the temperature was difficult — a clumsy affair. Techniques are now naturally far more advanced although some, and often the best, discoveries are still made by accident. There are many claimants to the fame of discovery both in antiquity and this century. For example, a geologist working for the Silver and Baryte Ores Mining Co. around the 1940s was holidaying on the Greek island of Milos when he threw beach sand on a picnic fire to dampen its vigour. He witnessed the 'popping' and expanding grains leap out of the fire onto cooler areas and claimed the discovery of perlite expansion. This review records some stages of heat treatment in the industrial mineral industry.

Pyroprocessing, thermal treatment, and heat treatment are just three terms used to describe an important and little recorded aspect of the minerals industry. This article is aimed at redressing the balance and describe some of the many process and techniques that face the mineral processor. Thermal treatment is one means of changing either either the chemical make-up or physical nature or a combination of both, in order to add value to a mineral. Products that will be covered here include magnesite, alumina, lime, vermiculite, perlite, gypsum, and molochite. And an insight into the plant and machinery required to process them is also given.

Fused minerals — the heat is on

Historical introduction

Fused minerals have been available since the turn of this century following the discovery of fused synthetic corundum. An engineer, Charles B. Jacobs, is credited with initiating the industry by discovering that hard abrasive alumina crystals could be manufactured by the fusion of bauxite in an electric arc furnace. A host of minerals including fused alumina, silicon carbide, and boron carbide, are now similarly processed to strict quality controlled guidelines, both physical and chemical, to supply diverse markets such as abrasive, refractory, foundry, ceramic, and filler. Natural occuring abrasive minerals, corundum, emery, and garnet were used until the turn of the last century. However for abrasive applications it was recognised that the contained crystalline alumina was responsible for the abrasive properties. Because of its high melting point the fusing of alumina bearing materials was only possible using electric arc furnaces. Fused alumina production began in earnest in the early 1900s drawing cheap power from the Niagara Falls hydro-electric development. I. Werlein in France and F. Hasslachler in Germany patented methods of fusing emery in 1893 and 1894, respectively. These processes were then superseded by Werleim's use of calcined bauxite as opposed to emery. In 1900 Jacobs introduced limited control to the process by installing a movable furnace bottom, a technology used initially by the *Norton Emery Wheel Co.* (now

Some thermal terminology

Calcination and roasting
Calcination can be defined as the heating of ores, concentrates, precipitates, or residues to decompose carbonates, hydrates, or other such compounds. The process differs from roasting because air is not supplied to the charge during heating. Roasting involves a chemical reaction between the gas and the solids but in calcination the surrounding hot gas serves merely to provide the necessary heat. Calcining occurs in a furnace or kiln in an oxidising atmosphere and is usually required to expel excess sulphur or carbon dioxide from the concentrate. If the maximum amount of sulphur is removed the operation is termed sweet roasting, whereas if CO_2 is all but completely removed the process is known as dead roasting.

Sintering
The agglomeration of small particles to form larger ones by heating without actually reaching melting point is known as sintering. An industrial mineral example of this is sinter magnesia, also known as dead-burned magnesite.

Norton Co.) in Niagara Falls, New York. Further important discoveries made by C. M. Hall included the mechanical removal of suspended metallic particles and impurities in the alumina melt by adding iron borings to the charge. A. C. Higgins then replaced the brick or carbon block lined furnace with a skull furnace consisting of a congealed, thin alumina layer with a water-cooled shell. These contributions by Hall and Higgins remain important features in the production of fused alumina production. Many different grades, colours, and specifications of product have been introduced to the market and are generally distinguishable by the following parameters:

alumina content,
percentage of contained impurities,
crystal size — a function of cooling rate.

Processing is heavily capital intensive, both to set up operations and to maintain plant and equipment, in highly abrasive environments. An immense demand for electrical power is required, presenting another barrier to new companies hoping to enter markets. Fusion is often made during off-peak hours when electricity rates are cheaper. Alumina, magnesia, silica, mullite, and zirconia are all minerals which can be fused to produce commercial products.

Alumina — what goes in . . .
Bauxite is the primary feed material used for production of regular and semi-friable alumina. Pure fused alumina, white, pink and ruby, is produced from calcined alumina. Calcined alumina is produced from bauxite by the caustic digestive process ie. the Bayer process. Australian, Chinese, Guinean or South American bauxites are often blended before fusion to achieve the best mix to optimise end product and cost effectiveness.

Run of mine bauxite contains free and bound moisture in quantities up to 40% H_2O. To avoid heating complications in the electric arc, raw bauxite is first crushed to one inch size and calcined in rotary kilns at a temperature of 1100°C, to reduce water content to below 1%. As the percentage impurities content of bauxite has increased, following exhaustion of higher grade material, so the amount of energy required to produce a unit of fused alumina has increased. For example, a 2% increase in silica in calcined bauxite requires 16% more energy in fusion while a 2% increase in Fe_2O_3 demands 8% more energy. This cost increase is also compounded by,

Higher energy costs,
Higher electrode costs,
Higher labour costs due to fall in output.

Raw bauxite can be used as feed material if the deposit is located near a cheap source of power and is of the low water-containing diaspore grade. However, the water released during dehydration gives rise to a water gas reaction with carbon resulting in unbalance in the carbon ratio and erratic furnace operation. Where sintered bauxite is used in preference to calcined bauxite it offers two specific advantages. The furnace can be kept covered 90–95% of operating time, so reducing heat and dust losses and, as the moisture has to be removed anyway, a combination of calcining and agglomeration can be achieved simultaneously by sintering. Sintered bauxite is not often used as a raw material by American producers because of the prohibitive domestic expense of sintering and the practical, mechanical, difficulties of transporting the material from South America or Australia.

. . . must come out
The accompanying table indicates characteristics of the main calcined alumina end products.

Major varieties of fused alumina

Regular or high titania fused alumina is of deep, dark brown colour and contains 94–96% Al_2O_3, 2–3.5% TiO_2, 1–2% SiO_2, and small amounts of Fe_2O_3, ZrO_2, CaO, and MgO. When fired the material turns blue. There are two kinds of regular fused alumina — one chill cooled with a smaller crystal size (300 microns average) and the other with larger crystal size (1,000 microns) as a result of slow cooling.

Semi-friable or low titania fused alumina has a higher Al_2O_3 content of 96–98%. TiO_2 content ranges from 1.5–2.5% and the SiO_2 content is below 1%. Its colour is brown to reddish brown which transforms into a light blue when fired. Two types are commercially available — slow cooled, semi-friable with an average crystal size of 600 microns, and chill cast semi-friable with an average crystal size of 200 microns.

White fused alumina contains <0.5% impurities of which NaO_2 is the most important as it influences the toughness of the alumina.

Pink and red fused alumina contain from 0.05–0.3% chromium oxide and **ruby fused alumina** contains some 2.5% Cr_2O_3. the chromium oxide is added when fusing calcined Bayer alumina.

Grey fused single crystal alumina cystallises from sulphide melts. It contains in excess of 99% Al_2O_3 and about 0.5% TiO_2.

Zirconia modified fused aluminas were introduced in 1961 and are commercially available in three varieties depending on zirconia content — 10%, 25% and 40%. Some of these abrasives contain only ZrO_2 and Al_2O_3, whereas in others the SiO_2 and TiO_2 content varies from 0.2% to 2.0%.

Source: P. Cichy, Fused alumina production

The fusing process
There are three types of furnace used:-
1. The block or pot furnace for batch operation eg. Higgins type,
2. The pour or tilt type, for continuous operation.
3. The tapping type resembles a ferroalloy furnace, for continuous operation.

The furnace type synonymous with the fusing process is the Higgins furnace. Pioneered by Norton Co. and engineer Aldous Higgins in 1904, its design relies on the cooling effect of a water jacket which prevents the intense heat generated in the melt from melting the mild steel shell. See accompanying diagram.

Block furnace (Higgins type) for regular fused alumina

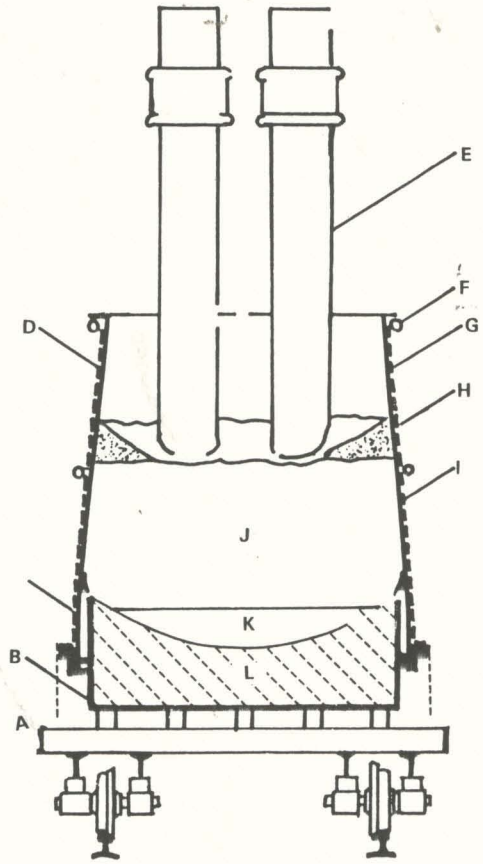

A – Base B – Furnace bottom C – Alumina grain seal
D – Furnace Shell E – Electrode F – Cooling ring
G – Water film H – Charge I – Alumina skull
J – Alumina melt K – Ferrosilicon L – Carbon

Source: Fused alumina production, P. Cichy

This water jacket surrounds a lined shell and creates a 'frozen' crystallised layer of unfused material of bauxite/alumina between the refractory and the melt. This prevents the shell from cracking or suffering breakouts as happened in the early stages of development.

Mr Higgins would easily recognise most of the furnaces still in use as they are little changed from his original water cooled cylindrical furnace shell model. Tilt furnaces, similar to those found in the steel industry, are also favoured. Melt from a tap and tilt type furnace is extracted via a water-cooled taphole located in the side of the pot, in a similar arrangement to the one used to remove ferrosilicon waste produced from ironboring additions to remove impurities. Advantages of this method are quoted as being easy emptying of the furnace (the hole is plugged with refractory cement and punched out), easy separation of ferrosilicon from the fused alumina slag, and a fairly unrestricted flow.

Depending on the feed, electric arc fusing takes between 12 and 24 hours at melt temperatures in the centre of the furnace in excess of 2,000°C. The AC arc is achieved by using three-phase graphite electrode systems, initially to fuse the charge. This charge is topped up with feed material to make a finished ingot averaging 6–10 tonnes in weight. During fusion the electrodes are continually adjusted vertically to keep the arc at the optimum height. This operation can be performed manually or automatically and is necessary to ensure that new material is continually exposed to the arc to achieve complete fusion. Once fusion is complete the electrodes are lifted from the melt and the furnace shell removed. The ingot at this stage has the appearance, shape, dimensions, and texture of a giant toasted marshmallow. The ingot is left to cool before crushing, grinding, and classifying in circuit which is subjected to severe wear because of abrasive nature of the material. The irony of the whole process is that a pure fused product is found in the ingot but during the communition process contamination is such a problem that it needs extensive and costly cleaning to regain the high purity levels.

Fused alumina — white and brown

Fused alumina primarily owes its existence to the rarity of occurrence of its natural forms, corundum and emery, and the suitability of the material as an abrasive. Brown fused alumina was first produced by Norton Co. in 1909 and sold to the refractories industry under the Alundum trade name. The following year white fused alumina was manufactured utilising high purity Bayer alumina as feed and was found to have harder and faster cutting properties than the brown material. The purer white material commands the higher price of the two, both of which have remained the volume choice electrofused minerals in their major markets of abrasives and refractories.

Nearly 80% of total output is of the brown variety, the production of which is based on the fusion of calcined abrasive-grade bauxite with ground coke and iron borings. The additions are required to clean the bauxite, removing such impurities as iron oxide, silica, and titanium dioxide, leaving a material with an Al_2O_3 content of 94–97%.

$$Fe_2O_3 + 3C \longrightarrow 3CO + 2Fe$$
$$SiO_2 + 2C \longrightarrow 2CO + Si$$
$$TiO_2 + 2C \longrightarrow 2CO + TiO_2$$

Coke or anthracite is also added to the bauxite to carry the electric current in the initial stages of the melting process.

Having been reduced, impurities are taken up by the iron borings in a ferrosilicon waste which separates out from the molten mass and sinks to the bottom. The iron addition in the slag also facilitates the magnetic removal of contaminated fused material. Fumes containing amorphous silica. and dust are also taken out. The fusing operation takes place in continuously working tilt furnaces with slag removed every few days by deep tapping from the larger furnaces. The resulting molten ingot is allowed to cool at a planned rate to allow for controlled crystal growth and thus toughness. Production of fused alumina at *Universal Abrasives'* plant in Hull England is achieved with one furnace operating continuously all year round. At temperatures of 2,400–2,500°C, some 6 tonnes of material is tapped off at regular intervals. The company taps the furnace once a day for ferrosilicon and markets are available for the product which, having a relatively high phosphorous content of 0.8%, falls outside most specifications demanded by the steel industry.

Alternative pot constructions used in the production of white fused alumina

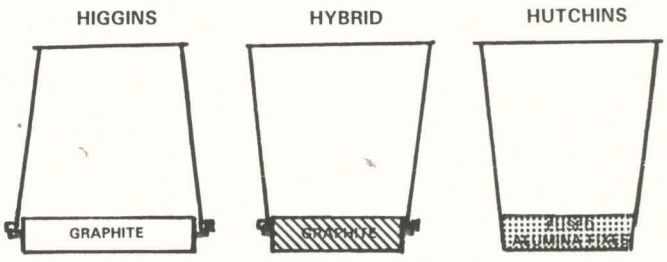

Source: Fused alumina production, P. Cichy

Pouring type furnace for semi-friable fused alumina

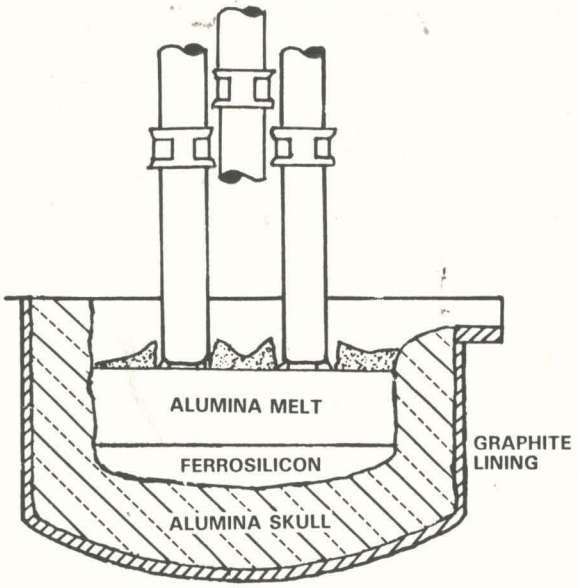

Source: Fused alumina production, P. Cichy

White fused material is obtained from an extremely pure alumina by-product from the Bayer process of aluminium production. Fusion of this material produces a 99.5%–99.9% Al_2O_3, which confers extreme hardness to the product but at the expense of toughness. Although brown fused alumina is softer than white, it possesses greater toughness which can be artificially enhanced by the addition of titanium. By the addition of chromium oxide a red or pink (2% or 2.5% respectively) fused alumina is produced with increased toughness for precision abrasive applications. Brown abrasive grain is often calcined before use to confer better hardness properties or to set ceramic coatings. These are sometimes applied to the grain to increase the roughened surface area and hence improve adhesion of any bonding media with the grain. This coating can be in the form of a metallic oxide or an organo-silicon compound such as silane.

Typical analyses of fused aluminas *(%)*

Chemical	*White*	*Brown*	*Physical*	*White*	*Brown*
Al_2O_3	99. 5	95. 2			
SiO_2	0.03	1.10	Sp. grav	3.94	3.95
Fe_2O_3	0.05	0.20	Hardness	1,800–2,300K_{100}	1,700–2,000
TiO_2	Trace	3.10	Moh's scale	9	9
CaO	0.04	0.05			
Na_2O	0.32	—			
K_2O	0.01	—			
MgO	—	0.35			

Source: Universal Abrasives

Lime and rotary kilns

Lime — the burning question

Lime is a term used to describe most forms of calcareous material and finely ground forms of limestone or dolomite, (See definitions in IM May '88 p. 23). Lime itself is the calcined product of limestone with pseudonyms of quicklime, calcium oxide, or calcia. Quicklime can be calcitic, dolomitic, or magnesian but does not refer to limestone or any carbonate form of lime. Lime production has historical roots dating back to the days of alchemy although the actual scientific processes were only really understood from the beginning of the nineteenth century. The basic process is, however, so simple that detailed investigation did not start until the 1960s when the mysteries of the thermodynamic and kinetic concepts began to be fully unravelled. A vast range of equipment is now available to achieve the burning of lime. The choice of kiln system essentially depends on the desired end product. This section will present an overview of the hows, whys, and wherefores of lime burning.

The reaction

Burning of lime is a chemically reversible reaction that can represented as follows:-

Heat (1,000°C to 1,300°C) + $CaCO_3$ (limestone) $\longrightarrow$ CaO (quicklime) + CO_2 or
$CaCO_3.MgCO_3$ + Heat (900°C to 1200°C) $\longrightarrow$ CaO. MgCO + $2CO_2$

Finer points of the chemistry involve the heat of reaction which is 42.2 kcal (176.6 kJ) per mol $CaCO_3$ at 20°C in 100% CO_2 atmosphere, corresponding to 753 kcal (3,152.1 kJ) per kg of CaO. At 900°C the heat of reaction is 39.8 kcal (165.8kJ).

Calcination is undertaken at high temperatures and pressures to release carbon dioxide. This dissociation starts at the surface of the mineral and proceeds towards the centre resulting in a shell of burnt lime and a core of non-calcined stone. The shell thickness is dependent on time spent in the kiln. At any time in the process, calcination takes place between these two layers at a temperature of 900°C minimum. Burnt lime, being a poor heat conductor, requires the outer shell to be hotter than the core material. Therefore a temperature of 1,100–1,250°C is often required to ensure a sufficient heat gradient. A weight loss of between 40% and 44% is effected during calcining but the volume is unchanged during low temperature burning. This product is highly porous and known as soft-burnt. Hard-burnt lime is produced at higher burning temperatures. As a result of hard burning shrinkage occurs, micropores contract, and the resultant calcium oxide crystallites agglomerate forms larger units with reduced free surface. This makes hard-burnt lime less chemically reactive than its soft-burnt counterpart. It is therefore less attractive to consumers. Soft burned lime has a particle size not exceeding 2 micron. It is produced at 900–1000°C irrespective of burning time. Dead burning (sintering) begins at 1,200°C after approximately 12 hours of calcining time at 1,300°C after 1–1½ hours of calcining time.

Diverse limestone types have been categorised according to their calcination behaviour by R. S. Boynton (Chemistry and Technology of Lime and Limestone, 2nd edition, 1980, John Wiley) as follows.

1. Limestones that fracture and decrepitate readily during preheating and at low calcination temperatures.
2. Limestones that yield a porous, reactive lime under most calcination conditions and are difficult to overburn.
3. Limestones that yield a dense, unreactive lime of low porosity even under the mildest calcining conditions.
4. Limestones that yield a porous, reactive lime under mild temperature conditions and denser, less porous lime under harder burning conditions.

Of these categories, 1 and 3 are rather undesirable, while for all round versatility 4 is preferred over 2. Time/temperature adjustments can be made by a kiln operator to produce lime for a specific task.

The cost of setting up a lime burning plant is within the reach of most industrial concerns who wish to get a foothold in the business. The barrier to market entry, in this case, is the sheer number of companies already active in the field. When choosing a lime kiln, as with any other capital investment, many factors